Relationship Between Ligand Structure and Reactivity for Copper(II) Complex Mediated Hydrolysis of Phosphate Diesters, Carboxylic Esters, and Amides

PART I

Hydrolysis of Phosphate Diesters Promoted by Cu(II) Complexes

PART II

Hydrolysis of Carboxylic Esters and Amides Catalyzed by Cu(II) Complexes

by

Vrej Jubian

A thesis submitted to the Faculty of Graduate Studies and Research of McGill University in partial fulfillment of the requirements for the degree of Doctor of Philosophy

March 1991
Department of Chemistry
McGill University
Montreal, Quebec, Canada

to my parents, Lucy and Avedis,

my grandmother, Victoria,

and Mihran, Mary and Christine

ABSTRACT

The efficiencies of several Cu(II) complexes in promoting the hydrolysis of bis(2,4-dinitrophenyl) phosphate (BDNPP) have been compared Copper complexes of the type $[(L)Cu(OH_2)_2]^{2+}$, where L represents a bidentate diamine ligand, can be effective in promoting the hydrolysis of BDNPP Furthermore, the activity of the Cu(II) complex is sensitive to the ligand structure. The structure-reactivity relationship has been explained in terms of a detailed mechanism of the reaction

The complex $[Cu(2,2'\text{-dipyridylamine})(OH_2)_2]^{2+}$ efficiently catalyzes the hydrolysis of carboxylic esters (4-nitrophenyl acetate, methyl trifluoroacetate, and methyl acetate). Methyl acetate, when bound to the copper complex, is hydrolyzed at a rate that is comparable to the k_{cat} values for chymotrypsin catalyzed hydrolyses of esters. The hydrolysis of N,N-dimethylformamide by $[Cu(2,2'\text{-dipyridylamine})(OH_2)_2]^{2+}$ at neutral pH, 100 °C, proceeds at least two hundred times faster than that by $[Cu(2,2',6',2''\text{-terpyridine})(OH_2)]^{2+}$. A detailed mechanism of the reaction has been given to explain the structural requirements of a metal catalyst necessary for hydrolyzing esters and amides, and a mechanism for Carboxypeptidase A catalyzed hydrolysis of peptides has been proposed

Résumé

L' efficacité de plusieurs complexes de Cu(II) pour la promotion de l'hydrolyse du bis(2,4-dinitrophényle) phosphate (BDNPP) a été comparée. Les complexes cuivriques du type $[(L)Cu(OH_2)_2]^{2+}$, où L représente un ligand bidentate diaminé, peuvent être des promoteurs efficaces de l'hydrolyse du BDNPP. De plus, l'activité du complexe Cu(II) est dépendante de la structure du ligand. La relation entre la structure et la réactivité peut être expliquée à partir du méchanisme détaillé de la réaction.

Le complexe $[Cu(2,2'\text{-dipyridylamine})(OH_2)_2]^{2+}$ est un catalyseur efficace de l'hydrolyse des esters carboxyliques (acétate de 4-nitrophényle, trifluoroacétate de méthyle, acétate de méthyle). L'acétate de méthyle en présence du complexe est hydrolysé à une vitesse comparable aux valeurs du k_{cat} pour l'hydrolyse d'esters par la Chymotrypsine. L'hydrolyse du DMP par le $[Cu(2,2'\text{-dipyridylamine})(OH_2)_2]^{2+}$ à pH neutre et à 100°C, procède au moins deux cent fois plus rapidement qu'en présence du $[Cu(2,2':6',2''\text{-terpyridine})(OH_2)]^{2+}$. Un méchanisme détaillé de la réaction est décrit pour expliquer les contraintes structurales dans un complexe pour qu'il soit un catalyseur efficace de l'hydrolyse d'esters et d'amides. Un méchanisme de l'hydrolyse de peptides par la Carboxypeptidase A est proposé.

ACKNOWLEDGEMENTS

I am deeply grateful to my research supervisor, Prof. Jik Chin, for his guidance, support, and encouragement throughout the course of this study.

I am indebted to NSERC for financial support in the form of a postgraduate scholarship.

I would also like to thank:

Dr. Stephen Kawai for his helpful discussions and friendship, and for proofreading parts of the manuscript.

Dr. Mariusz Banaszczyk, Karen Mrejen, Jung-Hee Kim, Dr Andrew Moore, Dr. Xiang Zou, Barry Linkletter, James Connolly, Bryan Takasaki, and Daphne Wahnon for their friendship and helpful discussions

Dr. Françoise Saurnol for her assistance in NMR experiments

Nancy Kawai for proofreading the manuscript.

Normand Hebert for translating the abstract of this thesis into French

GLOSSARY OF SYMBOLS AND ABBREVIATIONS

~	approximately
δ	chemical shift
ε	extinction coefficient
λ	wavelength
AcCh	acetylcholine
AcOH	acetic acid
anal.	analysis
Arg	arginine
b.p.	boiling point
BDNPP	bis(2,4-dinitrophenyl) phosphate
BNPP	bis(4-nitrophenyl) phosphate
bpy	2,2'-bipyridine
calcd	calculated
cAMP	3',5'-cyclic adenosine monophosphate
cGMP	3',5'-cyclic guanosine monophosphate
CHES	[2-(cyclohexylamino)ethanesulfonic acid]
CPA	carboxypeptidase A
cyclen	1,4,7,10-tetraazacyclododecane
dien	diethylenetriamine
5,5'-dimethyldpa	bis[2-(5-methylpyridyl)]amine
6,6'-dimethyldpa	bis[2-(6-methylpyridyl)]amine
disp.	dispersion
DMAP	4-dimethylaminopyridine
DMF	N,N-dimethylformamide
DMSO	dimethyl sulfoxide
DNA	2'-deoxyribonucleic acid
DNPP	2,4-dinitrophenyl phosphate
dpa	2,2'-dipyridylamine
dpk	2,2'-dipyridylketone
dpm	2,2'-dipyridylmethane
dps	2,2'-dipyridylsulfide
DSS	3-(trimethylsilyl)-1-propanesulfonic acid (2,2-dimethyl-2-silapentane-5-sulfonate)
E-coli	Escherichia coli

EDTA	ethylenediaminetetraacetic acid
en	ethylenediamine
eq.	equation
eq.	equivalent(s)
EtOAc	ethyl acetate
g	gram(s)
Glu	glutamic acid
h	hour(s)
His	histidine
Hz	Hertz
L	bidentate diamine ligand
L	Litre(s)
M-OH	metal-hydroxide
m.p.	melting point
MeOAc	methyl acetate
MES	4-morpholineethanesulfonic acid
min	minute(s)
mol	mole(s)
MTA	methyl trifluoroacetate
N_4	tetraamino ligand
neo	neocuproine (2,9-dimethyl-1,10-phenanthroline)
5-NO_2neo	5-nitroneocuproine
NMedpa	bis(2-pyridyl)methylamine
NMR	nuclear magnetic resonance
NPP	4-nitrophenyl phosphate
Phe	phenylalanine
phen	1,10-phenanthroline
pNPA	4-nitrophenyl acetate
ppm	parts per million
py	pyridine
RNA	ribonucleic acid
t.l.c	thin layer chromatography
terpy	2,2':6',2''-terpyridine
TFP	trifluoperazine
THF	tetrahydrofuran

tmen	N,N,N',N'-tetramethylethylenediamine
TMP	trimethyl phosphate
TMS	tetramethylsilane
tn	1,3-diaminopropane
tren	tris(2-aminoethyl)amine
trien	triethylenetetramine
trpn	tris(3-aminopropyl)amine
Tyr	tyrosine
UV-vis	ultraviolet-visible
v	volume
s	second(s)
w	weight

STRUCTURES OF LIGANDS

Abbreviation	*Structure*
5-NO_2neo	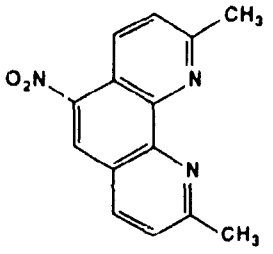
5,5'-dimethyldpa	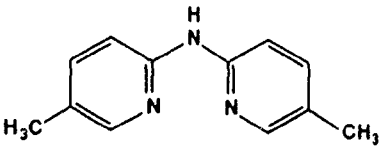
6,6'-dimethyldpa	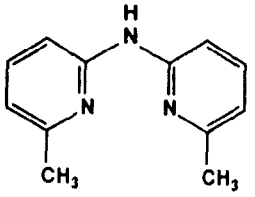
bpy	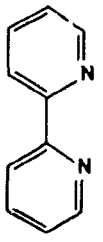

cyclen

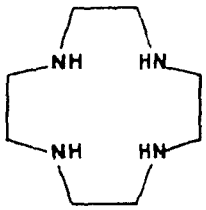

dien

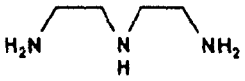

dpa

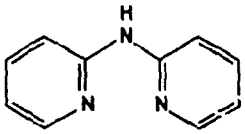

dpk

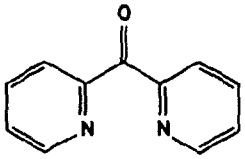

dpm

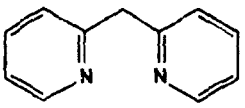

dps 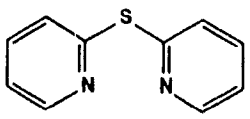

en 

neo 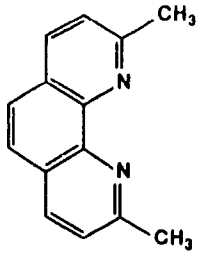

NMedpa 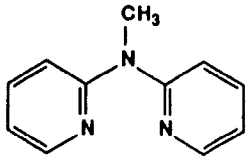

terpy 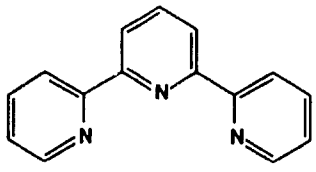

tmen 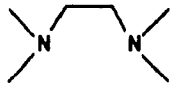

tn 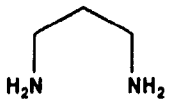

tren 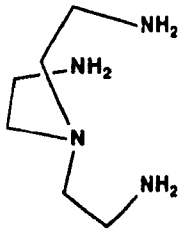

trien 

trpn 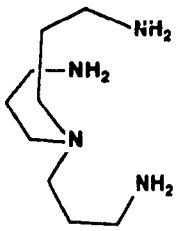

TABLE OF CONTENTS

2 RESULTS

3 DISCUSSION

PART II HYDROLYSIS OF CARBOXYLIC ESTERS AND AMIDES CATALYZED BY Cu(II) COMPLEXES

4 INTRODUCTION

5 RESULTS

1. INTRODUCTION

1.1 THE BIOLOGY OF PHOSPHATE ESTERS

Phosphate esters play a very important role in biological systems. The polymeric molecule that functions to both store and pass on genetic information is deoxyribonucleic acid (DNA) The related polymer, ribonucleic acid (RNA) helps in the passage of this genetic information. Both DNA and RNA are diesters of phosphoric acid. The molecules of heredity are not the only phosphate esters which serve an important role in the chemistry of life processes. Phosphate esters are ubiquitous in biochemistry

Most of the coenzymes are esters of phosphoric or pyrophosphoric acid. For example, pyridoxal-5'-phosphate is the coenzyme form of vitamin B_6 and has the structure shown in figure 1.1. It is involved in a variety of reactions in the metabolism of α-amino acids including transaminations, α-decarboxylations, racemizations, α,β-eliminations, aldolizations and the β-decarboxylation of aspartic acid.

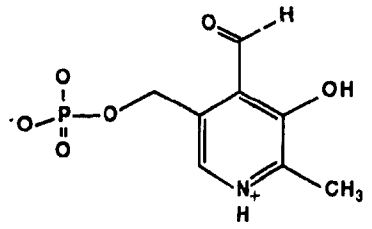

Figure 1.1. Pyridoxal-5'-phosphate.

Phospholipids are another important class of biologically important phosphate esters. They are the major structural lipids of all biological membranes in eukaryotic and prokaryotic cells. The phosphoglycerides are the most abundant structural group in this lipid class. All the phosphoglycerides have a glycerol-3-phosphate backbone. The hydroxyls are usually acylated with fatty acids. The phosphoglycerides are classified according to the substituent X on the phosphate group (fig. 1.2). If X is a hydrogen, the compound is phosphotidic acid. If X is choline, the lipid is called phosphatidylcholine (or more commonly referred to as lecithin) and is the most abundant phospholipid in animal tissues. Phospholipids can be thought of as phosphate monoesters or phosphodiesters.

Cyclic nucleotides, 3', 5'-cyclic guanosine monophosphate (cGMP) and 3', 5'-cyclic adenosine monophosphate (cAMP) function to regulate cell-to-cell communication processes (fig. 1.3). In general, there are primarily three pathways to follow for cellular

communication. The first involves the transmission of electrical impulses via the nervous system. The second involves chemical messengers or hormonal secretions, and the third involves *de novo* protein synthesis All three processes are usually in response to some demand or stimulus and involve, to some extent, regulation by cyclic nucleotides

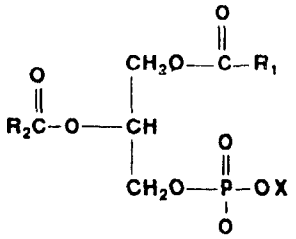

Phosphatidic acid, X = H

Phosphatidylcholine, X = $CH_2CH_2N(CH_3)_3$

Figure 1.2 Examples of phospholipids

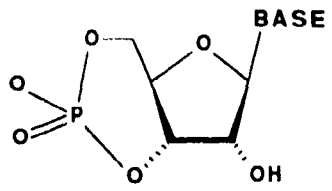

Base = adenine or guanine

Figure 1.3 cAMP and cGMP

Many enzymes are regulated by phosphorylation or dephosphorylation.

Many metabolites are phosphate monoesters which are essential intermediates in biochemical synthesis and degradations. Phosphoenolpyruvate, an enol ester of phosphoric acid, is an intermediate in the glycolytic pathway It is a principal reservoir of biochemical energy along with adenosine triphosphate (ATP, an anhydride of phosphoric acid) and creatine phosphate (an amide of phosphoric acid).

The variety of phosphate esters present in nature is a clear indication of its importance. Nature has evolved to develop highly specialized enzymes that hydrolyze or form esters of phosphoric acid The significance of these esters in biological processes has lead many researchers to study the hydrolysis of phosphate esters

1.2 ARTIFICIAL RESTRICTION ENZYMES

DNA strand cleavage reactions are of considerable interest both in understanding the ubiquitous phosphate ester hydrolysis reactions carried out in nature and in designing new artificial restriction enzymes.

1.2.1 The Need for an Artificial Restriction Enzyme

Over the past decade, much progress has been made in designing artificial restriction enzymes.[1-13] The advantage of an artificial restriction enzyme over the natural enzyme is that one would be able to cleave DNA at any desired nucleotide sequence. This cannot be done with natural restriction endonucleases. The natural enzymes recognize and bind to certain sequences in DNA ranging from four to eight base pairs in length and then hydrolyze DNA at that site.[2] This limits the molecular biologist in manipulating the DNA. The ability to hydrolyze DNA at any desired site would be an invaluable tool in recombinant DNA technology.

Sequence specific artificial restriction enzymes may find use in mapping the human genome and in helping molecular biologists locate individual genes on chromosomes There are three thousand human genetic diseases that have been identified but it is not known where most of the genes responsible for those diseases are located and what proteins they encode. With the development of an artificial restriction enzyme, it may be possible to control disease states at the level of DNA itself.[1a]

1.2.2 Previous Work

The first man-made catalyst which exhibited nuclease activity was discovered by Sigman et al.[3] The catalyst was $[(phen)_2Cu^+]$ complex and the cleavage reaction occurred by an oxidative process requiring hydrogen peroxide as a coreactant. The process includes binding of the cuprous complex to DNA followed by the generation of a metal ion associated hydroxyl radical-like species by one-electron oxidation of the cuprous complex by hydrogen peroxide This oxidant is responsible for the scission of DNA (fig. 1.4).

The phenanthroline cuprous complex showed little sequence specificity Like natural restriction enzymes there are two structural domains for an artificial DNAse. One binds DNA sequence specifically and the other cleaves DNA. A lot of work has been done

---

[1]a) R. M Baum, *Chem Eng News*, **1988**, 66(1), 20 , b) D P Mack, B. L Iverson, and P B. Dervan, *J Am Chem Soc* , **1988**, 110, 7527 , c) J K Barton, *Science*, **1986**, 233, 727 , d) A M. Pyle, E. C Long, and J K Barton, *J Am Chem Soc* , **1989**, 111, 4520 ; e) D. S. Sigman, *Acc Chem Res* , **1986**, 19, 180

[2]P B Dervan, *Science*, **1986**, 232, 464

[3]D S. Sigman, D Graham, V D'Aurora, and A. M Stern, *J Biol Chem* , **1979**, 254, 12269

on DNA recognition and in the past several years advances have been made in coupling recognition to reactivity.

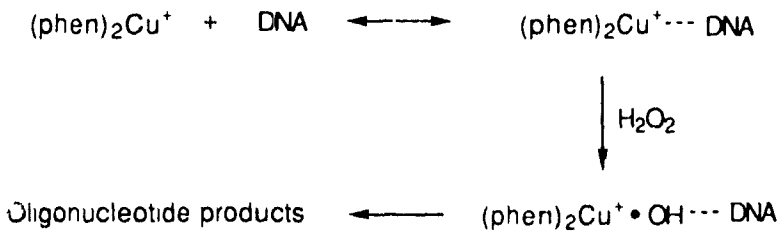

Figure 1.4 The oxidative nuclease activity of the 1,10-phenanthroline cuprous complex (ref 3)

The nuclease activity of the phenanthroline cuprous complex was targeted to specific DNA sequences by covalently attaching it to the 5' end of complementary deoxyoligonucleotides via a phosphoramidate linkage [4] The phenanthroline metal complex was also attached to the DNA binding protein, E-coli trp repressor [5] Both systems generated a site specific nuclease (fig. 1 5)

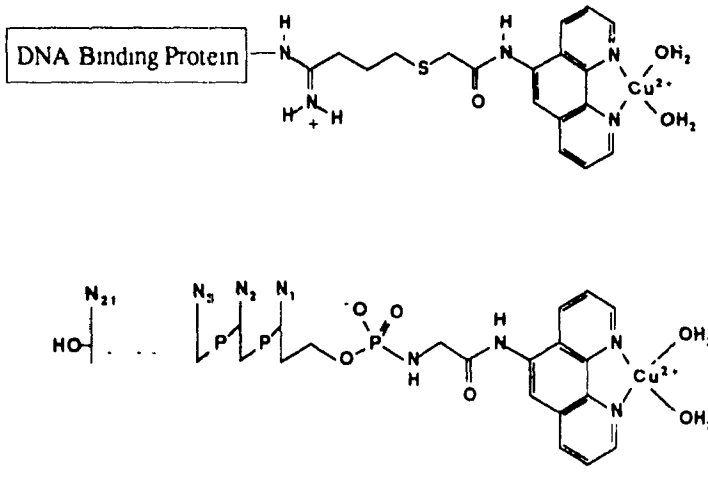

(ref 4,5)

Figure 1.5. DNA binding groups covalently linked to phenanthroline-copper complex

[4]C. B Chen and D S Sigman, *Proc Natl Acad Sci USA*, **1986**, 83, 7147
[5]C B Chen and D S Sigman, *Science*, **1987**, 237, 1197

on DNA recognition and in the past several years advances have been made in coupling recognition to reactivity.

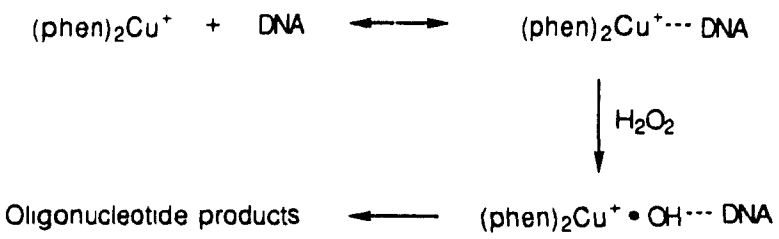

Figure 1.4 The oxidative nuclease activity of the 1,10-phenanthroline cuprous complex (ref 3)

The nuclease activity of the phenanthroline cuprous complex was targeted to specific DNA sequences by covalently attaching it to the 5' end of complimentary deoxyoligonucleotides via a phosphoramidate linkage.[4] The phenanthroline metal complex was also attached to the DNA binding protein. E-coli trp repressor.[5] Both systems generated a site specific nuclease (fig. 1 5).

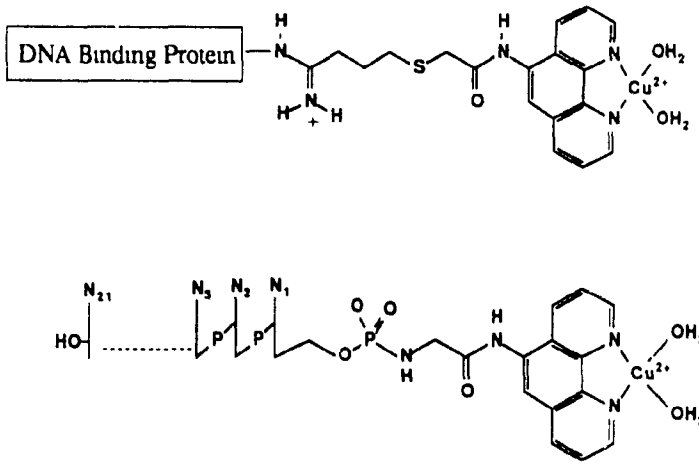

(ref 4,5)

Figure 1.5. DNA binding groups covalently linked to phenanthroline-copper complex.

[4]C B. Chen and D S. Sigman, *Proc Natl Acad Sci USA*, **1986**, 83, 7147
[5]C. B. Chen and D S. Sigman, *Science*, **1987**, 237, 1197

Dervan and co-workers took advantage of the Fe(II)/Fe(III) redox activity to cleave DNA.[1,2,6-8] Ferrous-EDTA was covalently bound by a short hydrocarbon tether to the DNA intercalator methidium[7] (fig 1.6). Greater specificity was achieved by changing the binding group. Fe(II)-EDTA was attached to DNA binders such as distamycin[2] and netropsin.[8]

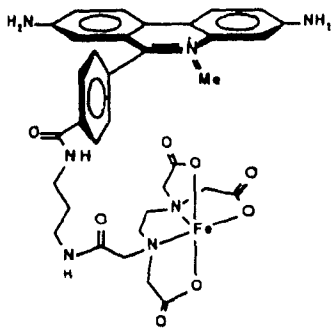

Figure 1.6 Methidiumpropyl-EDTA-Fe(II) (ref 7)

In an elegant experiment, Dervan and Griffin[8] attached the EDTA-Fe(II) group to two molecules of netropsin linked together with a polyether tether that can close around and bind an appropriate metal cation (fig 1.7b). Sequence specific DNA cleavage was observed only by the addition of Sr^{2+} or Ba^{2+} cations. The presence of these metal cations facilitated binding of both netropsin units simultaneously with an additional DNA binding subunit attributable to the macrocycle that formed around the metal cation.

Transition metal complexes which bind to DNA along conformationally distinct sites have also been coupled to metal mediated redox reactions to cause cleavage of the DNA strand at the bound site. For example, the complex $Ru(DIP)_2Macro^{n+}$ was prepared in which one of the three diphenylphenanthroline ligands is modified with two polyamine segments that can, themselves, complex to metal ions (fig. 1.8).[9] The complex binds to DNA and the polyamine arms deliver complexed metal ions, such as Cu^{2+} to each strand of duplex DNA for strand cleavage. The result is a shape selective DNA cleaving molecule.

---

[6]a) S. A. Strobel, H. E. Moser, and P. B. Dervan, *J. Am. Chem. Soc.*, **1988**, 110, 7927. b) H. E. Moser and P. B. Dervan, *Science*, **1987**, 238, 645.
[7]R. P. Hertzberg and P. B. Dervan, *J. Am. Chem. Soc.*, **1982**, 104, 313.
[8]J. H. Griffin and P. B. Dervan, *J. Am. Chem. Soc.*, **1987**, 109, 6840.
[9]L. A. Basile and J. K. Barton, *J. Am. Chem. Soc.*, **1987**, 109, 7548.

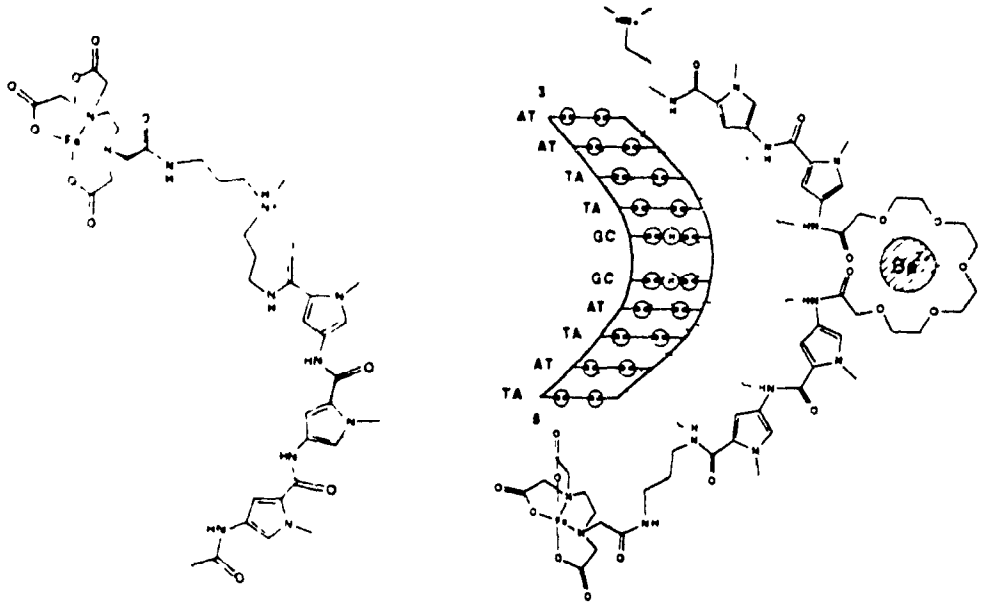

Figure 1.7. A) EDTA-distamycin-Fe(II) (ref 7), **B)** Bis(netropsin)-3,6,9,12,15-pentaoxaheptanediamide-EDTA-Fe(II) Molecule displays nuclease activity in the presence of Ba^{2+} or Sr^{2+}. (ref 8)

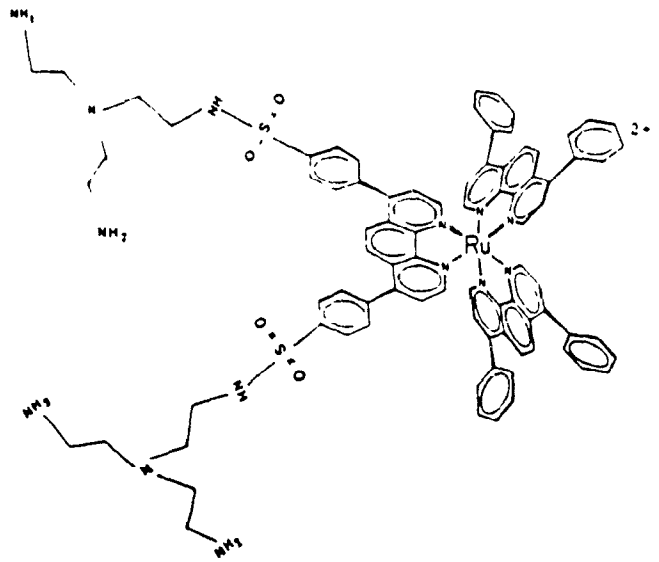

Figure 1.8. $Ru(DIP)_2Macro^{n+}$ Complex Binds to DNA and the polyamine groups bind metal ions for cleavage of DNA (ref 9)

1.2.3 Importance of a Hydrolytic System

In all of the models described thus far, there exists one major drawback. the DNA cleavage is accomplished by an oxidative process that requires an oxidant or reducing agent as coreactant. Unlike real restriction endonucleases, the DNA fragments obtained cannot be pieced back together. The primary products of oxidative cleavage on DNA are free bases and 5-methylene-2-furanone.[10] The products required to religate two pieces of DNA are 5' or 3'-phosphomonoester termini. In other words, "oxidative cleavage is like a small bomb going off next to the DNA."[11] The enzymes that cut DNA, by contrast, catalyze the hydrolysis of the nucleic acid's phosphodiester backbone to produce 3' or 5'-phosphomonoester termini Such a cleavage reaction results in DNA fragments that can be religated by other enzymes.

Some of the oxidative artificial restriction enzymes that have been mentioned have had their applications as footprinting and affinity cleaving agents [2] However, chemists who are designing molecules that site specifically bind DNA want to ultimately incorporate hydrolytic cleavage chemistry into their molecules Such molecules would be, in fact, true artificial restriction enzymes useful in molecular biology applications [11]

Progress has been made in cleaving DNA hydrolytically Hydrolysis of DNA was detected using Barton's Ru(DIP)Macro^{n+} complex with a redox non-active metal ion such as Zn(II).[9,12] However, the reaction is not very efficient especially in comparison to oxidative chemistry Furthermore, the DNA studied was a strained closed circular supercoiled double stranded plasmid. Hydrolysis has yet to be reported for this system using linear DNA.

Sequence selective hydrolysis of supercoiled DNA was achieved by Schultz's group at Berkeley.[13] Their approach was to design a hybrid nuclease consisting of a short oligonucleotide fused to staphylococcal nuclease.

One of the problems in developing hydrolytic artificial restriction enzymes is the unique stability of the phosphodiester bond in DNA. It has been estimated that the half-life for the hydroxide catalyzed hydrolysis of the phosphodiester bond of DNA at pH 7, 25 °C

---

[10]T. E. Goyne and D S Sigman, *J Am Chem Soc*, **1987**, 109, 2846
[11]R. M. Baum, *Chem Eng News*, **1989**, 67(24), 22.
[12]L. A. Basile, A. L Raphael, and J K Barton, *J Am Chem Soc*, **1987**, 109, 7550
[13]D. R Corey, D Pei, and P G Schultz, *J Am Chem Soc*, **1989**, 111, 8523

is 200 million years.[14] It is suggested that phosphate diesters evolved as part of the make-up of genetic material because of its exceptional stability.[15]

Although there have been great advances in DNA recognition, there is still a need to develop catalysts that can hydrolyze unreactive phosphate diesters with great efficiency. Part of our research is focussed on developing metal complexes that hydrolyze phosphate esters efficiently.

1.3 MECHANISM OF PHOSPHATE ESTER HYDROLYSIS

In order to study the effects of metal complexes on the rate of hydrolysis of phosphate esters, it is necessary to first understand the mechanisms of phosphate ester hydrolysis in the absence of metal complexes.

Compared to carboxylate ester reactions, phosphate ester hydrolyses have proven more difficult and less attractive to study for a number of reasons, despite their considerable biological importance. First, the reactions are considerably slower than the reactions of carboxylic esters with comparable leaving groups (table 1.1). Second, the

TABLE 1.1 Rate constants for hydrolysis of carboxylic esters and phosphate esters (P-O bond cleavage) at pH 7.0, 25°C #

ESTER	k (s^{-1})	Relative rate	Ref.
$(CH_3O)_3PO$	1.6×10^{-11} **	2.4×10^{7}	a
$(CH_3O)_2PO_2^-$	6.8×10^{-19} **	1	a
$(CH_3O)HPO_3^-$	2.6×10^{-10} *	3.8×10^{8}	a
CH_3COOCH_3	1.5×10^{-8} **	2.2×10^{10}	b

\# Values are measured rate constants, or obtained by extrapolation from data at higher temperatures

** Hydroxide rate constant extrapolated to pH 7.0

* Metaphosphate mechanism is predominant at pH 7.0

a) J. P. Guthrie, *J. Am. Chem. Soc.*, **1977**, 99,3991

b) J. P. Guthrie, *J. Am. Chem. Soc.*, **1973**, 95,6999

---

[14] J. Chin, M. Banaszczyk, V. Jubian, and X. Zou, *J. Am. Chem. Soc.*, **1989**, 111, 186.

[15] F. H. Westheimer, *Science*, **1987**, 235, 1173

mechanisms of phosphate ester hydrolysis can be very complex since there are frequently three competitive paths:[16,17] (fig. 1.9) i) Attack at phosphorus to expand its coordination number from four to five. This intermediate is usually trigonal bipyramidal that decomposes to yield the products. ii) Unimolecular cleavage to give a metaphosphate intermediate In this pathway, the coordination number of phosphorus decreases from four to three to produce the metaphosphate which then adds a nucleophile to yield the products. iii) Attack at carbon to give products of nucleophilic substitution. It is necessary to sort out these possibilities carefully to assign mechanistic significance to rate constants.

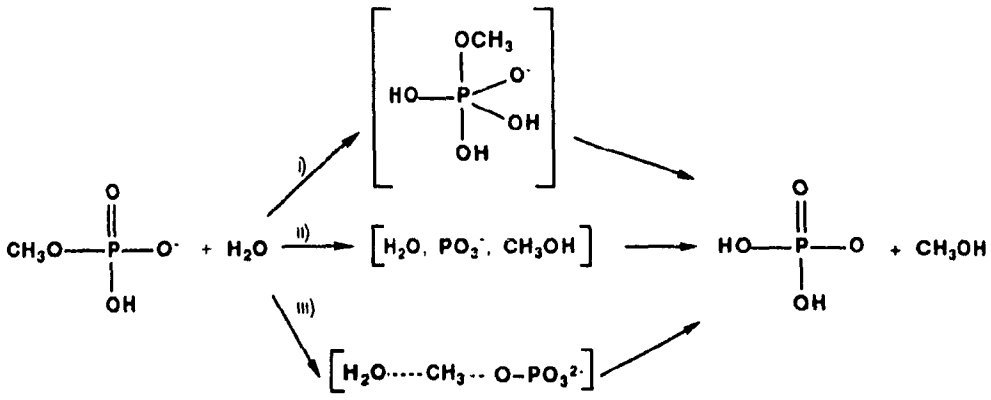

Figure 1.9. Possible paths for phosphate ester hydrolysis (ref 16)

1.3.1 Phosphate Monoesters

The mechanism of phosphate monoester hydrolysis is very complex. All three possible mechanistic pathways can be operative depending on the pH. The complexity can be illustrated by the different shapes of the pH-rate profiles for different phosphate monoesters of varying leaving group basicity (fig. 1.10).[18]

In general, there are two distinct types of pH-rate profiles observed for phosphate monoesters. One has a rate maximum near pH 4 as exemplified by p-nitrophenyl

[16] J. P. Guthrie, *Acc Chem Res*, **1983**, 16, 122
[17] F. H. Westheimer, *Chem Rev*, **1981**, 81, 313.
[18] A. J Kirby and A G Varvoglis, *J Am Chem Soc*, **1967**, 89, 415.

phosphate[19] and monoalkyl phosphates.[20] The second type of curve displays a higher rate for the hydrolysis of the dianion than that for the monoanion. This type is obtained for aryl esters of which the pKa of the conjugate acid of the leaving phenol is less than about 5.45. The pH-rate profile for 2,4-dinitrophenyl phosphate is one example of this type of curve.[21] A special case is for 2-chloro-4-nitrophenyl phosphate (pKa of phenol = 5.45) where the hydrolysis is virtually pH independent. The monoanion and the dianion are hydrolyzed at almost identical rates.[18]

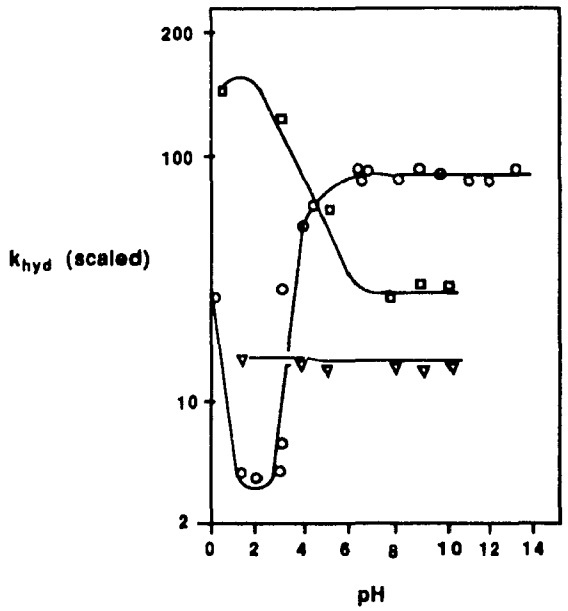

Figure 1.10. pH rate profiles for three phosphate monoesters at 39°C, on adjusted scales: □ , k_{hyd} x 10^7 min^{-1} for 2,4,6-trichlorophenyl phosphate, ▽, k_{hyd} x 10^6 min^{-1} for 2-chloro-4-nitrophenyl phosphate; ○ , k_{hyd} x 10^4 min^{-1} for 2,4,-dinitrophenyl phosphate. (ref 18)

For the hydrolysis of monomethyl phosphate, all three possible mechanisms are operative depending on the pH. The pH-rate profile is shown in figure 1.11. The rate is at a maximum at pH 4 and falls to lower values at more acidic or alkaline pH. In strong acid solution the rate of hydrolysis again rises. This phenomenon is due to the facile reaction of the monoanion which is the predominant ionic species in solutions of most phosphate

---

[19]P. W C Barnard, C A Bunton, D. Kellerman, M M Mhala, B. Silver, C A. Vernon, and V. A. Welch, *J Chem Soc Sect B* , **1966**, 227

[20]C A. Bunton, D R. Llewellyn, K. G. Oldham, and C. A. Vernon, *J Chem Soc* , **1958**, 3574.

[21]C. A. Bunton and S. J Farber, *J Org Chem.*, **1969**, 34, 767.

esters between pH 2 and 6. Isotope labelling experiments reveal that hydrolysis of the monoanion proceeds with P-O bond fission.[20]

The rapid hydrolysis of the monoanion is due to the formation of an unstable monomeric metaphosphate ion intermediate **IV** (fig. 1.12) which reacts rapidly with water to give inorganic phosphate. Proton transfer occurs to convert the alkoxide group, OR, to an energetically more favourable leaving group. At the same time, transfer of the proton to the leaving group leaves the phosphate moiety of the molecule with two negative charges which provides a driving force for expulsion of the leaving group (fig. 1.12). Proton transfer can occur in three different ways: i) a pre-equilibrium transfer to give the zwitterion (I); ii) a concerted proton transfer via a four membered ring which accompanies the P-O bond scission (II); and iii) proton transfer is carried out through a six membered ring formed by the participation of a molecule of water (III). It is the metaphosphate mechanism which makes the monoanion of a phosphate monoester more reactive towards hydrolysis than the monoanion of the corresponding phosphate diester.

At pH less than one, both C-O and P-O bond cleavages occur. The mechanism involves an S_N2 nucleophilic attack by water on either the phosphorus or carbon atom of the conjugate acid of the phosphate ester.

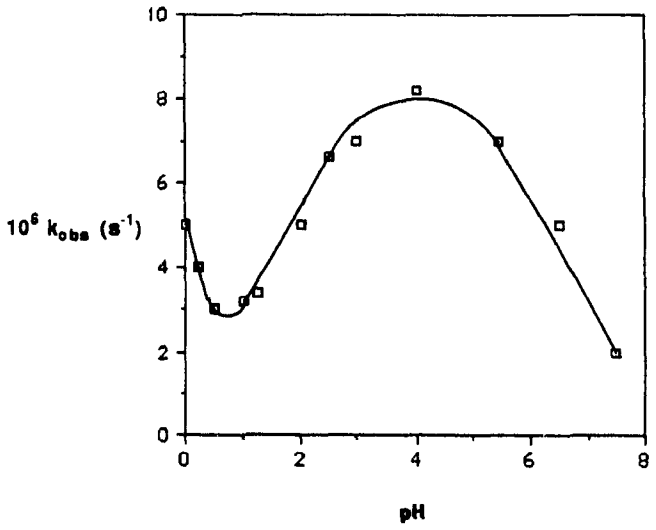

Figure 1.11. Hydrolysis of monomethyl phosphate at 100°C (ref. 20)

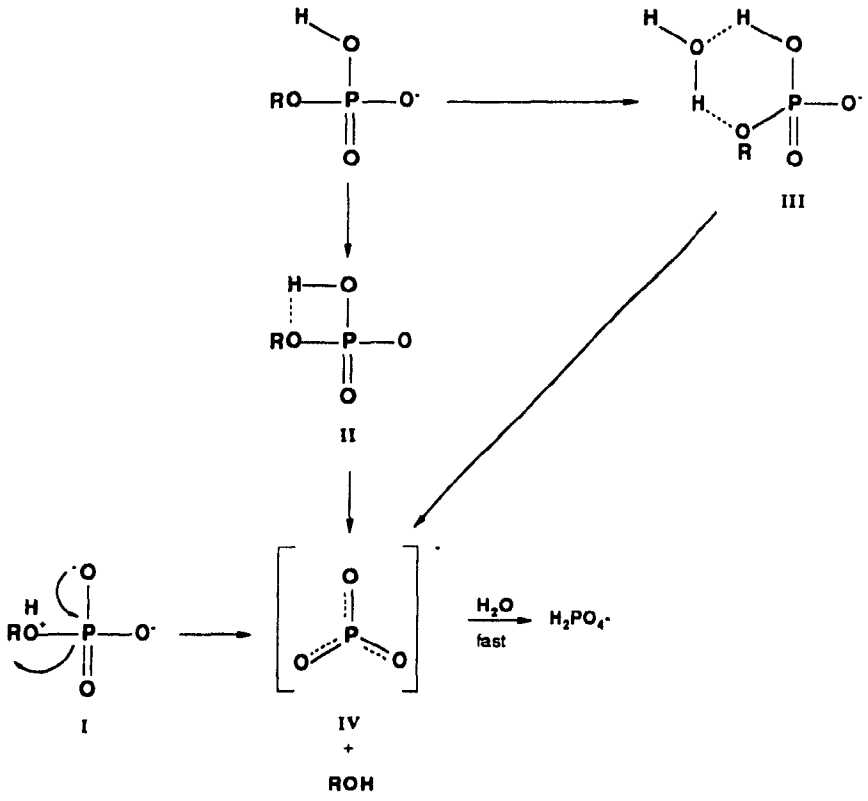

Figure 1.12 Metaphosphate mechanism for the hydrolysis of phosphate monoesters

1.3.2 Phosphate Diesters

Hydrolysis of a phosphate diester differs significantly from that of phosphate monoesters (fig. 1.13).[21] Unlike phosphate monoesters, no rate maximum is evident in the pH-rate profile for phosphate diesters. For BDNPP (fig. 1.13) there is a pH-independent rate between pH 2 and 6, however, for less reactive phosphate diesters, the hydronium and hydroxide catalyzed reactions account for the observed rates over almost the entire pH range.[22]

Since the pKa of a disubstituted hydrogen phosphate lies between one and two, the species present under most physiological conditions is the anion. Because of unfavourable electrostatic interactions, the anion of phosphate diesters resists attack by anionic nucleophiles, such as hydroxide, thereby making phosphate diesters hydrolytically very unreactive. It is the stability of the anion of the diester that makes the study of phosphate

[22]A. J. Kirby and M. Younas, *J Chem Soc Sect B.*, **1970**, 510.

diester hydrolysis very difficult. The hydrolysis of the anion of dimethyl phosphate is very slow.

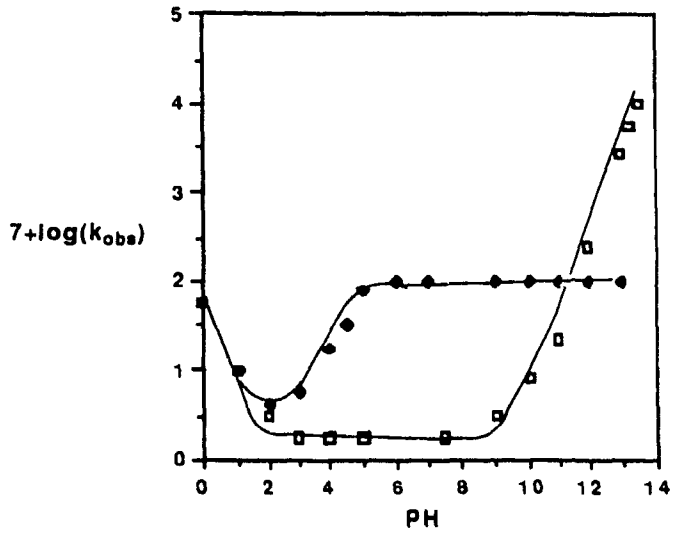

Figure 1.13. Hydrolysis of bis-2,4-dinitrophenyl phosphate □ and 2,4-dinitrophenyl phosphate ◇ (ref 21)

It is estimated that the monoanion of dimethyl phosphate undergoes hydrolysis 10^8 times slower than the monoanion of methyl phosphate.[23] Because of the slow rate of hydrolysis of simple dialkyl phosphates, and the rather good correlation between leaving group basicity and reactivity,[21] attention has focussed on hydrolysis of phosphate diesters with fairly acidic phenols which hydrolyze at measurable rates in aqueous solution

The mechanism of hydrolysis for the anion of phosphate diesters (P-O bond fission) proceeds through a nucleophilic displacement process as shown in figure 1.14.

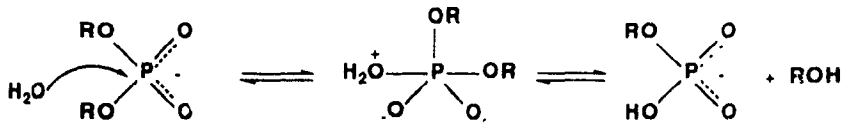

Figure 1.14. Mechanism of phosphate diester hydrolysis

[23] See table 1.1 (page 8)

Although the anions of simple dialkyl phosphates have very low reactivity, five membered cyclic phosphate esters are known to be hydrolyzed at greatly enhanced rates.[24] For example, compared to dimethyl phosphate, ethylene phosphate is far more reactive. The rate factor in favour of the cyclic phosphate, for P-O bond cleavage, is approximately 10^8. This high reactivity is attributed to release of ring strain upon hydrolysis. Compounds with neighbouring functional groups such as hydroxy and carboxy are also known to be hydrolyzed at greatly increased rates.[24]

1.3.3 Phosphate Triesters

Phosphate triesters are not prominent naturally occurring substances, however, the hydrolysis of phosphate triesters has received considerable interest due to the importance in detoxification of acetylcholinesterase inhibiting insecticides and chemical warfare agents Unlike phosphate diesters, phosphate triesters are neutral. Therefore, unfavourable electrostatic interactions do not occur between an anionic nucleophile and the triester. As a consequence, rapid hydrolysis is observed in alkaline solution. It has been shown that alkaline hydrolysis of trimethyl phosphate and triphenyl phosphate proceeds with P-O bond scission at pH greater than ten and C-O bond cleavage predominates at pH less than ten.[25,26]

1.4 METAL CATALYZED HYDROLYSIS OF PHOSPHATE ESTERS

In order to design an efficient metal catalyst that can efficiently hydrolyze phosphate esters, or for that matter, carboxylic esters and amides in general, it is important to examine the possible mechanistic pathways available for the metal ion or metal complex in hydrolyzing its substrate.

Many hydrolytic enzyme reactions are directly metal ion dependent. The addition of chelating agents to some metalloenzymes leads to a loss of activity but it is regained if further metal ion is added. The importance of metal ions on enzyme catalyzed reactions has

---

[24]For a review see T C Bruice and S J Benkovic, 'Bioorganic Mechanisms', W A Benjamin Inc., New York, 1966, vol 2, Chap. 5

[25]P. W. C. Barnard, C A Bunton, D R. Llewellyn, C A. Vernon, and V A. Welch., *J Chem Soc.*, **1961**, 1636.

[26]J. P. Guthrie, *J Am Chem Soc* , **1977**, 99, 3991.

lead to numerous studies employing transition metal complexes for ester and amide promoted hydrolysis.[27]

1.4.1 Mechanisms of Metal Catalysis

In general, there are two mechanisms for metal ion or metal complex promoted hydrolysis reactions: i) Lewis acid mechanism and ii) metal-hydroxide mechanism

In the Lewis acid mechanism, the metal ion or metal complex coordinates to the substrate and activates it towards nucleophilic attack This type of mechanism can be illustrated in the metal(II) ion catalyzed hydrolysis of amino acid esters.[28] The esters are chelated to the metal by the amino and carbonyl group. Metal coordination of the carbonyl polarizes the C-O bond and enhances its susceptibility towards nucleophilic attack by hydroxide ion (fig. 1.15). Metal ions like Cu^{2+}, Co^{2+}, and Mn^{2+}, were found to promote the hydrolysis of ethylglycinate in the pH range 7 3 to 7 9 at 25 °C, under which conditions the free ester is ordinarily stable The rate of hydrolysis increased with increasing tendency of the metal ion to coordinate with the ester. Rate enhancements up to 10^6 were observed with Cu^{2+} ion.

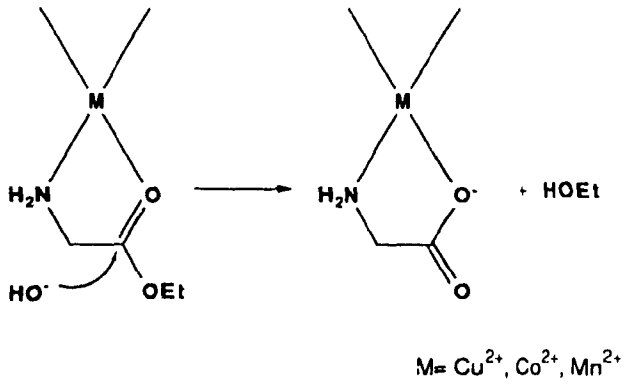

Figure 1.15 Lewis acid mechanism proposed for metal(II) ion catalyzed hydrolysis of ethylglycinate.

In the metal-hydroxide mechanism, a coordinated hydroxide anion can act as a reactive nucleophile towards an appropriate substrate. A classic example of this type of

[27] A. E. Martell, *Metal Ions in Biological Systems*, Vol. 2, Helmut Sigel Ed , Marcel Dekker Inc N Y , **1973**, Ch. 5.
[28] H. Kroll, *J Am Chem Soc* **1955**, 74, 2036

mechanism was the Cu(II) mediated hydrolysis of **1** (fig. 1.16) displayed by Groves and Dias.[29] Because of the rigidity of the molecule, the metal cannot coordinate to the carbonyl oxygen, thus, a Lewis acid mechanism was ruled out. The mechanism proceeded by a nucleophilic addition of metal-bound hydroxide. The metal ion reduces the effective negative charge of the coordinated hydroxide thus making the metal-bound hydroxide a weaker nucleophile than a free hydroxide. However, since the metal is able to lower the pKa of coordinated water,[30] it acts as a buffer for hydroxide around neutral pH. For metal hydroxide mechanisms, the reduced reactivity of the metal-bound hydroxide can be considered more than compensated by the increased effective local concentration of the hydroxide. At pH 7 6 the reaction proceeded 10^6 times faster than calculated for the base catalyzed hydrolysis of **1** at the same pH in absence of any metal ion.

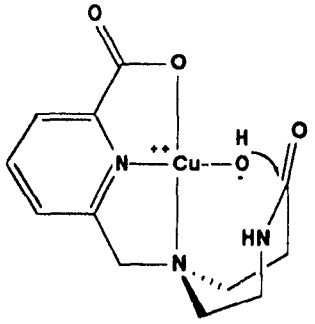

1

Figure 1.16. Metal hydroxide mechanism. (ref. 29)

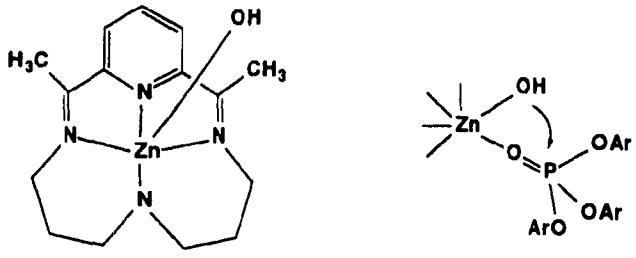

2

Figure 1.17 Bifunctional mechanism proposed for **2** catalyzed hydrolysis of phosphate triesters (ref. 31)

[29] J. T. Groves and R. M Dias, *J Am Chem Soc* , **1979**, 101, 1033.
[30] The pKa of the Cu^{2+} bound water was found to be 7.3.

A third mechanism is also possible, a bifunctional mechanism, where the effects of the Lewis acid and metal-hydroxide mechanisms are combined into one. As an example, Breslow and co-workers[31] showed that the zinc complex, **2** (fig 1.17) catalyzed the hydrolysis of a phosphate triester ten times faster than the free hydroxide rate.[32] They reasoned that a simple metal-hydroxide mechanism could not account for this difference, a bifunctional mechanism was taking place making the Zn-OH a better nucleophile than free hydroxide.

1.4.2 Co(III) Complex Hydrolysis of Phosphate Diesters

Numerous reports exist on metal complex catalyzed hydrolysis of phosphate monoesters,[33,34] triesters,[31,35,36] fluorophosphonates,[37] fluorophosphates[37] and phosphoric anhydrides.[38] Remarkably, only a few publications exist on metal complex catalyzed hydrolysis of phosphate diesters. My interest lies in a rational design of metal complexes that hydrolyze phosphate diesters efficiently. Although hydrolysis of phosphate diesters promoted by transition metal complexes are scarce, one can still get a great deal of insight from previous work done on metal complex promoted hydrolysis of phosphorus esters and anhydrides.

Most of the work has focussed on substitutionally inert metal complexes such as Co(III) complexes and to a lesser extent Ir(III) complexes. Attention has centred on inert metal complexes because the use of labile metal complexes seriously complicates reliable identification of the species actually involved in the ester hydrolysis. By using

---

[31] S. H. Gellman, R. Petter, and R. Breslow, *J. Am. Chem. Soc.*, **1986**, 108, 2388.

[32] Based on second-order rate constants.

[33] a) F. J. Farrell, W. A. Kjellstrom, and T. G. Spiro, *Science*, **1969**, 164, 320. b) J. Harrowfield, D. R. Jones, L. F. Lindoy, and A. M. Sargeson, *J. Am. Chem. Soc.*, **1977**, 99, 2652. c) D. R. Jones, L. F. Lindoy, and A. M. Sargeson, *J. Am. Chem. Soc.*, **1983**, 105, 7327. d) J. Harrowfield, D. R. Jones, L. F. Lindoy, and A. M. Sargeson, *J. Am. Chem. Soc.*, **1980**, 102, 7733.

[34] D. R. Jones, L. F. Lindoy, and A. M. Sargeson, *J. Am. Chem. Soc.*, **1984**, 106, 7807. b) R. A. Kenley, R. H. Fleming, R. M. Laine, D. S. Tse, and J. S. Winterle, *Inorg. Chem.*, **1984**, 23, 1870. c) P. R. Norman, and R. D. Cornelius, *J. Am. Chem. Soc.*, **1982**, 104, 2356.

[35] a) P. Hendry and A. M. Sargeson, *Aust. J. Chem.*, **1986**, 39, 1177. b) P. Hendry and A. M. Sargeson, *J. Chem. Soc. Chem. Commun.*, **1984**, 164.

[36] a) J. R. Morrow and W. C. Trogler, *Inorg. Chem.*, **1989**, 28, 2330. b) F. M. Menger, L. H. Gan, E. Johnson, and D. H. Durst, *J. Am. Chem. Soc.*, **1987**, 109, 2800.

[37] T. Wagner-Jauregg, B. E. Hackley Jr., T. A. Lies, O. O. Owens, and R. Proper, *J. Am. Chem. Soc.*, **1955**, 77, 922. b) J. Epstein, and D. H. Rosenblatt, *J. Am. Chem. Soc.*, **1958**, 80, 3596. c) R. C. Courtney, R. L. Gustafson, S. J. Westerback, H. Hyytiainen, S. C. Chabarek Jr., and A. E. Martell, *J. Am. Chem. Soc.*, **1957**, 79, 3030.

[38] a) R. M. Milburn, M. Gautem-Basak, R. Tribolet, and H. Siegel, *J. Am. Chem. Soc.*, **1985**, 107, 3315. b) R. M. Milburn, G. Rawji, and M. Hediger, *Inorg. Chim. Acta*, **1983**, 79, 247. c) R. M. Milburn, S. S. Massoud, and F. Tafesse, *Inorg. Chem.*, **1985**, 24, 2593. d) R. M. Milburn, and F. Tafesse, *Inorg. Chim. Acta*, **1987**, 135, 119.

substitutionally inert metals, characterization of all species present in solution is possible. Also, the kinetics and mechanism of Co(III) and Ir(III) complex substitution reactions are well understood[39] and this knowledge should facilitate identifying mechanisms involved in metal-complex promoted phosphate ester hydrolysis In order to gain useful mechanistic information, the approach has been to synthesize and study the reactions of well characterized substitutionally inert metal ion phosphate complexes. This would allow unambiguous conclusions to be made about the reactivity of a particular type of complex.

Hendry and Sargeson[35], showed that metal complexes acting solely by a Lewis acid mechanism are very inefficient at promoting the hydrolysis of phosphate triesters The hydrolysis of trimethyl phosphate (TMP) coordinated to penta-ammine Iridium(III) ion was studied in an alkaline medium. The study revealed that coordination of the phosphate ester to the metal complex increased the rate of attack of hydroxide at the phosphorus atom by only four hundred fold. For the analogous Co(III) complex, the products of base hydrolysis were found to be trimethyl phosphate and the $[(NH_3)_5Co(OH)]^{2+}$ ion; the rate of loss of the TMP ligand was faster than the rate of attack of hydroxide [40]

The efficiency of the bifunctional mechanism was tested on phosphate monoesters It was demonstrated that the hydroxide[33c] and amido (NH_2^-)[33d] ions bound to Co(III) were efficient intramolecular nucleophiles for cleaving 4-nitrophenol from the coordinated 4-nitrophenol phosphate (fig. 1.18) The mechanism of an intramolecular metal-bound nucleophilic attack was elucidated by elegant isotope labelling experiments. Rate enhancements of 10^5 (for the metal hydroxide) and 10^8 (for the metal amido) relative to the uncoordinated ester were obtained for these complexes.

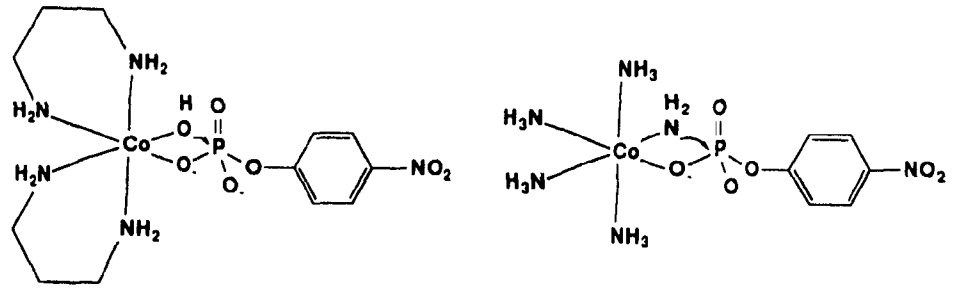

Figure 1.18. Intramolecular metal-hydroxide and metal-amido attack on coordinated phosphate monoester. (ref 33c, 33d)

[39]a)F. A. Cotton, and G Wilkinson, *Advanced Inorganic Chemistry*, 4th ed , Wiley-Interscience. New York 1980 b) F Basolo, and R. G Pearson, *Mechanisms of Inorganic Reactions*, 2nd ed , Wiley: New York 1967.

[40]a) W Schmidt and H. Taube, *Inorg Chem* , **1963**, 2, 698 b) N. E. Dixon, W G. Jackson, W Marty, and A M. Sargeson, *Inorg Chem* , **1982**, 21, 688.

It is not surprising that the metal-amido complex displayed a greater rate enhancement than that for the metal-hydroxide complex. The metal-amide is much more basic than the metal-hydroxide. The pKa of the metal-aqua complex was found to be 7.6 whereas the pKa of the metal-ammine complex was estimated to be near 1[41]. If one assumes a direct relationship between nucleophilic strength and basicity for these type of reactions, then the difference in reactivity is presumably due to the much greater nucleophilic character of the metal-amide. However, the unique attribute of the metal-aqua complex is its ability to generate a high concentration of the reactive nucleophile (M-OH) at the physiological pH range. The metal-amido complex can only be generated in very high alkaline solutions. At neutral pH, the metal-ammine complex predominates and is inactive at hydrolyzing the ester.

We have seen that the bifunctional mechanism is by far the most efficient mechanism for hydrolyzing phosphate monoesters. For this mechanism to be operative, one requires a complex in which two coordination sites, cis to each other, are available for phosphate chelation. One site would bind to the phosphoryl oxygen and the other would deliver the intramolecular metal-bound hydroxide nucleophile. Cis-aquohydroxotetraazacobalt(III) complexes, $[(N_4)Co(III)(OH)(OH_2)]^{2+}$, fit this criterion. The N_4 represents a bis bidentate or a tetradentate ligand. In the past few years, several groups have studied the effects of these type of complexes on phosphate diester hydrolysis.[14,34b,38b,41,42]

We have recently reported the largest rate enhancement for metal promoted hydrolysis of a phosphate diester.[14] BNPP when bound to $[Co(trpn)(OH)(OH_2)]^{2+}$ is hydrolyzed 10^{10} times more rapidly than the free phosphate diester. The rate of phosphate diester hydrolysis can vary significantly depending on the N_4 ligand. Milburn et al.[38b] observed that $[Co(tn)_2(OH)(OH_2)]^{2+}$ reacted 25 times slower than $[Co(trpn)(OH)(OH_2)]^{2+}$ at hydrolyzing BDNPP. No mechanistic interpretation was given to account for this difference.

In our lab, Chin and Zou[41] reported the effects of four Co(III) complexes on the rate of hydrolysis of BNPP and BDNPP. Not surprisingly, the $[(N_4)Co(OH)(OH_2)]^{2+}$ complexes were the most efficient at hydrolyzing the phosphate diester, BNPP. However, the reactivity pattern changed when hydrolyzing the more reactive phosphate diester, BDNPP (Table 1.2). The difference in the reactivity patterns was explained in terms of a change in the rate-determining step with change in the phosphodiester reactivity.

---

[41] J. Chin and X. Zou, *J. Am. Chem. Soc.*, **1988**, 110, 223.

[42] J. Chin, M. Banaszczyk, and V. Jubian, *J. Chem. Soc., Chem. Commun.*, **1988**, 735.

The cobalt complex promoted hydrolysis of BNPP was explained in terms of the mechanism shown in figure 1.19. It was determined that k_2 was the rate-determining step since the rates of anation of $[Co(trien)(OH)(OH_2)]^{2+}$, $[Co(en)_2(OH)(OH_2)]^{2+}$, and

Table 1.2. Observed first-order rate constants (k_{obs}, s^{-1}) for cobalt complex promoted hydrolysis of phosphate esters at 50°C, pH 7.0 (ref. 41)

Cobalt complex	BNPP	BDNPP
$[Co(en)_2(OH)(NH3)]^{2+}$	$<10^{-6}$	2.4×10^{-4}
$[Co(en)_2(OH)(OH_2)]^{2+}$	2.7×10^{-5}	4.2×10^{-4}
$[Co(trien)(OH)(OH_2)^{2+}$	4.8×10^{-4}	5.2×10^{-3}
$[Co(dien)(OH)(OH_2)_2]^{2+}$	$<10^{-6}$	8.6×10^{-2}
none	3×10^{-10}	2.1×10^{-6}

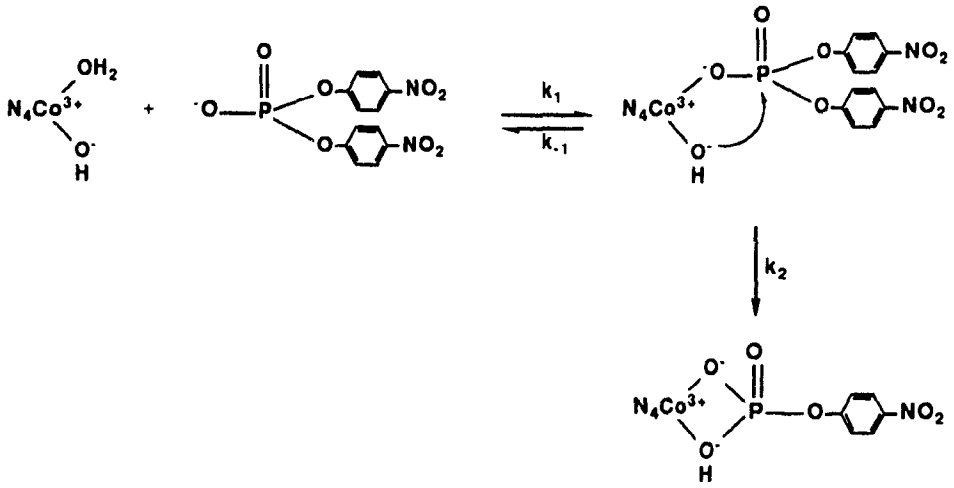

Figure 1.19. Co(III) complex promoted hydrolysis of BNPP (ref. 41)

$[Co(dien)(OH)(OH_2)_2]^{2+}$ were greater than the rates of the cobalt complex promoted hydrolysis of BNPP. It is well known that the rate of ligand exchange on Co(III)

complexes is sensitive to the ligand structure[39b] but what accounts for the difference in the rate for phosphate ester hydrolysis when anation is not rate determining? In this particular study, it was difficult to evaluate any structure-reactivity relationship on the phosphorus-oxygen cleavage step because both $[Co(trien)(OH)(OH_2)]^{2+}$ and $[Co(en)_2(OH)(OH_2)]^{2+}$ complexes undergo rapid cis-trans equilibration with the trans forms being inactive

In order to minimize the complications arising from cis-trans isomerizations, we studied and compared the reactivities of three rigidly held cis-aquohydroxytetraazacobalt(III) complexes,[14,42] $[(cyclen)Co(OH)(OH_2)]^{2+}$, $[(trpn)Co(OH)(OH_2)]^{2+}$, and $[(tren)Co(OH)(OH_2)]^{2+}$ (fig 1.20), in promoting the hydrolysis of BNPP. All three complexes are ideal for studying the structure-reactivity relationship since they exist only in the active cis form. The $[(cyclen)Co(OH)(OH_2)]^{2+}$ complex exists only in the cis form because of the small ring size of the cyclen ligand [43] The complexes $[(tren)Co(OH)(OH_2)]^{2+}$ and $[(trpn)Co(OH)(OH_2)]^{2+}$ exist only in the cis form for obvious structural requirements.

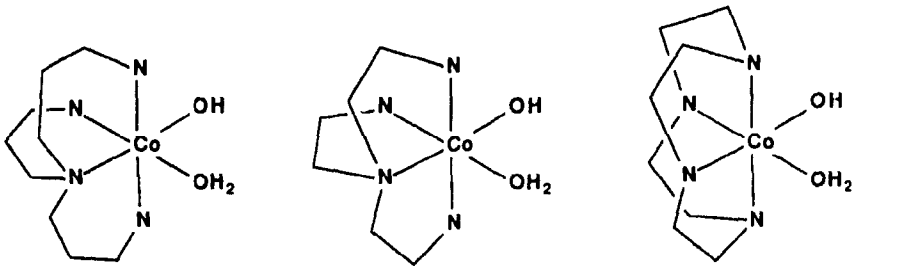

Figure 1.20 Structures of rigidly held cis-aquohydroxotetraazacobalt(III) complexes

The mechanism for the Co(III) complex promoted hydrolysis of BNPP is identical to the one shown in figure 1.19 which involves rapid coordination of the phosphate ester followed by rate-determining intramolecular metal-hydroxide attack All Co(III) complexes are in the cis form yet there are significant differences in hydrolyzing the phosphate diester For example, $[(trpn)Co(OH)(OH_2)]^{2+}$ is 300 times more reactive than $[(tren)(OH)(OH_2)]^{2+}$ for hydrolyzing BNPP. The equilibrium constant for binding of phosphate diesters to the Co(III) complexes and the basicities of the respective metal

[43] Y. Iitaka, M. Shina, and E. Kimura, *Inorg Chem*, **1974**, 13, 2886

hydroxides are comparable. The difference in reactivity is due to the different rates of the k_2 step, thus, the rate-determining step is highly sensitive to the tetraamine ligand (N_4) structure.

The result is striking in view that the two cobalt complexes are so closely related structurally. The k_2 step involves formation of a four-membered ring. In general four-membered rings are unstable, however, four-membered rings involving Co(III) can be very stable. For example, X-ray structures of four-membered Co(III) carbonato[44] and Co(III) phosphato[45] complexes are known. X-ray structures of $[(trpn)Co(CO_3)]^+$ and $[(tren)Co(CO_3)]^+$ reveal that the trpn ligand is better able to stabilize four-membered rings. Both O-Co-O bond angles in $[(trpn)Co(CO_3)]^+$ (68°) and $[(tren)Co(CO_3)]^+$ (68°) are highly distorted from that found in regular octahedral complexes (90°). All the N-Co-N bond angles are rigidly held (87°) with the tren ligand whereas the N-Co-N bond angle opposite the O-Co-O bond angle in $[(trpn)Co(CO_3)]^+$ is free to expand to 100°. It appears that a major factor in stabilizing the four-membered Co(III) complexes is increasing the bond angle opposite the four-membered ring.

It is the ability of $[(trpn)(Co)(OH)(OH_2)]^{2+}$ to stabilize four-membered rings that makes it such a very efficient complex for promoting phosphate ester hydrolysis. Additional evidence comes from the observation that sodium acetate readily forms the four-membered ring acetato complex with $[(trpn)Co(OH)(OH_2]^{2+}$ but not with the corresponding tren complex.[46] The $[(tren)Co(OH)(OH_2)]^{2+}$ complex binds with acetate only by a monodentate fashion. For $[(tren)Co(OH)(OH_2)]^{2+}$, a larger strain is developed in the chelation step (k_2 in fig. 1.19) and hence a slower rate for phosphate diester hydrolysis is observed.

1.4.3 Co(III) Complex Promoted Hydrolysis of Phosphate Monoesters

Hydroxide coordinated to Co(III) were efficient intramolecular nucleophiles for hydrolyzing coordinated phosphate monoesters with good leaving groups. Our success in determining the structural requirements of simple $[(N_4)Co(CH)(OH_2)]^{2+}$ complexes for phosphate diester hydrolysis led Chin and Banaszczyk to investigate Co(III) complex promoted hydrolysis of phosphate monoesters with poor leaving groups[47]. The complexes

[44]E.C Niederhoffer, A E Martell, P Rudolf, and A Clearfield, *Inorg Chem*, **1982**, 21, 3734.
[45]B Anderson, R M. Milburn, and A. M Sargeson, *J Am Chem Soc*, **1977**, 99, 2654
[46]J Chin, and M Banaszczyk, *J Am Chem Soc*, **1989**, 111, 2724
[47]J Chin and M Banaszczyk, *J Am Chem Soc*, **1989**, 111, 4103.

$[(trpn)Co(OH)(OH_2)]^{2+}$ and $[(tren)Co(OH)(OH_2)]^{2+}$ were used to promote the hydrolysis of AMP and methyl phosphate.

The mechanism of Co(III) complex promoted hydrolysis of phosphate monoesters with poor leaving groups can be very different compared to hydrolysis of phosphate monoesters with good leaving groups. The mechanism of Co(III) complex promoted hydrolysis of p-nitrophenyl phosphate involves intramolecular metal-hydroxide attack on the metal coordinated phosphate monoester. Addition of one equivalent of $[(trpn)Co(OH)(OH_2)]^{2+}$ to p-nitrophenyl phosphate, at neutral pH, rapidly produces p-nitrophenol. In contrast, Phosphate monoesters with poor leaving groups initially form stable cobalt complexes **3** (fig. 1.21). Upon addition of a second equivalent of $[(trpn)Co(OH)(OH_2)]^{2+}$, rapid hydrolysis of the phosphomonoester occurs with concomitant formation of a novel binuclear Co(III) complex **4** (fig 1.21). The mechanism of hydrolysis of **3** involves complexation to $[(trpn)Co(OH)(OH_2)]^{2+}$ followed by cleavage of the ester bond as depicted in **5** (fig. 1.22). Co(III) complex promoted hydrolysis of phosphate monoesters with good leaving groups involves a 1:1 complex between the metal and the substrate whereas a 2:1 $[(trpn)Co(OH)(OH_2)]^{2+}$ to substrate ratio is observed for the hydrolysis of phosphate monoesters with poor leaving groups.

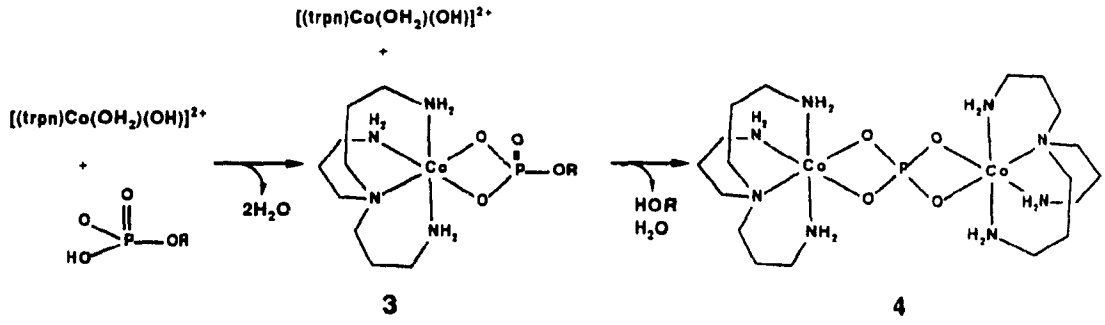

Figure 1.21 $[(trpn)Co(OH)(OH_2)]^{2+}$ promoted hydrolysis of AMP (ref 47)

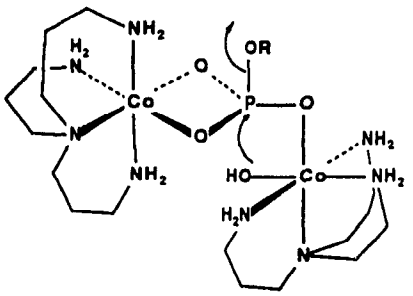

5

Figure 1.22. Mechanism of AMP hydrolysis and concomitant formation of binuclear complex.

Interestingly, $[(tren)Co(OH)(OH_2)]^{2+}$ does not hydrolyze phosphate monoesters with poor leaving groups under the same conditions employed for the trpn complex. Again, it is the ease of formation of a four-membered ring imposed by the structure of the N_4 ligand that enables $[(trpn)Co(OH)(OH_2)]^{2+}$ to hydrolyze phosphate monoesters with poor leaving groups very efficiently.

1.4.4 Cu(II) Complex Catalyzed Hydrolysis of Phosphate Esters

In the past, most studies involving Cu(II) ions were based on hydrolyzing phosphate monoesters covalently attached to a metal chelate. Cu(II) catalyzed hydrolysis of salicyl phosphate[27,48] and 2-(1,10-phenanthroyl) phosphate[49] are two typical examples.

In the case for Cu(II) catalyzed hydrolysis of salicyl phosphate, it was observed that the catalytic effect of the metal ion was greatest (about 10^8 rate enhancement) for the trianion of the salicyl phosphate. The trianionic species does not have the possibility of an intramolecular proton catalysis route as is the case for the mono and dianionic species. The metal ion exerts its catalytic effect by taking the place of a proton. The availability of a metaphosphate elimination process and the stability of the metal chelate structure as final product are the driving forces in the Cu(II) catalyzed reaction (fig. 1.23).

---

[48]Y. Murakami and A. E. Martell, *J Am Chem Soc*, **1964**, 85, 2119.
[49]T. H. Fife and M. P. Mujari, *J Am Chem Soc*, **1988**, 110, 7790.

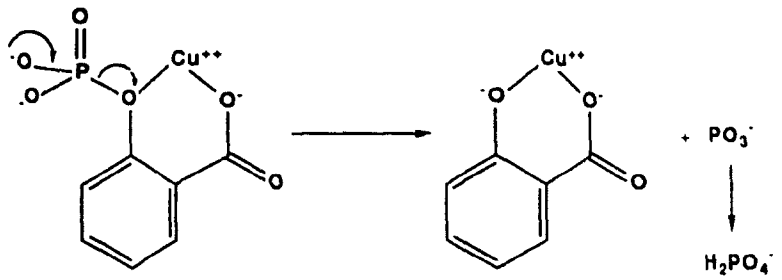

Figure 1.23. Copper(II) ion catalyzed hydrolysis of salicylphosphate. (ref 27)

For the hydrolysis of 2-(1,10-phenanthrolyl) phosphate, it was observed that at pH 8, 85 °C, the Cu(II) catalyzed hydrolysis of the dianionic phosphate ester was 300 times greater than in the absence of any metal ion. A metaphosphate mechanism was not involved since the metal ion could not chelate to the leaving group oxygen of the phosphate ester. The reaction involved nucleophilic attack of H_2O on phosphorus (fig. 1 24).

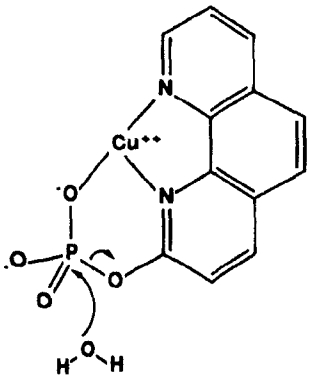

Figure 1.24. Cu(II) ion catalyzed hydrolysis of 2-(1,10-phenanthrolyl) phosphate (ref 49)

Only a few examples exist for Cu(II) complex hydrolysis of phosphate esters in which the ester is not covalently linked to the metal complex. Martell and his co-workers studied the hydrolysis of Sarin (isopropylmethylphosphonofluoridate) and DFP (diisopropylphosphorofluoridate) by a series of Cu(II) complexes.[27,50] As was the case for Co(III) complex promoted hydrolysis of phosphate esters, it was observed that the most catalytically active Cu(II) complexes were those which had two free (aqua) coordination sites. Rate maximums were obtained in the neutral to weakly alkaline pH

[50]R. L. Gustafson, S. Chabarek, and A. E Martell, *J Am Chem Soc*, **1964**, 85, 2119

range where aqua-hydroxy Cu(II) chelates were the predominant species in solution. Highly stable chelates containing terdentate or tetradentate amine ligands showed very little or no catalytic activity. Two kinetically indistinguishable mechanisms were proposed (fig. 1.25). In path A, the metal hydroxide attacks the coordinated substrate. In path B, the substrate is chelated to the metal complex and external hydroxide attacks the phosphorus atom.

More recently, metallomicelles[36b] using Cu(II) ions have been used to accelerate the hydrolysis of phosphate triesters and diesters. Trogler and his co-workers have studied the effect of Cu(bpy) complex catalyzed hydrolysis of phosphate diesters[51] and triesters.[36a] The proposed mechanisms are identical to the bifunctional mechanism proposed for Co(III) complex promoted hydrolysis of phosphate diesters.

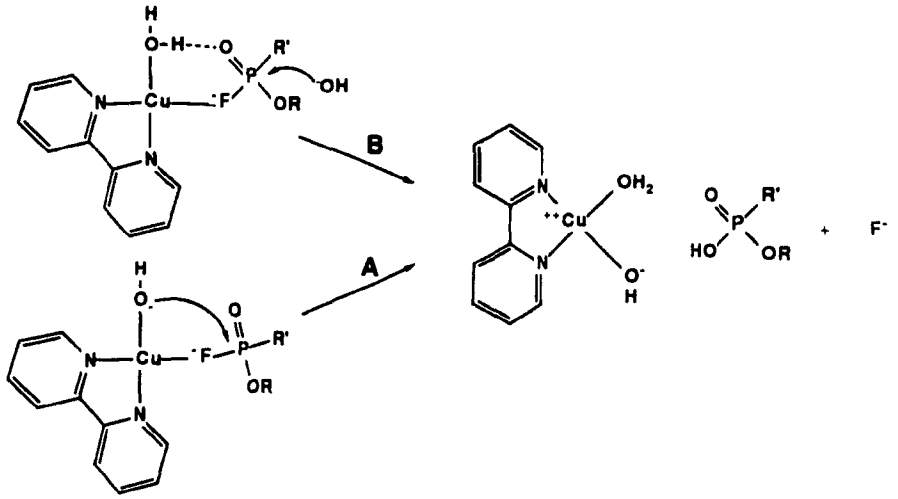

(ref. 27)

Figure 1.25. Proposed mechanisms of Cu(II) catalyzed hydrolysis of phosphofluoridate esters.

[51]a) J. R. Morrow and W. C. Trogler, *Inorg Chem*, **1988**, 27, 3387. b) M. A. De Rosch and W. C. Trogler, *Inorg Chem*, **1990**, 29, 2409

1.5 PLAN OF STUDY

It has recently been shown[14] that cis-aquahydroxytetraazacobalt(III) complexes, $[(N_4)Co(OH)(OH_2)]^{2+}$, are highly efficient at hydrolyzing phosphate esters. Furthermore, the reactivity of these octahedral cobalt complexes is highly sensitive to the tetraamine ligand structure.

My plan is to investigate if this structure-reactivity relationship is applicable to different metal-ligand systems. It is well known that Cu(II) ions are efficient catalysts for hydrolyzing phosphate esters covalently attached to metal chelating units.[27,48,49] We therefore chose to study Cu(II) complexes. No systematic study has been done on determining the structure-reactivity relationship for simple Cu(II) complexes of the type, $[(L)Cu(OH_2)_2]^{2+}$, where L represents a bidentate diamine ligand.

The plan is to prepare and study a series of 1,10-phenanthroline, and 2,2'-dipyridylamine ligands in order to determine whether slight changes in the ligand structure would affect the efficiency of the corresponding Cu(II) complex for promoting the hydrolysis of phosphate esters. A detailed kinetic analysis shall be given to provide a mechanistic rationale to account for the different reactivities for these metal complexes.

2. RESULTS

For all the hydrolyses reactions, 1mM metal complex and 2.5 x 10^{-5} M phosphate ester concentrations were used unless stated otherwise. 0.01 M concentration of buffer was used to maintain a constant pH. For pH 5.5 to 6.5 MES buffer was utilized, pH 7 to 8 N-ethylmorpholine buffer, and for pH 8.5 to 10 CHES buffer was used. Rate constants were obtained under pseudo first-order conditions by monitoring the initial rate of production of 4-nitrophenolate (BNPP hydrolysis) or 2,4-dinitrophenolate (BDNPP and DNPP hydrolysis) at 400 nm (see experimental section for details). Figure 2.1 shows the UV-vis absorbance change during the hydrolysis of BDNPP promoted by $[Cu(dpa)(OH_2)_2]^{2+}$.

All rate constants which are reported in the tables represent the average value of at least three runs with deviations within 5%.

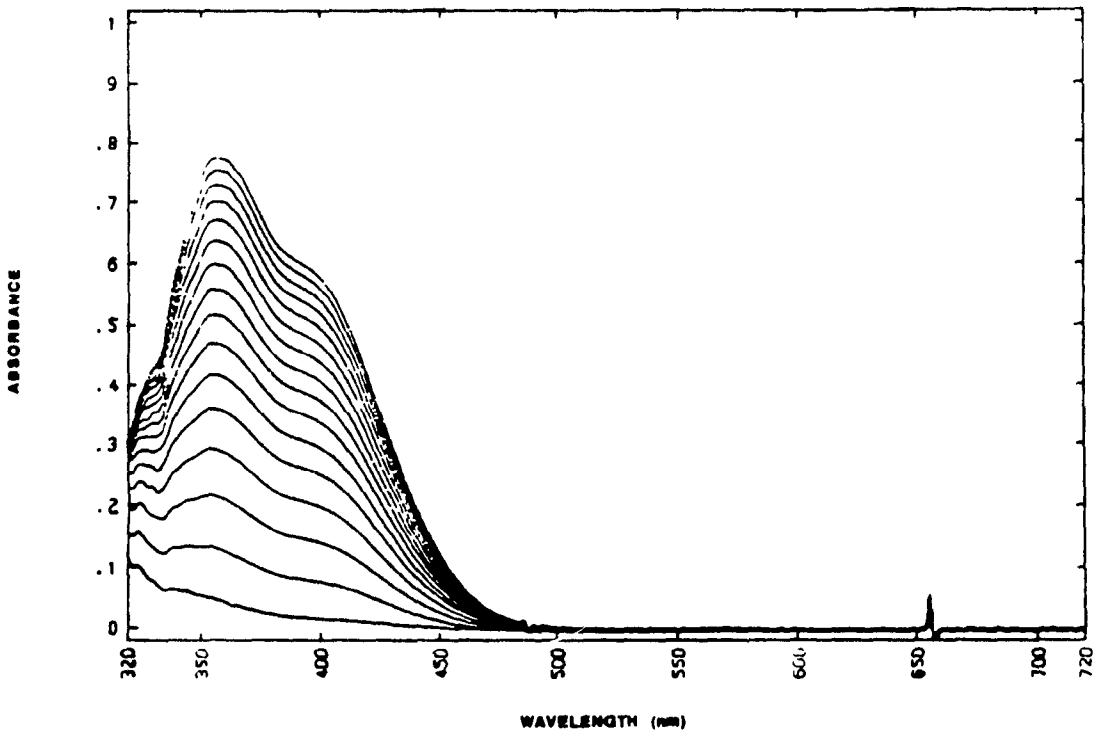

Figure 2.1 UV-vis spectrum for $[Cu(dpa)(OH_2)_2]^{2+}$ (1 mM) promoted hydrolysis of BDNPP (5 x 10^{-5} M) at pH 8, 25 °C

2.1 Acid Dissociation and Dimerization Constants for Cu(II) Complexes

Table 2.1 lists the acid dissociation constants and dimerization constants for the Cu(II) complexes used in this study. Determination of the pKa values are complicated by the dimerization process of these complexes. The pKa and K_{dim} (dimerization constant) values are determined by potentiometric titrations at various Cu(II) complex concentrations.

Table 2.1 Acid Dissociation constants and dimerization constants for Cu(II) complexes used in this study

Cu(II) complex	pKa	K_{dim} (M^{-1})
$[Cu(terpy)(OH_2)]^{2+}$	8 0	-
$[Cu(phen)(OH_2)_2]^{2+}$	7 8 *	2 54 x 10^4 *
$[Cu(neo)(OH_2)_2]^{2+}$	7 0	-
$[Cu(5\text{-}NO_2neo)(OH_2)_2]^{2+}$	6 7	-
$[Cu(dpa)(OH_2)_2]^{2+}$	7 2	2 3 x 10^2
$[Cu(NMedpa)(OH_2)_2]^{2+}$	7 2	1 7 x 10^2
$[Cu(5,5'\text{-dimethyldpa})(OH_2)_2]^{2+}$	7 3	1 3 x 10^2
$[Cu(dpm)(OH_2)_2]^{2+}$	7 25	1 15 x 10^2

*Gustafson and Martell (ref 59) report pKa = 7 8 and K_{dim} = 1 x 10^5 M^{-1} for this complex

The dependence of the midpoint of the titraion curves on the total Cu(II) complex concentration present in solution is given in equation 3.15 (see discussion),

$$pH_{mid} = pKa + \log 2 - \log\left(1 + \sqrt{1 + 4K_{dim}C_T}\right) \qquad (3\ 15)$$

where pH_{mid} is the midpoint of the titration curve at a given Cu(II) complex concentration, C_T, and K_{dim} is the dimerization constant of the Cu(II) complex. Figure 2.2 shows representative titration curves at various concentrations of $[Cu(dpa)(OH_2)_2]^{2+}$ The second

acid dissociation constants for $[Cu(L)(OH_2)_2]^{2+}$, where L represents a bidentate diamine ligand, occur at pH>10. These values are not attainable by direct pH titrations. At pH>10 the copper complexes decompose to give a precipitate of $Cu(OH)_2$.

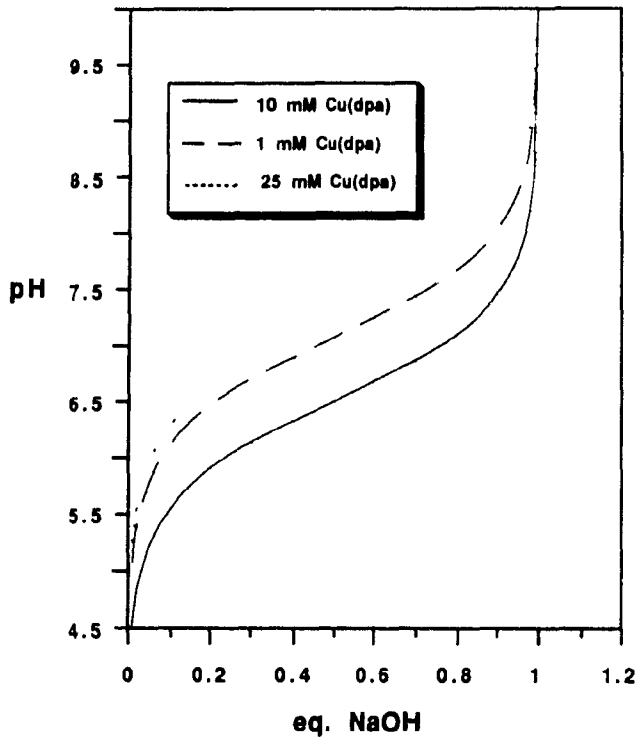

Figure 2.2 Representative titration curves for $[Cu(dpa)(OH_2)_2]^{2+}$ at various concentrations

Figure 2.3 shows the dependence of pH_{mid} on C_T for $[Cu(phen)(OH_2)_2)]^{2+}$ and $[Cu(dpa)(OH_2)_2]^{2+}$. The experimental points were fit according to equation 3.15 using a non-linear least square curve fitting program.†

† *Kaleidograph*, version 2.0.2, developed by Abelbeck software.

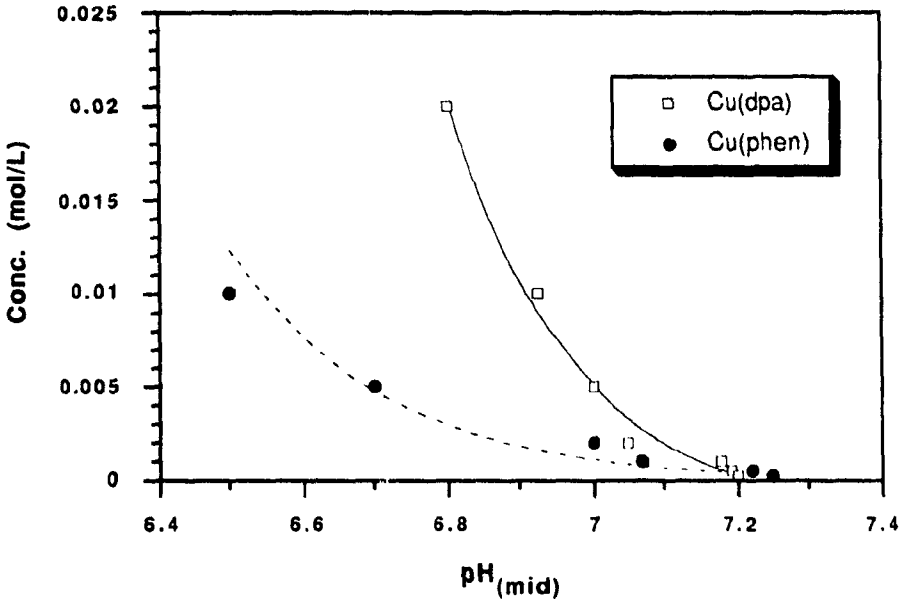

Figure 2.3 Relationship between pH_{mid} and the total Cu(II) complex concentration used

2.2 METAL(II) COMPLEX PROMOTED HYDROLYSIS OF BDNPP

2.2.1 pH-rate profiles

The pH-rate profiles for M(II) complex promoted hydrolysis of BDNPP are shown in figures 2.4 to 2.6. The data were fit according to equation 3.7,

$$k_{obs} = \left[\frac{k_1 \cdot [H^+] + k_2 \cdot Ka}{[H^+] + Ka} \right] \qquad (3.7)$$

where Ka is the acid dissociation constant for the coordinated water molecule, and. k_1 and k_2 are the first-order rate constants for BDNPP hydrolysis promoted by the diaqua and the hydroxy-aqua species, respectively. The constants obtained from the fitted curve are listed underneath the appropriate pH-rate plot. The data for the pH-rate plots are listed in tables 2.2, 2.3 and 2.4.

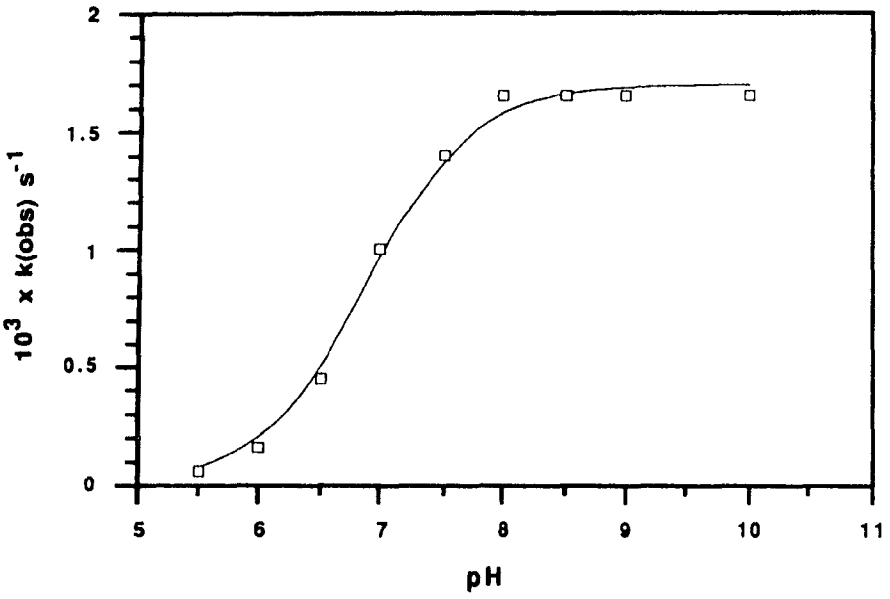

Figure 2.4 pH-rate profile for the hydrolysis of BDNPP by **Cu(dpa)** (1mM, 25 °C) Ka = 1.31 x 10^{-7}, k_1' = 1.23 x 10^{-5} s^{-1}, k_2' =1 65 x 10^{-3} s^{-1}.

Table 2.2 Observed first-order rate constants for $[Cu(dpa)(OH_2)_2]^{2+}$ (1 mM) promoted hydrolysis of BDNPP (2.5 x 10^{-5} M) at 25 °C.

pH	10^3 x k_{obs} (s^{-1})
5.5	061
6.0	.16
6.5	.45
7 0	1.0
7 5	1.4
8 0	1 65
8.5	1.65
9.0	1 65
10 0	1 65

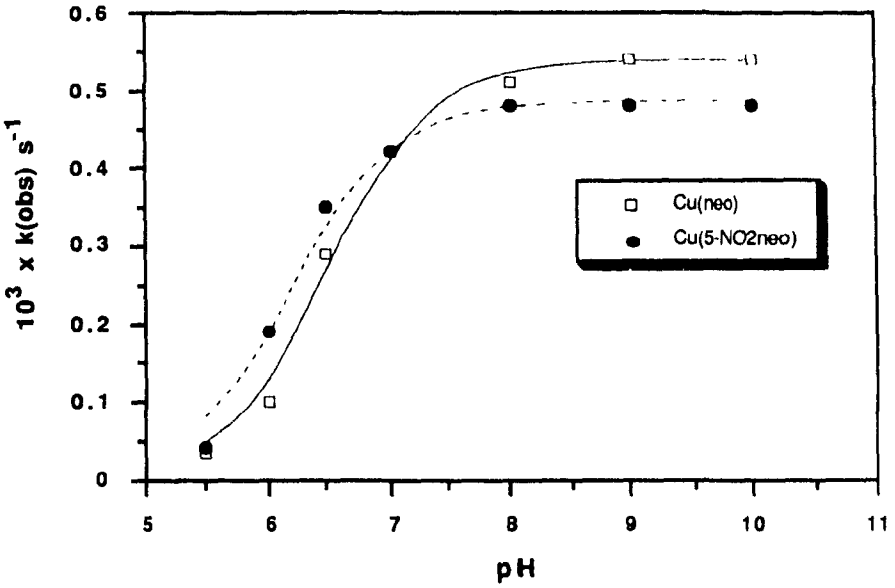

Figure 2.5 pH-rate profile for the hydrolysis of BDNPP by **Cu(neo)** and **Cu(5-NO_2neo)** (1mM, 25 °C). For Cu(5-NO_2neo) Ka = 6 4 x 10^{-7}, $k_{2'}$ = 4 9 x 10^{-4} s^{-1} Cu(neo): Ka = 3 2 x 10^{-7}, $k_{2'}$ = 5 4 x 10^{-4} s^{-1}.

Table 2.3 Observed first-order rate constants for $[Cu(neo)(OH_2)_2]^{2+}$ and $[Cu(5\text{-}NO_2neo)(OH_2)_2]^{2+}$ (1 mM) promoted hydrolysis of BDNPP (2 5 x 10^{-5} M) at 25 °C

pH	10^3 x k_{obs} (s^{-1})	
	$[Cu(neo)(OH_2)_2]^{2+}$	$[Cu(5\text{-}NO_2neo)(OH_2)_2]^{2+}$
5.5	035	042
6.0	10	19
6 5	29	35
7.0	42	42
8.0	51	48
9.0	54	48
10 0	54	48

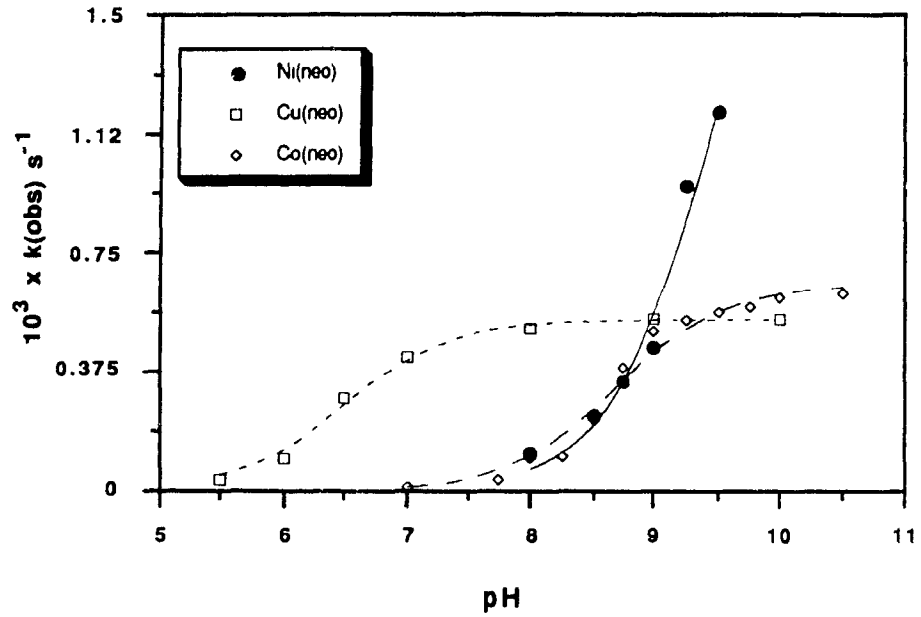

Figure 2.6 pH-rate profiles for the hydrolysis of BDNPP by **Ni(neo)**, **Cu(neo)**, and **Co(neo)** (1 mM, 25 °C) For Co(neo)· Ka = 2.05 x 10^{-9}, k_2· = 6 5 x 10^{-4} s^{-1}. Cu(neo)· Ka = 3 2 x 10^{-7}, k_2· = 5 4 x 10^{-4} Ni(neo)· values are unattainable due to precipitation at pH> 9.5

Table 2.4 Observed first-order rate constants for $[M(neo)(OH_2)_2]^{2+}$ (1 mM) promoted hydrolysis of BDNPP (2.5 x 10^{-5} M) at 25 °C

pH	10^3 x k_{obs} (s^{-1})		
	Co^{2+}	Cu^{2+}	Ni^{2+}
5.5		035	
6.0		10	
6.5		29	
7 0	0122	42	
7.75	034		
8.0	11	51	.12
8 25	12		
8.5	22		23
8 75	39		.34
9 0	50	54	.49
9 25	54		96
9.5	56		1.2
9.75	58		
10 0	61	54	
10.5	62		

2.2.2 Dependence of BDNPP Hydrolysis Rate on the Concentration of Cu(II) Complex

The rate of hydrolysis of BDNPP increases linearly with the increase of the concentration of the Cu(II) neocuproine complex (fig. 2.7). For the Cu(II) phenanthroline complex and the Cu(II) dipyridylamine complex, the rate of BDNPP hydrolysis levels at increasing complex concentration (fig. 2.7). The data for these plots are listed in table 2.5. Metal complex concentrations range from 0.1mM to 5 mM. Slow precipitation of the metal complexes occurs at concentrations greater than 5mM.

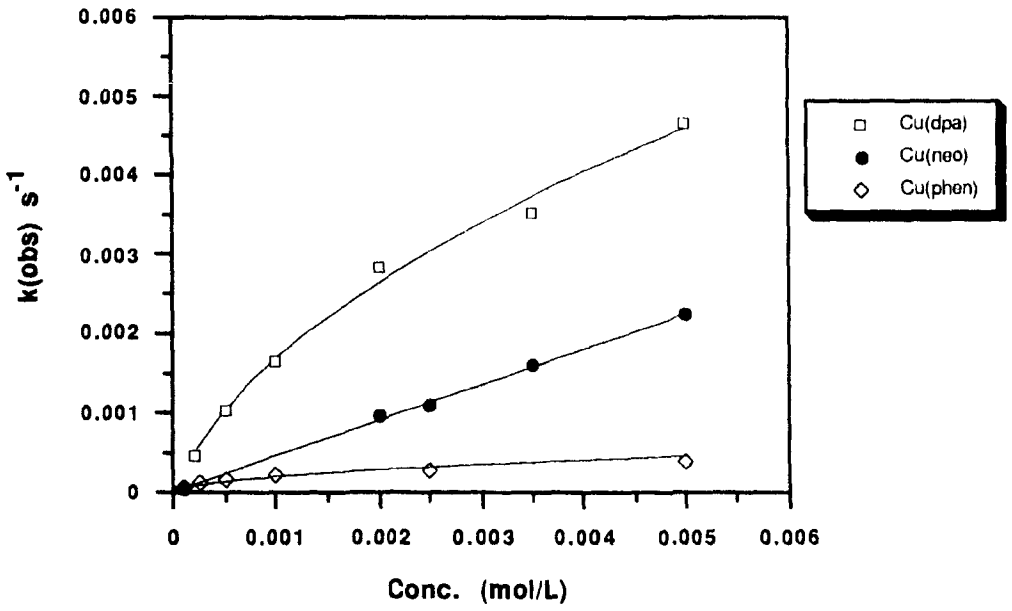

Figure 2.7 Dependence of k_{obs} for the hydrolysis of BDNPP on Cu(phen), Cu(neo), and Cu(dpa) concentration

Table 2.5 First-order rate constants for BDNPP (2.5×10^{-5} M) hydrolysis by Cu(II) complexes at pH 8, 25 °C with dependence on the metal complex concentration

Conc. (mM)	k_{obs} (s^{-1})		
	$[Cu(dpa)(OH_2)_2]^{2+}$	$[Cu(neo)(OH_2)_2]^{2+}$	$[Cu(phen)(OH_2)_2]^{2+}$
0.1		4.5×10^{-5}	6.5×10^{-5}
0.2	4.6×10^{-4}		
0.25			1.2×10^{-4}
0.5	1.0×10^{-3}		1.6×10^{-4}
1.0	1.65×10^{-3}		2.2×10^{-4}
2.0	2.8×10^{-3}	9.6×10^{-4}	
2.5		1.1×10^{-3}	2.7×10^{-4}
3.5	3.5×10^{-3}	1.6×10^{-3}	
5.0	4.6×10^{-3}	2.2×10^{-3}	3.8×10^{-4}

The data for Cu(dpa) and Cu(phen) were fit according to equation 2.1 (see appendix) where k is the second-order rate constant for $[Cu(dpa)(OH)(OH_2)]^+$ or $[Cu(phen)(OH)(OH_2)]^+$ mediated hydrolysis of BDNPP, C_T is the total concentration of copper complex used, and K_{dim} is the dimerization constant for the copper complex. The values for K_{dim} were taken from table 2.1.

$$k_{obs} = k \left[\frac{-1 + \sqrt{1 + 8K_{dim}C_T}}{4K_{dim}} \right] \qquad (2.1)$$

2.2.3 Rates of M(II) complex promoted hydrolysis of BDNPP

The observed pseudo-first-order rate constants for the hydrolysis of BDNPP promoted by different Cu(II) complexes are summarized in tables 2.6 and 2.7.

Table 2.6 Rate constants for BDNPP (2.5×10^{-5} M) hydrolysis promoted by various Cu(II) complexes (5×10^{-3} M) at pH 8, 25 °C

Cu(II) complex	$^{*}k_{(obs)}$ (s^{-1})	rel. rate	$^{*}k$ ($M^{-1}s^{-1}$)	rel. rate
$[Cu(dpa)(OH_2)_2]^{2+}$	4.6×10^{-3}	12	1.93	4.4
$[Cu(neo)(OH_2)_2]^{2+}$	2.2×10^{-3}	5.7	44	1
$[Cu(phen)(OH_2)_2]^{2+}$	3.84×10^{-4}	1	1.25	2.84
$[Cu(terpy)(OH_2)]^{2+}$	1.42×10^{-6}	0.037	2.84×10^{-3}	0064
NaOH	3.0×10^{-9}**	7.8×10^{-6}	3.0×10^{3}	0068

* as defined in equation 2.1 Values of K_{dim} taken from table 2.1

** Hydroxide rate at pH 8 from ref 21

Table 2.7 Observed pseudo-first-order rate constants for BDNPP (2.5×10^{-5} M) hydrolysis by Cu(II) complexes (1×10^{-3} M) containing modified dpa ligands at pH 8, 25 °C.

Cu(II) complex	$k_{(obs)}$ (s^{-1})	rel. rate
$[Cu(dpa)(OH_2)_2]^{2+}$	1.63×10^{3}	1
$[Cu(NMedpa)(OH_2)_2]^{2+}$	4.16×10^{-4}	0.26
$[Cu(5,5'\text{-dimethyldpa})(OH_2)_2]^{2+}$	1.78×10^{3}	1.1
$[Cu(dpm)(OH_2)_2]^{2+}$	6.24×10^{4}	0.38

Table 2.8 lists the observed pseudo-first-order rate constants for BDNPP hydrolysis promoted by the M(II) neocuproine complexes used in this study. The acid dissociation constants are also given in the table. The Ni(II) neocuproine complex precipitates out at pH>9.5. The Zn(II) neocuproine complex precipitates out as $Zn(OH)_2$ at pH>6.5, and therefore it was not possible to study its kinetics towards phosphate ester hydrolysis.

Table 2.8 Observed pseudo-first-order rate constants for BDNPP (2.5×10^{-5} M) hydrolysis promoted by Metal(II) neocuproine complexes (1×10^{-3} M) at pH 9.5, 25 °C

M(II) complex	pKa	k_{obs} (s^{-1})	rel. rate
$[Cu(neo)(OH_2)_2]^{2+}$	7.0	5.4×10^{-4}	1
$[Co(neo)(OH_2)_2]^{2+}$	8.7	6.1×10^{-4}	1.1
$[Ni(neo)(OH_2)_2]^{2+}$	>9.5	1.2×10^{-3}	2.2

2.2.4 Comparison Between Cu(II) and Co(III) Complex Promoted Hydrolysis of BDNPP and BNPP.

Table 2.9 lists the rates of hydrolysis for BDNPP and BNPP promoted by $[Cu(dpa)(OH_2)_2]^{2+}$ and compares them to the rates promoted by Co(III) complexes as reported in ref. 14. For the Co(III) complexes, the maximal rate for phosphate diester hydrolysis is observed at pH 7 whereas the maximal rate for the Cu(II) complex is at pH $\geq$ 8.

Table 2.9 Rate constants for BDNPP (2.5 x 10^{-5} M, 25 °C) and BNPP (2.5 x 10^{-5} M, 50 °C) hydrolysis promoted by Cu(II) (pH 8) and Co(III) (pH 7) complexes**

Phosphate Diester	Metal Complex	k(obs) (s^{-1})	k (M^{-1} s^{-1})	Rel. rate
BDNPP	$[Cu(dpa)(OH_2)_2]^{2+}$ (1 mM)	1.6 x 10^{-3}	1.93*	1
BDNPP	$[Co(trpn)(OH_2)_2]^{3+}$ (10 mM)	1.1 x 10^{-1}	11	57
BNPP	$[Cu(dpa)(OH_2)_2]^{2+}$ (1 mM)	1.3 x 10^{-4}	0.179*	1
BNPP	$[Co(trpn)(OH_2)_2]^{3+}$ (10 mM)	2.5 x 10^{-2}	2.5	14
BNPP	$[Co(tren)(OH_2)_2]^{3+}$ (10 mM)	8.1 x 10^{-5}	0.0081	0.042

*as defined in equation 2.1 K_{dim} = 230 M^{-1}

** Rate constants for Co(III) complexes obtained from ref. 14

2.3 Cu(II) PROMOTED HYDROLYSIS OF PHOSPHATE MONOESTERS

Table 2.10 lists the rates of hydrolysis for DNPP and BDNPP promoted by $[Cu(dpa)(OH_2)_2]^{2+}$. The hydrolysis reaction was followed spectrophotometrically at 400 nm. The conditions used were similar to those employed for phosphate diester hydrolysis. The symbol k_{uncat} refers to the spontaneous rate of hydrolysis of the phosphate ester, under the conditions specified, in absence of any metal catalyst.

Table 2.10 Observed pseudo-first-order rate constants for phosphate ester hydrolysis (2.5×10^{-5} M) promoted by $[Cu(dpa)(OH_2)_2]^{2+}$ (1×10^{-3} M) at pH 8, 25 °C.

Substrate	k_{obs} (s^{-1})	Rel. rate	k_{uncat} (s^{-1})	$\frac{k_{obs}}{k_{uncat}}$
DNPP	1.38×10^{-4}	1	2.22×10^{-5} (ref 18)	6.12
BDNPP	1.65×10^{-3}	12	2.42×10^{-7} (ref 21)	6300

Metal complex promoted hydrolysis of methyl phosphate was monitored by ^1H NMR. Methanol was produced after several days (pD 7, 40 °C) from the 1:1:1 addition of methyl phosphate, $[Co(trpn)(OH_2)_2]^{3+}$, and $[Cu(dpa)(OH_2)_2]^{2+}$ (fig. 2.8) Under similar conditions, rate promoted hydrolysis of methyl phosphate was not detected to any significant extent when $[Cu(terpy)(OH_2)]^{2+}$ was substituted for $[Cu(dpa)(OH_2)_2]^{2+}$. In the absence of copper complex, (i.e. the 1:1 addition of methyl phosphate to $[Co(trpn)(OH_2)_2]^{3+}$) minimal production of methanol was observed (approx. 10%) at the end of the same time interval used to study the system involving $[Cu(dpa)(OH_2)_2]^{2+}$. No hydrolysis was detected from the 2:1 addition of $[Cu(dpa)(OH_2)_2]^{2+}$ to methyl phosphate after three days at pD 7, 55 °C. The reaction could not be monitored further due to precipitation of the reaction solution.

It is well established that methyl phosphate binds to $[Co(trpn)(OH_2)_2]^{3+}$ in a bidentate fashion within a few minutes[47]. Figure 2.8 shows the ^1H NMR spectra of the hydrolysis of $[Co(trpn)(PO_3OMe)]^+$ (5 mM) promoted by $[Cu(dpa)(OH_2)_2]^{2+}$ (5 mM). Methanol was detected as the final product of the hydrolysis.

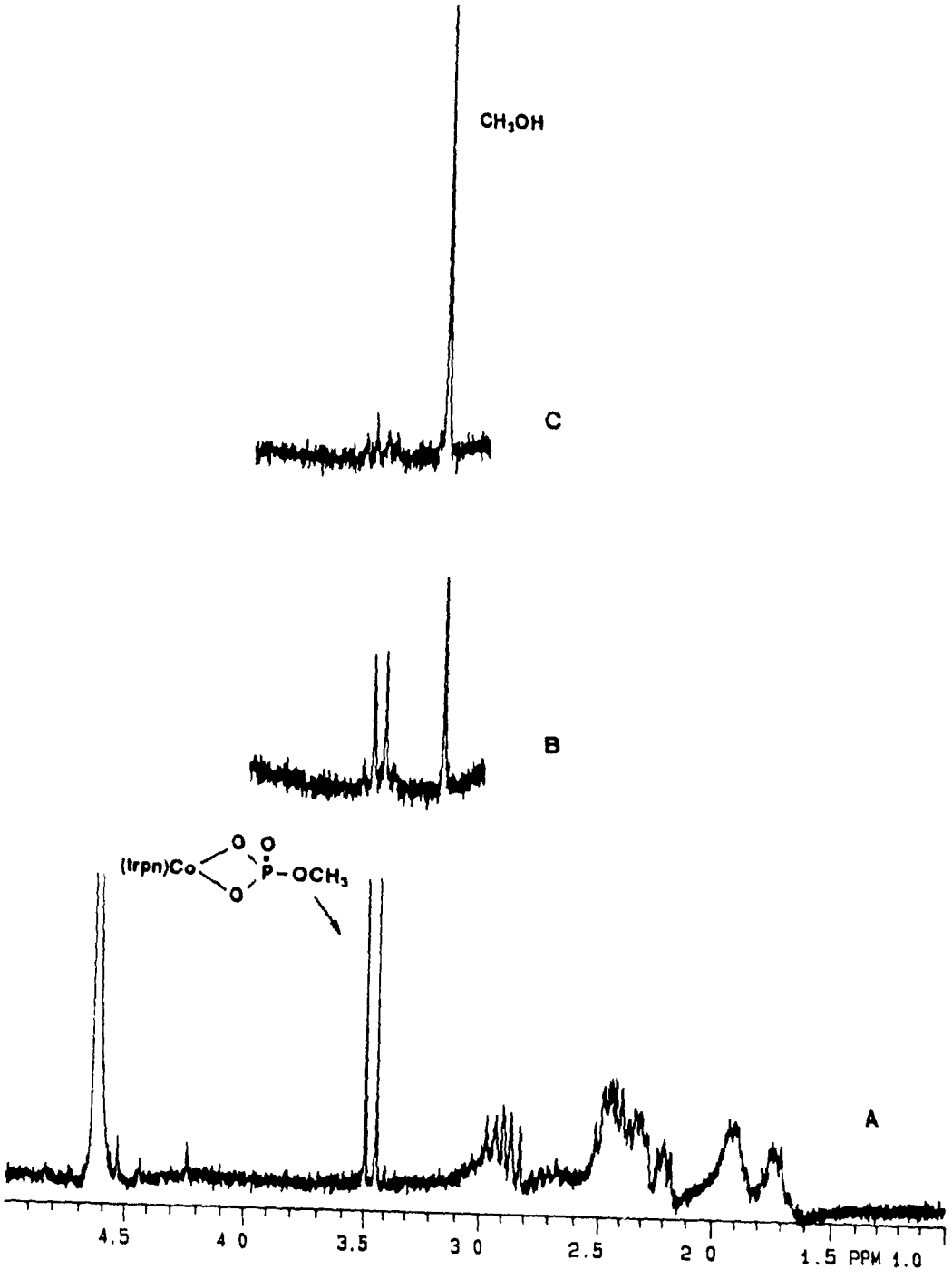

Figure 2.8 ^1H NMR spectra of methyl phosphate (5 mM) in D_2O after adding $[Co(trpn)(OH_2)_2]^{3+}$ (5 mM) and $[Cu(dpa)(OH_2)_2]^{2+}$ (5 mM), pD 7, 40 °C Elapsed time **A)** 0 hr, **B)** 70 hrs, **C)** 214 hrs

3. DISCUSSION

3.1 Cu(II) COMPLEX PROMOTED HYDROLYSIS OF PHOSPHATE DIESTERS.

3.1.1 Mechanism for BDNPP Hydrolysis.

The mechanism proposed for $[Cu(dpa)(OH_2)_2]^{2+}$ mediated hydrolysis of BDNPP is shown in figure 3.1. This mechanism is valid for all the $[(L)Cu(OH_2)_2)]^{2+}$ complexes studied, where L denotes a bidentate diamine ligand. The hydrolysis of the resulting phosphate monoester is slower than the hydrolysis of the diester and shall be discussed in section 3.5.1.

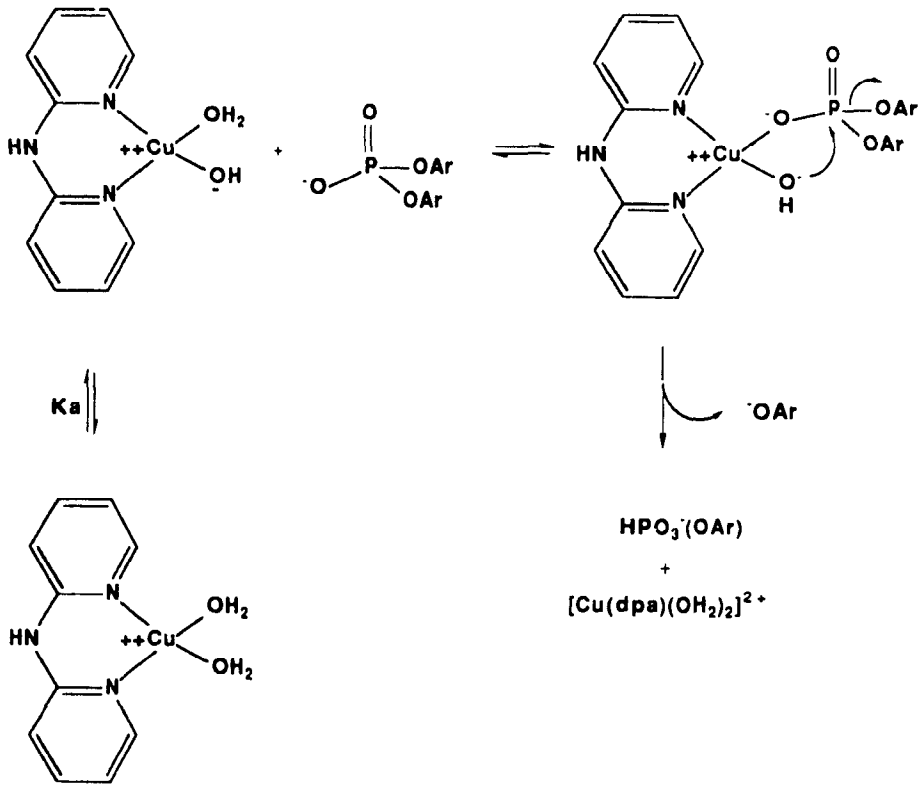

Figure 3.1. Mechanism of $[Cu(dpa)(OH_2)_2]^{2+}$ hydrolysis of BDNPP.

The pH-rate profiles for $[LCu(OH_2)_2]^{2+}$ promoted hydrolysis of BDNPP are consistent with the proposed mechanism. The profiles show sigmoidal shaped curves. For $[Cu(dpa)(OH_2)_2]^{2+}$, a pH-independent plateau is observed at neutral to alkaline pH and a pH-dependent region is observed at pH 6 to 7 The sigmoidal pH-rate profile suggests that the removal of a proton from the copper complex is necessary to form the dominant catalyst. The similarity between the kinetic pKa (6.9) and that obtained by direct titration (7.2) for $[Cu(dpa)(OH_2)_2]^{2+}$ suggests formation of a copper-bound hydroxide or its kinetic equivalent.

The pH-rate data can be fit to the expression shown in eq. 3.1

$$k_0 = k_1 [(L)Cu] + k_2 [(L)Cu(OH)] \qquad (3\ 1)$$

where k_1 and k_2 are the second-order rate constants for BDNPP hydrolysis promoted by the diaqua and hydroxy-aqua species, respectively. [(L)Cu] and [(L)Cu(OH)] represent the diaqua and hydroxy-aqua copper complexes, respectively. The acid dissociation constant, Ka, for the diaqua copper complex is given by equation 3.2.

$$Ka = \frac{[(L)Cu(OH)]\,[H^+]}{[(L)Cu]} \qquad (3\ 2)$$

The total concentration of copper complex used, C_T, can be expressed by eq. 3.3

$$C_T = [(L)Cu] + [(L)Cu(OH)] \qquad (3\ 3)$$

By substituting eq. 3.2 into eq. 3.1 the rate law can be expressed as a function of the concentration of the hydroxy-aqua species (see eq. 3.4). Also, C_T can be expressed as a function of the concentration of the hydroxy-aqua species (eq. 3.5) by substituting eq. 3.2 into eq. 3.3.

$$k_0 = \frac{k_1 [(L)Cu(OH)]\,[H^+]}{Ka} + k_2 [(L)Cu(OH)] \qquad (3\ 4)$$

$$C_T = [(L)Cu(OH)] \left[\frac{[H^+] + Ka}{Ka} \right] \qquad (3\ 5)$$

The pH-rate law can now be expressed as a function of the total copper complex concentration used by substituting eq. 3.5 into eq. 3.4. This is given by eq. 3.6.

$$k_0 = \left[\frac{k_1 [H^+] + k_2 Ka}{[H^+] + Ka} \right] [C_T] \qquad (3\ 6)$$

Therefore, the pseudo-first-order rate constant, k_{obs}, is expressed in eq. 3.7 where k_1' and k_2' are the pseudo-first-order rate constants for BDNPP hydrolysis promoted by the diaqua and hydroxy-aqua species respectively [†]

$$k_{obs} = \left[\frac{k_1' [H^+] + k_2' Ka}{[H^+] + Ka} \right] \qquad (3\ 7)$$

The proposed mechanism for $[(L)Cu(OH_2)_2]^{2+}$ promoted hydrolysis of BDNPP is similar to the mechanism suggested for $[(N_4)Co(OH_2)_2]^{3+}$. As is the case for the Co(III) complexes, the Cu(II) complex plays a bifunctional role effecting hydrolysis by electrophilic activation of the coordinated phosphate ester and by providing a cis proximity for the metal-hydroxide nucleophile. In support of this mechanism, it is observed that Cu(II) complexes with one less available coordination site, such as $[Cu(terpy)(OH_2)]^{2+}$, do not promote the hydrolysis of BDNPP very efficiently (table 2.6); therefore, the Lewis acid and the metal hydroxide mechanism can be ruled out. Kinetically equivalent mechanisms must incorporate the dual features of phosphate diester complexation and evidence for a copper-hydroxide species as active catalyst. Other possible paythways are shown in figure 3.2.

Figure 3.2a depicts an intramolecular general base mechanism which can be ruled out. The Cu(II) complexes used in this study of the type $[(L)Cu(OH_2)_2]^{2+}$, where L represents a bidentate diamine ligand, are structurally related and have similar pKa values (table 2.1) yet they hydrolyze BDNPP at significantly different rates (table 2.6 and 2.7). If the general base mechanism is valid then one should expect to observe similar reactivities for these Cu(II) complexes

In figure 3.2b, the phosphate diester coordinates to the copper complex in a bidentate fashion followed by external hydroxide attack. In general, intramolecular nucleophilic catalysis is much more efficient than the corresponding intermolecular reaction.[52,53] For example, the phosphate diester **6** (fig. 3.3) reacts by intramolecular

[†] $k_1' = k_1[C_T]$ and $k_2' = k_2[C_T]$

[52] F. M. Menger, *Acc. Chem. Res.*, **1985**, 18, 128.

attack of alkoxide anion at the phosphorus centre.[54] It is estimated that the intramolecular reaction proceeds 10^7 times faster than the corresponding intermolecular attack of hydroxide.[53]

As mentioned in the introduction, several reports exist in the literature of an intramolecular pathway for metal complex promoted hydrolysis of phosphate esters. Hydrolysis of $[(en)_2Co(^{18}OH)(4\text{-}NO_2C_6H_4OPO_3)]$ to yield ^{18}O-labelled coordinated inorganic phosphate and hydrolysis of $cis\text{-}[(en)_2Ir(OH)O_2P(OR)_2]^+$, where the phosphate diester, ethyl 4-nitrophenyl phosphate is precoordinated to the metal ion, provide the strongest evidence for intramolecular hydrolysis of phosphate esters by transition metal complexes. Recently, the same mechanism was proposed by Morrow and Trogler for $[(bpy)Cu(OH_2)_2)]^{2+}$ hydrolysis of phosphate diesters[51a] and triesters[36a]

In the present study, no mechanistic discrimination between inter- and intramolecular nucleophilic hydrolysis is possible by ^{18}O-labelling experiments because, unlike the Co(III) and Ir(III) complexes, Cu(II) complexes exchange aqua ligands very rapidly on the time scale of phosphate ester hydrolysis. In this respect, it is difficult to disprove the kinetically indistinguishable mechanism of figure 3.2b. However, based on the conclusions from the above examples, it is most likely that the intramolecular mechanism (fig. 3.1) is the dominant pathway for the hydrolysis reaction.

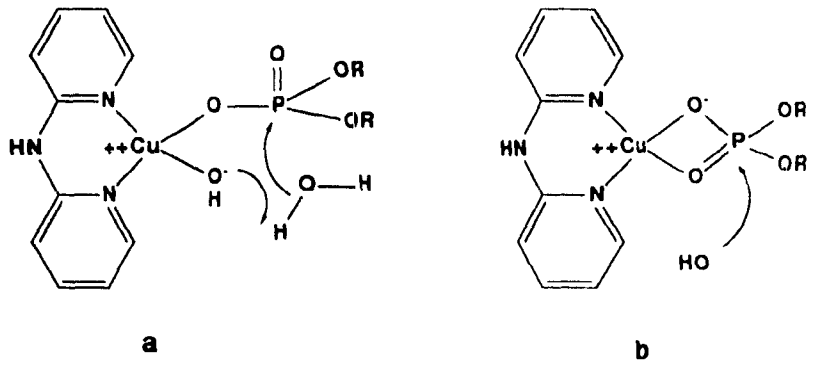

a b

Figure 3.2 **a)** General base mechanism **b)** Intermolecular nucleophilic mechanism for $[(L)Cu(OH_2)_2)^{2+}$ promoted hydrolysis of BDNPP

[53] A. J. Kirby, *Adv Phys Org Chem*, **1980**, 17, 183

[54] D. A. Usher, D. I. Richardson Jr., and D. G. Oakenfull, *J Am Chem Soc*, **1970**, 92, 4699

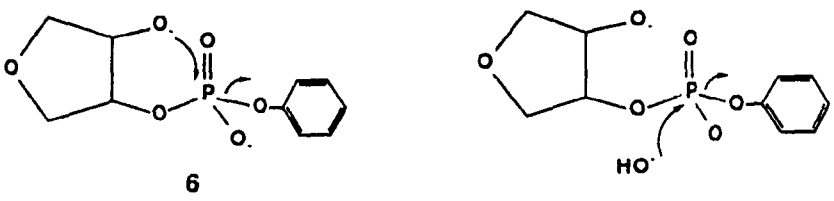

	6	
Relative rates	10^7	1

Figure 3.3 Intramolecular vs. intermolecular nucleophilic catalysis (ref 53 & 54)

As is the case for $[N_4Co(OH_2)_2]^{3+}$, the rate-limiting step for the Cu(II) complex promoted hydrolysis of BDNPP involves the P-O cleavage step (fig. 3.1) since the rate of solvent exchange with anionic ligands occurs extremely rapidly for Cu(II) complexes.[55]

Since the mechanism of phosphate ester hydrolysis promoted by $[(L)Cu(OH_2)_2]^{2+}$ and $[(N_4)Co(OH_2)_2)]^{3+}$ are the same, the aim is to determine if there is a substantial ligand effect in Cu(II) complexes as was the case for Co(III) complexes.

3.2 LIGAND EFFECT ON $[(L)Cu(OH_2)_2]^{2+}$ COMPLEXES

It is clear that the reactivity of Cu(II) complexes is highly sensitive to the ligand structure (table 2.6 and 2.7). For example, at 5 mM metal complex concentration (25 °C, pH 8), it is observed that $[Cu(neo)(OH_2)_2]^{2+}$ hydrolyzes BDNPP almost 6 times more rapidly than $[Cu(phen)(OH_2)_2]^{2+}$ while $[Cu(dpa)(OH_2)_2]^{2+}$ is 12 times more efficient at hydrolyzing the phosphate diester. The mechanism for hydrolysis of BDNPP is the same for all the $[(L)Cu(OH_2)_2]^{2+}$ complexes studied. The complexes are structurally related and have similar pKa values (table 2.1) yet they hydrolyze BDNPP at significantly different rates. The structure of the ligand can affect the efficiency of the Cu(II) catalyst.

In what way does the ligand influence the efficiency of the Cu(II) complex? Some of the answers to this question are obvious. For instance, the ligand should impart aqueous solubility to the metal ion. Also, it should not dissociate appreciably from the metal ion in the pH range of interest for the reaction being studied. More importantly, the ligand should leave two free coordination sites on the metal ion to allow it to "combine" with the substrate. The complex $[Cu(terpy)(OH_2)]^{2+}$ has only one free coordination site and therefore is inactive towards BDNPP hydrolysis.

[55]C. M Frey and J Struehr, *Metal Ions in Biological Systems*, Dekker, New York, 1974, Vol. 1.,51-116

3.2.1 Geometry of Cu(II) Complexes

In aqueous solution, the Cu(II) ion has a distorted octahedral structure which arises from the Jahn-Teller effect.[56] Four of the coordinated water molecules are situated in an equatorial square plane about the central Cu(II) ion, while the remaining two water molecules are located at a greater distance along the central axis perpendicular to the square plane.[57] In its complexes, Cu(II) shows a strong preference for square planar (or grossly distorted octahedral) structures. That is, the strong donor atoms are bound in the tetragonal plane and the coordination tendency of the axial positions is very low. In this respect, the Cu(II) complexes used in this study are four coordinate and will be referred to as having a 'square planar' geometry. As will be discussed, complexes of the type $[(L)Cu(OH_2)_2]^{2+}$, where L represents a bidentate diamine ligand, will distort from a regular square planar geometry depending on the structure of the ligand.

3.2.2 Dimerization

An interesting comparison can be made between $[Cu(neo)(OH_2)_2]^{2+}$ and $[Cu(phen)(OH_2)_2]^{2+}$. A significant difference towards BDNPP hydrolysis is observed by placing methyl groups ortho to the heterocyclic nitrogens of the phenanthroline ligand. As illustrated from the concentration vs. rate plot in figure 2.5, for the neocuproine complex, the rate of BDNPP hydrolysis increases linearly with increase in the concentration of the copper complex. Such is not the case for $[Cu(phen)(OH_2)_2]^{2+}$, where the rate levels off at increasing copper complex concentrations. At 5 mM copper complex concentration, the neocuproine complex is 5.7 times more reactive than the phenanthroline complex at hydrolyzing BDNPP. However, this difference becomes minor at lower concentrations, and in fact, at 0.1mM, the phenanthroline complex is slightly more reactive at hydrolyzing the phosphate diester (see table 2.5).

The non-linear plot for $[Cu(phen)(OH_2)_2]^{2+}$ is attributable to the known dimerization reaction for copper(II) chelates and is consistent with the dimer being inactive

---

[56]L. E. Orgel, *An Introduction to Transition Metal Chemistry: Ligand Field Theory*, Wiley and Sons, London, 1966, p. 59.

[57]H. Sigel, *Angew. Chem. Internat. Ed.*, **1975**, 14, 394.

Martell and coworkers[58,59] determined that copper(II) diamine chelates have the tendency to dimerize to the hydroxy-bridged dimer as shown in figure 3.4. The dimer cannot be active towards ester hydrolysis since there are no free coordination sites available for the substrate to bind to the metal ion. $[Cu(neo)(OH)(OH_2)]^+$ does not dimerize because of unfavourable steric effects brought about by the methyl groups.

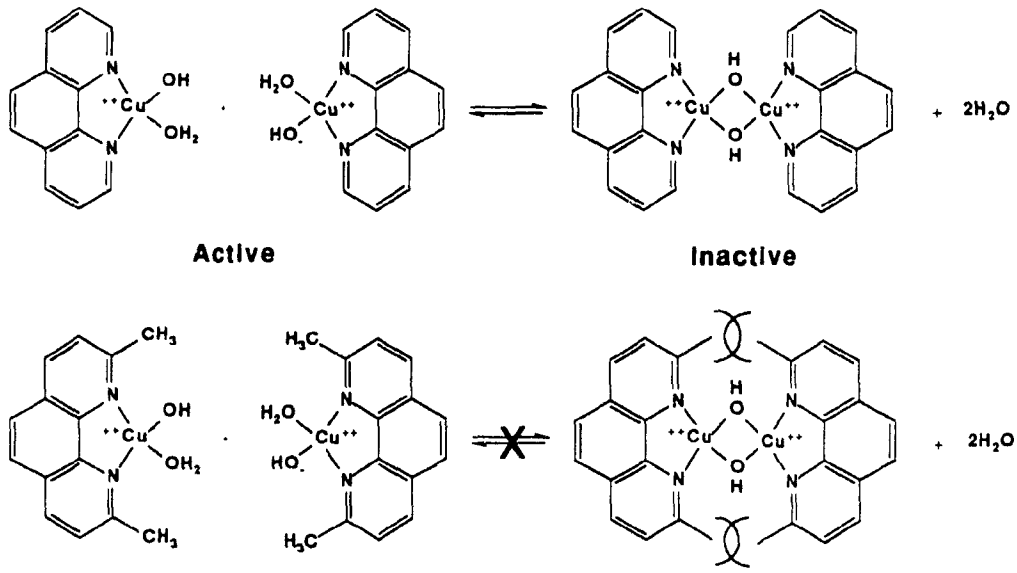

Figure 3.4. Dimerization of Cu(II) phenanthroline complex and formation of an inactive hydroxy-bridged dimer The neocuproine complex does not dimerize due to steric effects.

In order to compare the efficiencies of the different Cu(II) complexes, it is necessary to determine the concentration of the hydroxo-aqua species present in solution. The dimerization constant, K_{dim}, can be obtained by potentiometric titrations of the copper complex at varying concentrations. Three species exist in solution in the pH-range studied: a diaqua chelate, $[(L)Cu]^{\dagger}$; a hydroxy-aqua compound, $[(L)Cu(OH)]^{\dagger}$; and the hydroxy-bridged dimer, $[(L)Cu(OH)]_2$ The solution equilibria may be defined by the following equations:

---

[58]R C Courtney, R L Gustafson, and S Chabarek Jr., A. E. Martell, *J Am Chem Soc* , **1959**, 81, 519

[59]R. L Gustafson and A E Martell, *J Am Chem Soc* , **1959**, 81, 525

†The aqua ligands are omitted for clarity.

$$[(L)Cu] \overset{Ka}{\rightleftharpoons} [(L)Cu(OH)] + [H^+]$$

$$Ka = \frac{[H^+]\,[(L)Cu(OH)]}{[(L)Cu]} \qquad (3\ 8)$$

$$2\,[(L)Cu(OH)] \overset{K_{dim}}{\rightleftharpoons} [(L)Cu(OH)]_2 + H_2O$$

$$K_{dim} = \frac{[(L)Cu(OH)]_2}{[(L)Cu(OH)]^2} \qquad (3\ 9)$$

$$C_T = [(L)Cu] + [(L)Cu(OH)] + [(L)Cu(OH)]_2 \qquad (3\ 10)$$

As evidence of the dimerization process, potentiometric titration curves show that an increase in copper complex concentration results in a shift of the buffer region to lower pH values (figures 2.2 and 2.3). On the basis of pH titrations, equilibrium constants involving the formation of hydroxo-aqua species, Ka, and the dimeric chelate species, K_{dim}, can be determined.

By substituting equations 3.8 and 3.9 into equation 3.10 one obtains the total copper complex concentration as a function of the concentration of the hydroxo-aqua species present in solution (eq. 3.11).

$$C_T = [(L)Cu(OH)] + \left[\frac{Ka}{[H^+]} + 2K_{dim}\left(\frac{Ka}{[H^+]}\right)^2 [(L)Cu(OH)] + 1 \right] \qquad (3\ 11)$$

At the midpoint of the titration curve, the concentration of the hydroxy-aqua species should be one half the total metal chelate concentration, $[(L)Cu(OH)] = C_T/2$, therefore,

$$C_T = \frac{C_T}{2}\left[\frac{Ka}{[H^+]} + K_{dim}\left(\frac{Ka}{[H^+]}\right)^2 C_T + 1 \right] \qquad (3\ 12)$$

and equation 3.12 produces the quadratic equation 3.13.

$$[H^+]^2 - Ka\,[H^+] - K_{dim}\,Ka^2\,C_T = 0 \qquad (3\ 13)$$

Solving the quadratic equation gives:

$$[H^+] = \frac{Ka\left(1 + \sqrt{1 + 4K_{dim}C_T}\right)}{2} \qquad (3.14)$$

thus,

$$pH_{mid} = pKa + \log 2 - \log\left(1 + \sqrt{1 + 4K_{dim}C_T}\right) \qquad (3.15)$$

where pH_{mid} is the pH at the midpoint of the titration curve at a given copper complex concentration

The dimerization constants are listed in table 2.1. For the phenanthroline copper complex $K_{dim} = 2.5 \times 10^4\ M^{-1}$. If we consider the actual concentration of the hydroxy-aqua species present in solution then the second-order rate constants at pH 8, 25 °C for $[Cu(neo)(OH)(OH_2)]^+$ and $[Cu(phen)(OH)(OH_2)]^+$ are .44 $M^{-1}s^{-1}$ and 1.25 $M^{-1}s^{-1}$ respectively for BDNPP hydrolysis. The $[Cu(phen)(OH)(OH_2)]^+$ complex is 2.84 times more reactive at hydrolyzing BDNPP than $[Cu(neo)(OH)(OH_2)]^+$, and $[Cu(dpa)(OH)(OH_2)]^+$ is 4.4 times faster than the neocuproine copper complex.

The neocuproine ligand prevents the metal ion from dimerizing, thus one of the important functions of the ligand is to maintain an appreciable concentration of the active hydroxy-aqua species. This does not explain why $[Cu(phen)(OH)(OH_2)]^+$ and $[Cu(dpa)(OH)(OH_2)]^+$ are intrinsically more reactive than $[Cu(neo)(OH)(OH_2)]^+$. The ligand must impart other effects on the metal complex.

3.2.3 Strain Effect

In order to design a more efficient catalyst, we must facilitate the rate-limiting phosphorus-oxygen cleavage step. The mechanism for the P-O cleavage reaction involves an intramolecular metal-hydroxide attack at phosphorus to produce a pentavalent phosphorane intermediate **II** (figure 3.5). This is analogous to the mechanism of hydrolysis of the phosphate diester **6** in figure 3.3. In a totally strain-free system, the O-Cu-O, Cu-O-P, O-P-O, and P-O-Cu bond angles in **II** should add up to 399° (90° + 109.5° + 90° + 109.5° respectively). However, in any four-membered ring, the sum of the angles must be less than or equal to 360°. Therefore, some of the angles in the four-

membered ring **II** must be compressed compared to the totally strain-free bond angles. In particular, the O-Cu-O bond angle in **II** must be considerably less than 90.

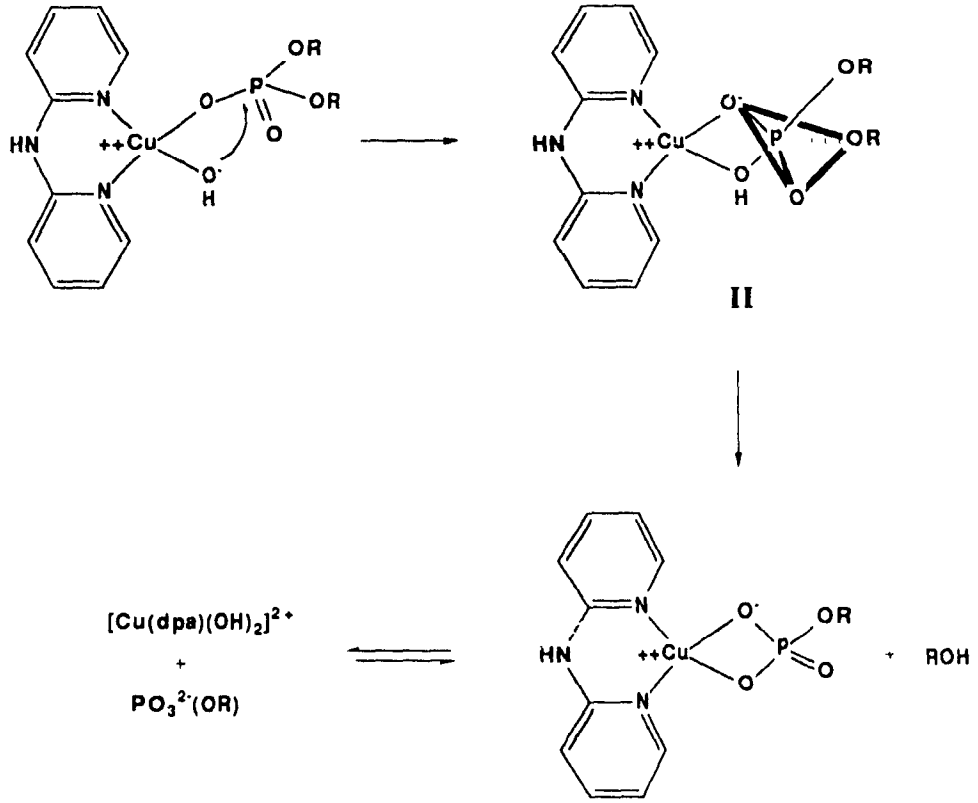

Figure 3.5. Proposed mechanism for Cu(II) complex mediated P-O cleavage reaction

The dipyridylamine ligand forms a six-membered chelate complex whereas a five-membered chelate complex is formed with the neocuproine ligand. It is more reasonable to make the comparison with the neocuproine complex instead of the phenanthroline complex since the former does not dimerize. Also, the pKa of the two complexes, $[Cu(dpa)(OH_2)_2]^{2+}$ (pKa = 7.2) and $[(Cu(neo)(OH_2)_2]^{2+}$ (pKa = 7.0) are very similar. As is the case for $[Co(tren)(OH)(OH_2)]^{2+}$ vs. $[Co(trpn)(OH)(OH_2)]^{2+}$, a major factor in stabilizing the four-membered transition state structure **II** is to increase the bond angle opposite the four-membered ring. The N-Cu-N bond angle in a six membered chelate complex should be larger than the N-Cu-N bond angle in a five membered chelate complex. It is proposed that $[Cu(dpa)(OH)(OH_2)]^{+}$ is more efficient at hydrolyzing phosphate

diesters than $[Cu(neo)(OH)(OH_2)]^+$ due to the greater ability of the former in stabilizing the four-membered ring

The $[Cu(dpa)(OH_2)_2]^{2+}$ complex is known to form four-membered rings easily For example, it was determined by X-ray crystallography that acetate binds to the copper(II) complex as a bidentate ligand.[60] It is the ability of the Cu(dpa)-complex to stabilize the four-membered ring in **II** that makes it a better catalyst for promoting the hydrolysis of phosphate diesters For five-membered diamine chelate complexes such as Cu(neo), a larger strain is developed in the chelation step and hence a slower rate for phosphate diester hydrolysis is observed.

3.2.4 Electronic Effect: Lowering Of pKa

The neocuproine copper(II) complex is appealing to study because complications arising from dimerization processes do not occur. An interesting comparison is between $[Cu(neo)(OH)(OH_2)]^+$ and $[Cu(5\text{-}NO_2neo)(OH)(OH_2)]^+$. Placing the electron withdrawing nitro group on the 5-position of the neocuproine ligand lowers the pKa of the corresponding copper(II) complex by 0.3 pH units (i.e . $[Cu(neo)(OH_2)_2]^{2+}$ pKa = 7.0, $[Cu(5\text{-}NO_2neo)(OH_2)_2]^{2+}$ pKa = 6.7). What then are the effects of lowering the pKa of the metal diaqua complex towards phosphate diester hydrolysis?

Figure 2.5 shows the pH-rate profiles for BDNPP hydrolysis promoted by the two complexes. The typical sigmoidal-shaped curves reveal inflection points near the pKa of their respective diaqua complexes. Lowering the pKa of the diaqua complex has the effect of generating the active hydroxy-aqua species at a lower pH. It is interesting to note that the maximal rate for both complexes are similar: ($k_2' = 5.4 \times 10^{-4}$ s^{-1} and 4.9×10^{-4} s^{-1} for $[Cu(neo)(OH)(OH_2)]^+$ and $[Cu(5\text{-}NO_2\text{-}neo)(OH)(OH_2)]^+$, respectively) It was anticipated that the 5-NO_2neo copper(II) complex would indeed display a lower maximal rate since its metal-hydroxide is less basic and hence less nucleophilic than the neocuproine complex. However, the difference in reactivity is not large. Perhaps the lower nucleophilicity is offset by the greater Lewis acidity of the 5-NO_2neo complex thereby making the phosphorus centre more electrophilic upon coordination.

[60] N Ray, S Tyagi and B Hathaway, *Acta Cryst* **1982**, B38, 1574

3.2.5 Other Ligands

Before we began our study with Cu(II) phenanthroline complexes, we anticipated that the introduction of methyl groups adjacent to the nitrogen atoms of 1,10-phenanthroline would enhance the activity of the copper complex in hydrolyzing phosphate diesters. We thought that steric interactions between the methyl groups and the metal bound oxygen atoms in $[Cu(neo)(OH)(OH_2)]^+$ would result in compression of the O-Cu-O bond angle compared to that for $[Cu(phen)(OH)(OH_2)]^+$. Constriction of the O-Cu-O bond angle should facilitate the rate-determining four-membered ring formation step. The evidence for the steric interaction is that although neocuproine (pKa = 5.85) is almost 10 times more basic than phenanthroline (pKa = 4.98), the equilibrium constant for binding of Cu(II) to neocuproine in water (log K = 6.1) is 500 times less than that for binding of Cu(II) to phenanthroline (log K = 8.8).[61] If steric factors are not involved then the formation constants for these type of complexes are approximately proportional to pKa.[62,69b]

The increased strain of the metal complex imposed by the methyl groups does not force the coordinated water molecules closer together but causes a progressive distortion towards a tetrahedral geometry[61] It is well known that the tetrahedral geometry prefers Cu(I) over Cu(II), thus, the Cu(II) neocuproine complex undergoes autoreduction to the Cu(I) complex.[63] Upon standing for a few weeks at room temperature, an aqueous solution of $[Cu(neo)(OH_2)_2]^{2+}$ produces an intense visible absorption maximum at 455 nm which is indicative of Cu(I) complexes.[63] At elevated temperatures, this process is accelerated. This is why $[Cu(neo)(OH_2)_2]^{2+}$ mediated hydrolysis of phosphate esters were carried out at 25 °C. At room temperature, the 'decomposition' of the Cu(II) complex was not significant during the course of the hydrolysis reaction. Hydrolysis of phosphate diesters promoted by the bulkier 2,9-diethylphenanthroline-Cu(II) complex could not be monitored even at room temperature since the reduction process interferes with the study of the phosphate ester hydrolysis reaction.

---

[61] H. Irving and D. H. Mellor, *J. Chem. Soc.*, **1962**, 5237.

[62] B. R. James and R. J. P. Williams, *J. Chem. Soc.*, **1961**, 2007.

[63] a) J. R. Hall, N. K. Marchant, and R. A. Plowman, *Aust. J. Chem.*, **1962**, 15, 480. b) J. R. Hall, N. K. Marchant, and R. A. Plowman, *Aust. J. Chem.*, **1963**, 16, 34. c) S. Kitigawa, M. Munakata, and A. Higashie, *Inorg. Chim. Acta.*, **1984**, 84, 79. d) H. Doine, Y. Yano, and T. W. Swaddle, *Inorg. Chem.*, **1989**, 28, 2319.

The trivial name 'neocuproine' was assigned to 2,9-dimethyl-1,10-phenanthroline by Smith and McCurdy[64] who first described its application as a specific chromogenic reagent for copper The common name 'cuproine' was assigned to 2,2'-biquinoline by Hoste[65] because its reaction with cuprous ion is analogous to the ferroin reaction between ferrous ion and 1,10-phenanthroline Wolden, Hammet, and Chapman[66], in 1931, introduced the use of tris(1,10-phenanthroline)iron(II) as a high potential redox indicator, but it was Gleu who first suggested, the now common name 'ferroin' as an abbreviation for, in his words, "this most important and best oxidimetric indicator,...the phenolphthalein of oxidimetry.. "[67] For the analytical chemist, neocuproine is superior to cuproine because of its greater solubility in aqueous solution and its greater molar absorptivity for its Cu(I) chelate[68]

The reasons given for the greater efficiency of $[Cu(dpa)(OH_2)_2]^{2+}$ compared to $[Cu(neo)(OH_2)_2]^{2+}$ for phosphate diester hydrolysis are still valid One may argue that the methyl groups will hinder the approach of the oncoming phosphate diester. It is unlikely that the Cu(II)-dipyridylamine complex is more reactive than the neocuproine complex due to steric considerations since both complexes have similar reactivities for hydrolyzing p-nitrophenol acetate (pNPA). The metal promoted hydrolysis of pNPA occurs via a nucleophilic metal-hydroxide mechanism (see sections 4 4 and 6 1 concerning metal complex hydrolysis of pNPA). If hindrance were a factor then $[Cu(neo)(OH_2)_2]^{2+}$ should hydrolyze pNPA less efficiently than $[Cu(dpa)(OH_2)_2]^{2+}$

Compared with the phenanthroline system, the Cu(II)-dpa complex is by far the most efficient complex at hydrolyzing phosphate diesters We wanted to ascertain if slight modifications to the dipyridylamine ligand would have an effect on the resulting Cu(II) complex towards phosphate diester hydrolysis. The ligands that were studied are shown in figure 3.6 and the rates of the Cu(II) complex promoted hydrolysis of BDNPP are listed in table 2.7

Addition of methyl groups adjacent to the nitrogen atoms of phenanthroline prevented dimerization of the Cu(II) complex. Similarly, we hoped that introduction of methyl groups ortho to the nitrogen atoms of dipyridylamine would also prevent dimerization of the resulting complex. Unfortunately, in aqueous solution, both metal and ligand precipitated out of solution. Metal complexation could not occur because of the

---

[64]G F Smith and W H McCurdy Jr , *Anal Chem* , **1952**, 24, 371
[65]J Hoste, *Anal Chim Acta* , **1950**, 4, 23
[66]G H Walden Jr , L P Hammet, and R P Chapman, *J Am Chem Soc* , **1931**, 53, 3908
[67]K Gleu, *Z Anal Chem* , **1933**, 95, 305
[68]A A Schilt, *Analytical Applications Of 1,10-phenanthroline and Related Compounds* , Pergamon Press, Oxford, 1969, p 71

inhospitable steric environment around the nitrogen atoms. Compared with $[Cu(dpa)(OH_2)_2]^{2+}$, no significant effect is observed for the metal complex promoted hydrolysis of BDNPP by $[Cu(5,5'\text{-dimethyldpa})(OH_2)_2]^{2+}$. Apparently, the methyl groups in 5,5'-dimethyldpa are too far away from the metal centre to have any significant effect on the copper complex.

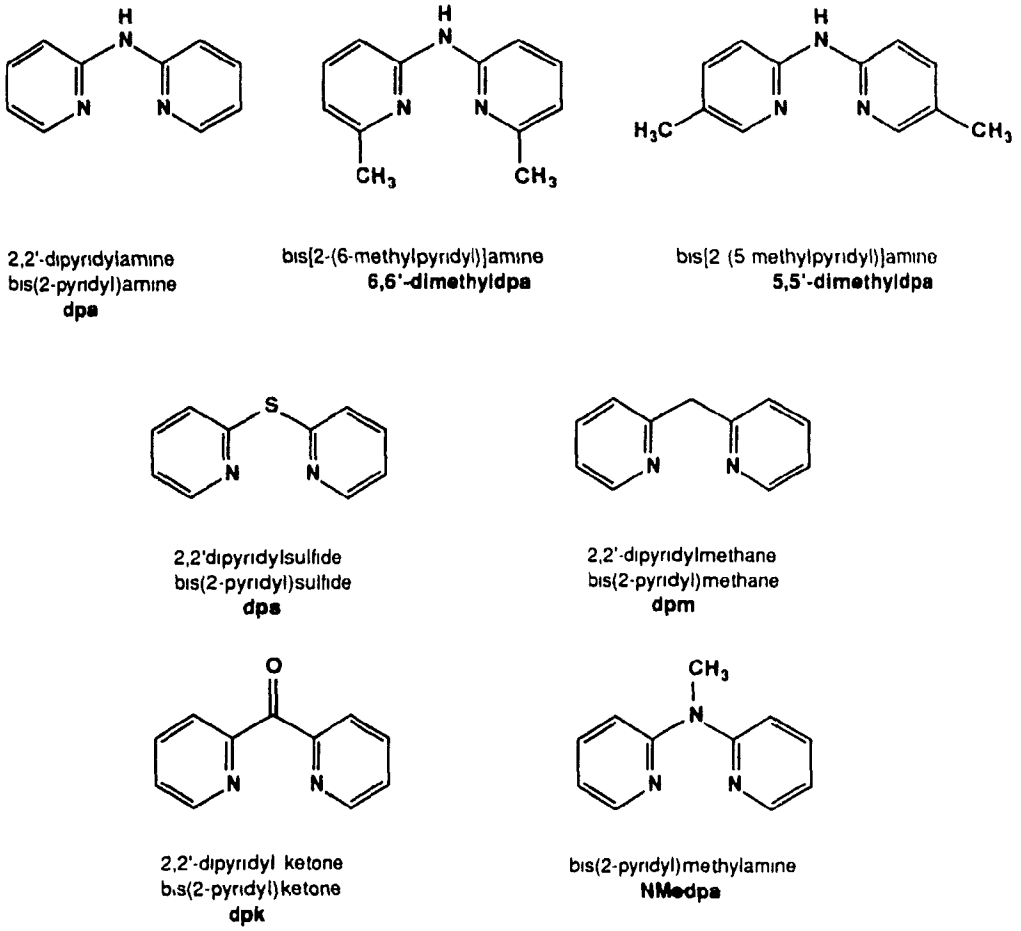

Figure 3.6. Modified dipyridylamine ligands used in this study

A significant difference for BDNPP hydrolysis is observed by changing the bridging group between the two pyridyl moieties. Hydrolysis of the phosphate diester could not be studied for $[Cu(dps)(OH_2)_2]^{2+}$ because of precipitation of the complex at neutral pH. The Cu(II) complex of dipyridyl ketone was also inactive at pH 8.

Studies have revealed[69] that dpk coordinates with Cu(II) via the two nitrogen atoms but the keto group is actually present in the form of a geminal diol. At pH above 4.5, one of the geminal hydroxy groups becomes deprotonated leading to a rearrangement of the binding sites from a six-membered N,N chelate to a five-membered N,O chelate as shown in figure 3 7. The resulting N,O chelate is inefficient for phosphate diester hydrolysis.

Of the four complexes listed in table 2 7, the Cu(II) complexes of dpm and NMedpa are the least efficient for promoting the rate for BDNPP hydrolysis In other words, the most efficient complexes are those which have a NH bridging group between the two pyridine rings. Compared with the Cu(II)-dpa complex, $[Cu(dpm)(OH_2)_2]^{2+}$ and $[Cu(NMedpa)(OH_2)_2]^{2+}$ are 2.6 and 3.9 times slower at hydrolyzing BDNPP respectively (table 2.7) The result is interesting considering all four complexes have similar pKa and K_{dim} values (table 2.1).

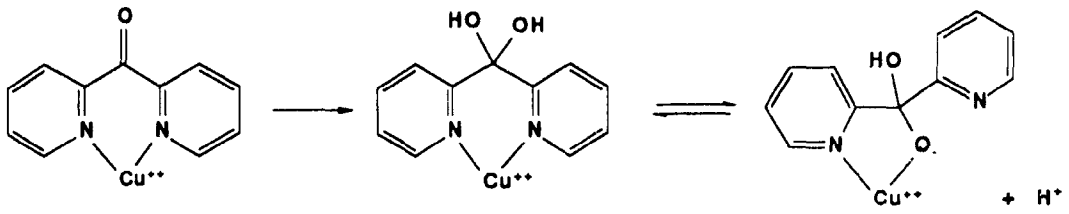

Figure 3.7. Hydration and rearrangement of Cu(II)-dpk complex (ref 69)

For Cu(II)-dpa and Cu(II)-5,5'-dimethyldpa complexes, the ligand is planar through resonance of the electron donating amino group into the pyridine rings. No such resonance is possible for the Cu(II)-dpm complex. X-ray structures show formation of a planar six-membered ring between dpa and Cu(II)[60,70] while the formation of a chelate in the boat form is achieved between a metal ion and the dpm ligand.[71] For phosphate ester hydrolysis, it should be easier to form the four-membered ring transition state structure from the geometry of the former complex; it follows that $[Cu(dpa)(OH_2)_2]^{2+}$ is more active than $[Cu(dpm)(OH_2)_2]^{2+}$ for BDNPP hydrolysis.

---

[69]a) B E Fischer and H Sigel, *Inorg Chem* , **1979**, 18, 425. b) B. E. Fischer and H Sigel, *J Inorg Nucl Chem* , **1975**, 37, 2127

[70]N Ray, S Tyagi and B Hathaway, *J Chem Soc , Dalton Trans* , **1982**, 143

[71]G Newkome, V K Gupta, C R Taylor, and R R Fronczek, *Organometallics*, **1984**, 3, 1549

For $[Cu(NMedpa)(OH_2)_2]^{2+}$, unlike $[Cu(dpa)(OH_2)_2]^{2+}$, coplanarity of the ligand and conjugation over the bridging N atom is difficult to maintain because of the unfavourable steric interactions that would result between the methyl group and the 3 and 3' hydrogens on the pyridine rings. Therefore, in order to avoid the steric hindrance, a geometry similar to the Cu(II)-dpm complex should be displayed. Thus $[Cu(NMedpa)(OH_2)_2)]^{2+}$ is not as efficient as $[Cu(dpa)(OH_2)_2]^{2+}$ for phosphate ester hydrolysis.

3.3 OTHER METAL(II) COMPLEX PROMOTED HYDROLYSIS OF PHOSPHATE DIESTERS

It has been shown in this study that, depending on the ligand structure, Cu(II) complexes can be efficient at hydrolyzing phosphate diesters. How does this compare to other divalent metal complexes? The complexes formed from the 1:1 addition of M(II) ion and the neocuproine ligand were studied. We chose the neocuproine ligand to avoid the complications arising from dimerization processes.

The pH-rate profile (fig. 2.6) for the Cu(II) complex promoted hydrolysis of BDNPP shows a pH independent region at pH>7, whereas the Co(II) complex displays a pH independent region at pH>9. These observations can be explained by the differing pKa values for the coordinated water molecules (table 2.8).

An important role of the metal ion, for phosphate ester hydrolysis, is to act as a Lewis acid activating the phosphorus towards nucleophilic attack. Although Co(II) is a weaker Lewis acid than Cu(II), its coordinated hydroxide anion is more nucleophilic. It seems that these two effects cancel each other since the maximal rates for Cu(II) and Co(II) complex mediated hydrolysis of BDNPP do not differ significantly (table 2.4 and 2.8). Interestingly, compared to Cu(II) and Co(II), the Ni(II) complex, at pH 9.5, is appproximately two times more reactive at hydrolyzing BDNPP. The full pH-rate profile could not be obtained because of precipitation of the complex above pH 9.5. The Zn(II) neocuproine complex precipitated out as $Zn(OH)_2$ at neutral pH.

It is difficult to draw general conclusions based upon the results of these three complexes. Several factors are involved other than differing Lewis acidities and acid dissociation constants. The three metal complexes have different geometrical structures. Cu(II) is square planar, Co(II) is tetrahedral[72a], and the Ni(II) complex is octahedral[72b].

[72a] F. Walmsley, A. A. Pinkerton, and J. A. Walmsley, *Polyhedron*, **1989**, 8, 689. b) H. S. Preston and C. H. L. Kennard, *J. Chem. Soc., Chem. Commun.*, **1967**, 1167.

(the axial positions are occupied by water). The geometry of the metal complex can significantly affect the efficiency of the metal catalyst.

The size of the metal ion can also play a major role For example, Hendry and Sargeson[73] showed that the rate of hydrolysis of the Ir(III) complex, cis-$[en_2Ir(OH)OP(O)(OC_2H_5)(OC_6H_4NO_2)]^+$, is 10^3 fold slower than the analogous Co(III) complex despite the more basic coordinated hydroxide on the Ir(III) ion The reduction in rate was ascribed to the larger size of the Ir(III) ion compared to Co(III) which made ring closure more difficult.

The advantage of the Ni(II) and Co(II) complexes over Cu(II) is that the former complexes are less redox active However, they are only active in the alkaline pH range whereas Cu(II) complexes are active at hydrolyzing phosphate esters in the preferred physiological pH range.

3.4 COMPARISON OF Cu(II) COMPLEXES WITH Co(III) COMPLEXES ON PHOSPHATE DIESTER HYDROLYSIS

Although the Cu(II) complexes are square planar and the Co(III) complexes are octahedral, there are important similarities between the two types of complexes on phosphate diester hydrolysis First, the metal bound water molecules are in the cis orientation in both the copper and cobalt complexes Second, the metal bound water molecules have comparable acidities. Third, maximum reactivity of the cobalt and copper complexes can be obtained at neutral to slightly alkaline pH The mechanisms for $[(L)Cu(OH_2)_2]^{2+}$ and $[(N_4)Co(OH_2)_2]^{2+}$ promoted hydrolysis of BDNPP are comparable For both types of complexes, the structure of the ligand can significantly influence the rate of hydrolysis on phosphate diesters. The comparison between $[Cu(neo)(OH)(OH_2)]^+$ vs. $[Cu(dpa)(OH)(OH_2)]^+$, and $[Co(tren)(OH)(OH_2)]^{2+}$ vs $[Co(trpn)(OH)(OH_2)]^{2+}$ are strikingly similar In both cases, the complexes containing a six-membered ring opposite the hydroxy and aqua ligands are better able to stabilize the proposed transition state four-membered ring structure than the complexes containing a five-membered ring opposite the hydroxy and aqua ligands

However, Co(III) complexes are still more efficient than Cu(II) complexes at hydrolyzing phosphate diesters. For example, compared with $[Cu(dpa)(OH)(OH_2)]^+$,

[73] P Hendry and A M Sargeson, *J Am Chem Soc*, **1989**, 111, 2521

$[Co(trpn)(OH)(OH_2)]^{2+}$ promotes the hydrolysis of BDNPP and BNPP 5 7 and 14 times more rapidly, respectively (table 2.5).

3.5 Cu(II) PROMOTED HYDROLYSIS OF PHOSPHATE MONOESTERS

3.5.1 Hydrolysis of Good Leaving Groups

Up to now the discussion has primarily focussed on Cu(II) complex promoted hydrolysis of phosphate diesters to monoesters As shown in table 2 10, the subsequent hydrolysis, that is, the hydrolysis of the phosphate monoester promoted by $[Cu(dpa)(OH_2)_2]^{2+}$ is not as efficient. At 1mM concentration of Cu(II) complex (pH 8, and 25 °C), only a six-fold rate enhancement, over the uncatalyzed rate, is observed for the Cu(II) complex promoted hydrolysis of DNPP whereas a 6 3 x 10^3 fold rate enhancement is observed for the hydrolysis of the phosphate diester, BDNPP In addition, $[Cu(dpa)(OH_2)_2]^{2+}$ hydrolyzes DNPP twelve times slower than the corresponding phosphate diester.

The observation that Cu(II) complexes hydrolyze phosphate monoesters less efficiently than phosphate diesters seems to be a general trend Morrow and Trogler [51a] observed that the rate for $[Cu(bpy)(OH_2)_2)]^{2+}$ promoted hydrolysis of NPP at 75 °C, pH 8, is three times slower ($k = 6.4 \times 10^{-3}\ M^{-1}s^{-1}$) compared to the hydrolysis of the analogous phosphate diester, BNPP ($k = 2 \times 10^{-2}\ M^{-1}s^{-1}$) The result is interesting considering that in the absence of any catalyst, phosphate monoesters hydrolyze more rapidly than phosphate diesters (see tables 1 1 and 2 10 and fig.1 13)

The Cu(II) promoted hydrolysis of DNPP can follow three possible reaction paths as outlined in figure 3.8. It is proposed that the Cu(II) complex promoted hydrolysis of DNPP occurs by the same mechanism to that presented for phosphate diesters as shown in figure 3.1. (and mechanism A in fig 3 8.) The hydrolysis reaction should not occur by the metaphosphate mechanism (mechanism B fig 3 8) since, for DNPP, the uncatalyzed hydrolysis of the monoanion is much slower than that for the dianion[18] (fig 1 10) If mechanism B is operative, then the Cu(II) complex will inhibit (or retard) phosphate monoester hydrolysis.

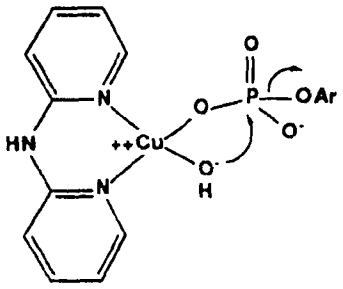

Mechanism A

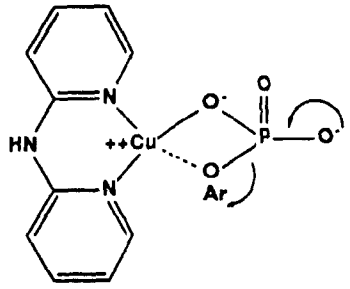

Mechanism B

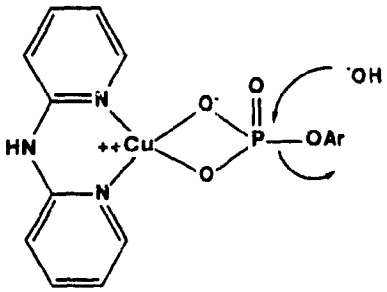

Mechanism C

Figure 3.8 Possible mechanisms for Cu(II) complex promoted hydrolysis of DNPP

Chelation of the phosphate monoester followed by attack by an external nucleophile as depicted by mechanism C can also be ruled out. This mechanism is analogous to $[Co(trpn)(OH_2)_2]^{3+}$ promoted hydrolysis of phosphate monoesters with poor leaving groups[47] (fig 1.21 and 1.22). This mechanism is unlikely since hydrolysis of methyl phosphate could not be detected (see sect. 3.5.2).

One of the reasons why phosphate diesters are stable towards hydrolysis is because of unfavourable electrostatic interactions between the the phosphate anion and the oncoming anionic hydroxide nucleophile [15] This electrostatic barrier is reduced when the diester is bound to the Cu(II) ion thus facilitating an intramolecular metal-hydroxide attack. For the dianionic phosphate monoester, unfavourable electrostatic interactions still exist between the coordinated monoester and the metal-hydroxide It follows that Cu(II) mediated hydrolysis of phosphate diesters are more efficient than that for phosphate monoesters. This does not explain why the trend is reversed for Co(III) complexes. Co(III) complexes promote the hydrolysis of phosphate monoesters much more efficiently

than for phosphate diesters,[33c,38b,41] yet the mechanisms for Co(III) and Cu(II) complex promoted hydrolysis of phosphate esters are the same.

3.5.2 Hydrolysis of Poor Leaving Groups

It has been shown in our lab by Chin and Banaszczyk[47] that $[Co(trpn)(OH_2)_2]^{3+}$ promoted hydrolysis of phospho-monoesters with poor leaving groups is different compared to hydrolysis of those with good leaving groups. Addition of one equivalent of $[Co(trpn)(OH_2)_2]^{3+}$ to methyl phosphate produces a stable cobalt complex **3** (fig 1.21) that subsequently hydrolyzes upon further addition of the Co(III) complex. It would be interesting to determine if this same mechanism would apply for $[Cu(dpa)(OH_2)_2]^{2+}$. Under the same conditions employed for the $[Co(trpn)(OH_2)_2]^{3+}$ case (50 °C for several hours), hydrolysis of methyl phosphate was not detected by the addition of two equivalents of the Cu(II) complex. This result is not surprising considering that the Cu(II) complex was not very efficient at hydrolyzing the more reactive phosphate monoester, DNPP. At pH 7, 25 °C, the spontaneous rate of hydrolysis for DNPP ($k = 2.22 \times 10^{-5}\ s^{-1}$) is 10^5 times more rapid than that for methyl phosphate ($k = 2.6 \times 10^{-10}\ s^{-1}$).

For the Co(III) complex promoted hydrolysis of methyl phosphate, it is the chelated phosphate monoester that acts as the 'true substrate'. Cu(II) complexes are not efficient at hydrolyzing phosphate monoesters, but would 'cooperative catalysis' occur for methyl phosphate hydrolysis by the 1:1 addition of $[Co(trpn)(OH_2)_2]^{3+}$ and $[Cu(dpa)(OH_2)_2]^{2+}$?

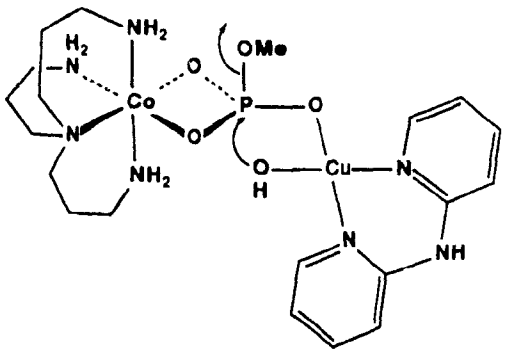

Figure 3.9 Proposed mechanism of methyl phosphate hydrolysis by the 1:1 addition of $[Co(trpn)(OH_2)_2]^{3+}$ and $[Cu(dpa)(OH_2)_2]^{2+}$

Figure 2.7 shows the ^1H NMR spectra for the production of CH_3OH from the $[Cu(dpa)(OH_2)_2]^{2+}$ promoted hydrolysis of $[Co(trpn)(PO_3OMe)]^+$. Cu(II) complexes with one less available coordination site, such as $[Cu(terpy)(OH_2)]^{2+}$, do not hydrolyze the Co(III) chelated phosphate monoester Therefore, the mechanism of hydrolysis should be similar to the one proposed for the $[Co(trpn)(OH_2)_2]^{3+}$ case, which is shown in figure 3.9.

The system which employs 2 eq. of $[Co(trpn)(OH_2)_2]^{3+}$ is still two times more reactive at hydrolyzing methyl phosphate than the system which involves the 1:1 addition of Co(III) and Cu(II) complex. However, at 5mM metal complex concentration, a significant amount of the Cu(II) complex is in its inactive dimer form. The actual amount of the active monomer present in solution is less than one half the concentration of the Co(III) complex[74], thus, the difference in reactivity is mainly due to the greater concentration of $[Co(trpn)(OH)(OH_2)]^{2+}$ over that for $[Cu(dpa)(OH)(OH_2)]^+$.

[74]The concentration of monomer is 2.38 mM calculated from eq. 5 using $K_{dim} = 230\ M^{-1}$ (see appendix)

4. INTRODUCTION

4.1 ARTIFICIAL ESTERASES AND PEPTIDASES

4.1.1 Importance of Developing an Artificial Esterase/Protease

The ability of proteolytic enzymes and chemical reagents to selectively cleave peptides and proteins at defined sequences has greatly facilitated studies of protein structure and function.[75] In comparison with the number of sequence selective nucleases available for analyzing and manipulating nucleic acid structure, only a limited number of selective peptide cleavage agents exist The development of an artificial protease that is capable of cleaving peptides at specific sites would greatly facilitate the mapping of protein structural domains and protein sequencing. In addition, such molecules would likely lead to the development of new therapeutic agents to selectively hydrolyze protein coats of viruses, cancer cells, or other physiological targets.[76]

The development of an artificial esterase would also lead to new therapeutic agents. Nature has made wide use of the carboxylic ester. For example, triacylglycerols serve as efficient reserves for the storage of energy, and acetylcholine, a neurotransmitter, is important for nerve impulse transmission. Phospholipids, the major structural lipids of all biological membranes are also comprised of carboxylic esters (fig 1.2) Many biochemical processes involve ester formation, transacylation, or hydrolysis.

For the organic chemist, artificial esterases may be used for stereoselective acylation and for kinetic resolution of alcohols. In the field of organic synthesis, one can imagine the use of these molecules for regioselectively removing blocking groups.

4.1.2 Previous Work

In the past decade, the strategy of most research teams for developing artificial esterases or proteases was to incorporate, into their systems, functional groups determined to be present in the enzyme's active site and which were essential for maintaining the enzyme's activity. The most often mimicked enzymes were esterases or peptidases like chymotrypsin, papain, and carboxypeptidase A.

---

[75]D Hoyer, H Cho, and P G Schultz, *J Am Chem Soc* , **1990**, 112, 3249 (references therein)
[76]P G. Schultz, R. A. Lerner, and S J Benkovic, *Chemical and Engineering News*, **1990**, 68(22), 26

D'Souza and Bender[77] have developed a 'miniature organic model' of chymotrypsin. The serine protease uses the imidazole group of histidine 57, the hydroxyl group of serine-195, and the aspartate-102 carboxylate group to perform the hydrolysis of peptides and esters. Bender and D'Souza's enzyme model contained the aforementioned triad of catalytic groups. The model consisted of an imidazole-benzoate group covalently attached to the secondary side of β-cyclodextrin (**6** in fig. 4.1). The kinetic constants for hydrolysis of m-(tert-butyl)phenyl acetate by **6** at its pH optimum of 10.7 were compared with those for hydrolysis of p-nitrophenyl acetate by chymotrypsin at its pH optimum of 8.0 Since K_{cat}/K_m for **6** catalyzed hydrolysis of m-(tert-butyl)phenyl acetate was very close to that for chymotrypsin catalyzed hydrolysis of p-nitrophenyl acetate, the authors believed that **6** catalyzed the hydrolysis of the ester by using the charge-relay mechanism as depicted in figure 4.1 Recently, however, the mechanism has been re-examined.[78] It is now generally accepted that the mechanism involves nucleophilic attack by an ionized cyclodextrin hydroxyl, without involvement of the imidazole-carboxylate moiety.

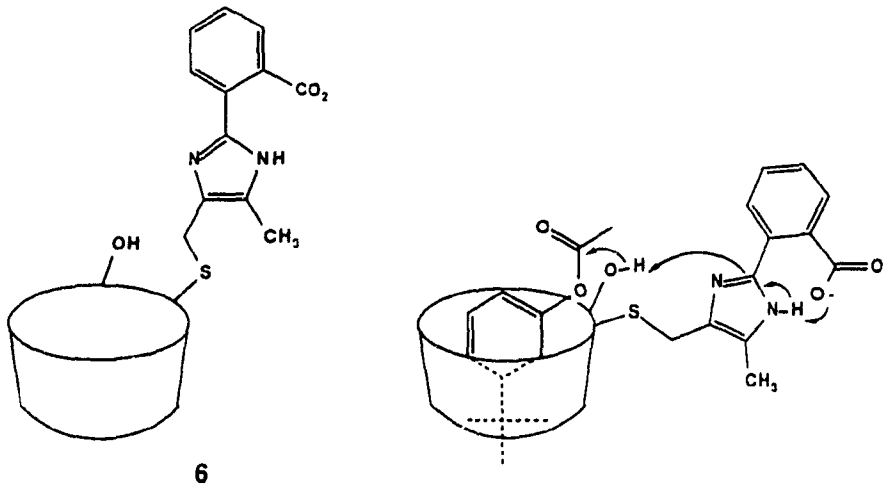

Figure 4.1 The 'miniature organic model' of chymotrypsin and the proposed charge-relay mechanism for ester hydrolysis (ref 77)

Lehn and Serlin[79] have prepared a chiral crown ether catalyst bearing cysteinyl residues to mimic the enzyme papain (fig. 4.2). The catalyst complexes primary

[77] V T D'Souza and M L Bender, *Acc Chem Res*, **1987**, 20, 146

[78] a) R Breslow and S Chung, *Tetrahedron Lett*, **1989**, 30, 4353 b) S C Zimmerman, *Tetrahedron Lett*, **1989**, 30, 4357

[79] J M Lehn and C Serlin, *J Chem Soc Chem Commun*, **1978**, 949

ammonium salts and displays enhanced rates of thiolysis for dipeptide ester substrates It also shows high chiral recognition for the L-enantiomer (70 times faster) of a racemic mixture of glycylphenylalanine p-nitrophenyl esters The 10^3-10^4 rate acceleration over uncomplexed substrates are due to complexation of the primary ammonium salt in the crown ether cavity and the participation of an SH group of the cysteinyl residues to give an S-acyl intermediate This artificial enzyme model displays molecular complexation, rate acceleration, and structural and chiral discrimination analogous to true biological catalysts

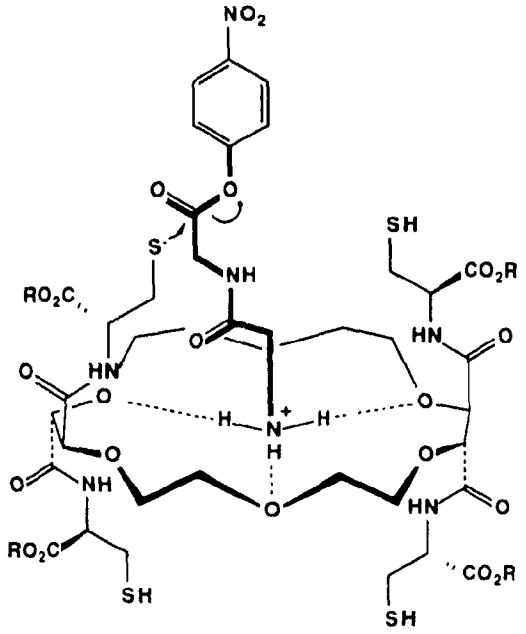

Figure 4.2 The dipeptide substrate, glycyl-glycine p-nitophenyl ester, binds to the macrocyclic receptor to undergo transacylation (ref 79)

More recently, Tecilla and Hamilton[80] have synthesized a catalytic system in which a peptide-like substrate is held, solely by hydrogen bonds, in proximity to an appended thiol nucleophile The researchers took advantage of the strong hexa-hydrogen bonding complementarity that exists between barbiturates and two 2,6-diamidopyridine units linked through an isophthalate spacer (fig 4 3) A barbiturate derivative with an acetate ester substituent in the 5-position, H-bonds (via 6-H-bonds as shown in fig 4 3) to the receptor

[80] P Tecilla and A D Hamilton, *J. Chem Soc , Chem Commun* , **1990**, 1232

and undergoes thiolysis. A rate acceleration of more than 10^4 is observed for the transacylation reaction

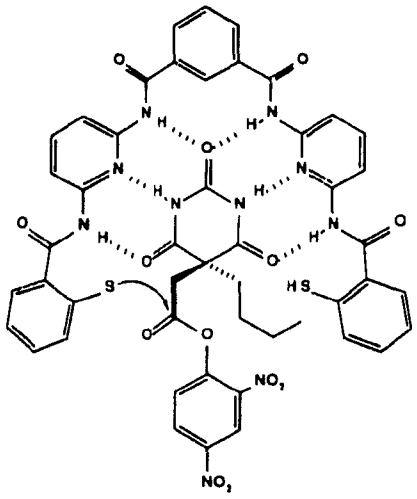

Figure 4.3 Thiolysis reaction of a H-bonding receptor complexed to a barbiturate acetate derivative (ref 80)

A strategy for the generation of selective protein cleaving agents is based on oxidative cleavage of the polypeptide backbone Schultz and his co-workers[81] have attached the metal chelator, EDTA, to biotin (fig 4.4a) This conjugate selectively delivers redox-active Cu^{2+} or Fe^{3+} in close proximity to the polypeptide backbone at the biotin binding site of streptavidin, resulting in selective protein cleavage at that site This strategy is similar to the one employed for developing artificial nucleases in which EDTA-Fe^{2+} conjugates of DNA binding groups are used to oxidatively cleave nucleic acids

A similar approach has been independently described by Schepartz and Cuenod[82] where EDTA was covalently tethered to the calmodulin antagonist, trifluoperazine (TFP), to produce an affinity cleavage reagent for calmodulin (fig 4.4b) The trifluoperazine-EDTA adduct binds to the protein in a Ca^{2+} dependent manner, thus, in the presence of Ca^{2+}, Fe^{2+}, O_2, and dithiothreitol, the TFP-EDTA conjugate cleaves calmodulin to produce six major cleavage fragments.

[81] D Hoyer, H Cho, and P G Schultz, *J Am Chem Soc*, **1990**, 112, 3249
[82] A Schepartz and B Cuenod, *J Am Chem Soc*, **1990**, 112, 3247.

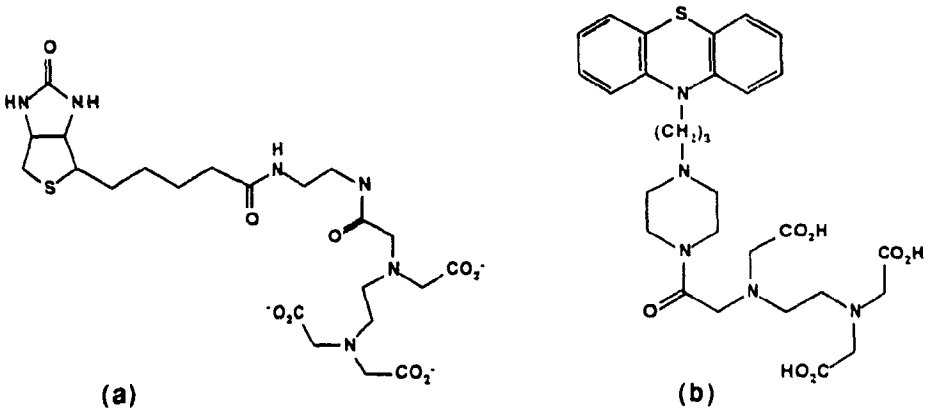

Figure 4.4 a) Biotin-EDTA conjugate (ref 81) **b)** Trifluoperazine-EDTA conjugate (ref 82)

In the past few years, antibodies have been used to catalyze the hydrolysis of esters and amides.[76,83] It has become possible, with the advent of hybridoma technology, to generate homogeneous, high affinity antibodies that selectively recognize virtually any molecule of interest. Catalysis is achieved by immunizing an animal with a transition state analogue that, in both shape and charge distribution, resembles a high energy structure thought to be a rate-limiting transition state in the reaction pathway. The generated antibodies catalyze the desired reaction through binding forces that lower the energy of the intermediate, and thus reduce the overall reaction barrier. The first examples of catalytic antibodies specific for transition state analogues bound tetrahedral, negatively charged phosphonate transition state anologues for the hydrolysis of esters. Monoclonal antibodies specific for a tetrahedral transition state analogue **7** (fig. 4.5) were found to selectively catalyze the hydrolysis of the corresponding ester **8**. Rate accelerations of 10^3-10^6 were observed. Since the first reports of antibody catalysis in 1986, hydrolysis of unactivated esters and amides have also been published, in addition, a considerable number of different reactions have been catalyzed with specificity and efficiency.

Remarkable as all of the above artificial protease and esterase models are, with the exception of catalytic antibodies, they fall considerably short of natural enzymes. Whereas natural enzymes hydrolyze unactivated esters and amides, the artificial esterases only transacylate activated esters or, as in the case of the protease models, oxidatively cleave

[83]P. G. Schultz, *Acc. Chem. Res.*, **1989**, 22, 287 (and references therein)

amide bonds. Although catalytic antibodies have been shown to hydrolyze simple esters

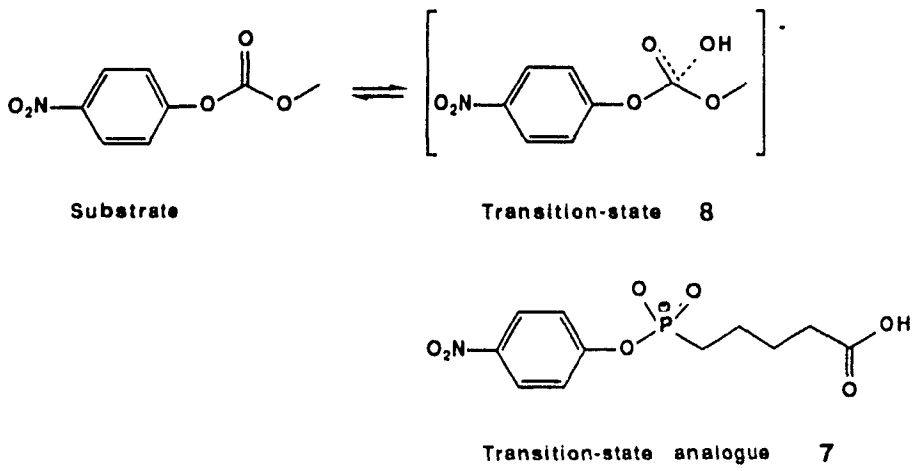

Figure 4.5 Phosphonate ester as transition-state analogue for antibody catalyzed hydrolysis of esters (ref 76)

and amides with great efficiency, their competency is greatly reduced when hydrolyzing more complex substrates This is because the tetrahedral phosphonate transition state analogue contributes less to the overall binding affinity of a large antigen to the antibody.[76] Clearly, there is a need to design a simple yet efficient system that hydrolyzes unactivated esters and amides. Part of my research has focussed on developing such catalysts

4.2 MECHANISM OF ESTER HYDROLYSIS

In order to design efficient catalysts for the hydrolysis of esters, it is necessary to understand the mechanisms of carboxylic ester hydrolysis in the absence of any catalyst. By doing so, one can also lay the groundwork for determining the catalytic mechanisms of hydrolytic enzymes.

The mechanism for ester hydrolysis is well understood [84] Carboxylic esters can be hydrolyzed in either basic or acidic solution. The mechanistic designations $A_{AC}2$ and $B_{AC}2$ are given to the acid and base catalyzed mechanisms, respectively. The letter A

[84]F A Carey and J Sundberg, *Advanced Organic Chemistry, Part A Structure and Mechanism*, Plenum Press New York, 1984, pp 421-430

stands for acid catalysis, B denotes base catalysis and AC indicates acyl-oxygen fission. The digit 2 represents the bimolecular nature of the rate determining step The acid and base mechanisms are shown in figures 4 6(a) and 4 6(b) respectively Evidence supporting these mechanisms include the expected dependence of hydrogen ion and hydroxide ion concentration, and isotope labelling studies that prove the acyl-oxygen, not the alkyl-oxygen bond, is cleaved during hydrolysis. Esters without special structural features hydrolyze by these mechanisms

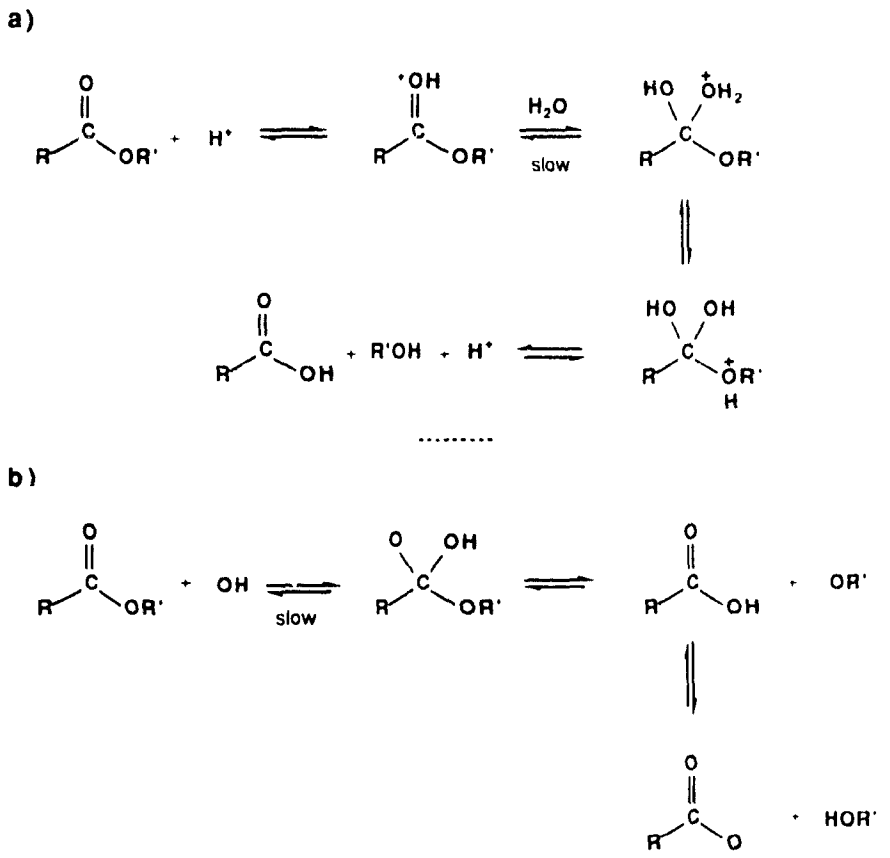

Figure 4.6 **a)** Acid catalyzed hydrolysis of esters ($A_{AC}2$ mechanism), **b)** Base catalyzed hydrolysis of esters ($B_{AC}2$ mechanism)

Alkyl-oxygen fission may occur when the ester is derived from a tertiary alcohol The change in mechanism is due to the stability of the carbonium ion that can be formed by

C-O heterolysis, and probably also to a decrease in the rate of nucleophilic attack at the carbonyl group because of steric factors.

The ester hydrolysis mechanisms discussed thus far have pertained to aqueous solutions of strong acids and strong bases. In media in which other acids and bases are present, general acid/base and nucleophilic catalysis must be considered It has been observed that general base catalysis occurs if the leaving group is several pK units more basic than the catalyst The transition state for esters undergoing hydrolysis by a general base catalyzed mechanism involves partial proton removal from the attacking water to the general base in the formation of the tetrahedral intermediate[85] (fig 4.7).

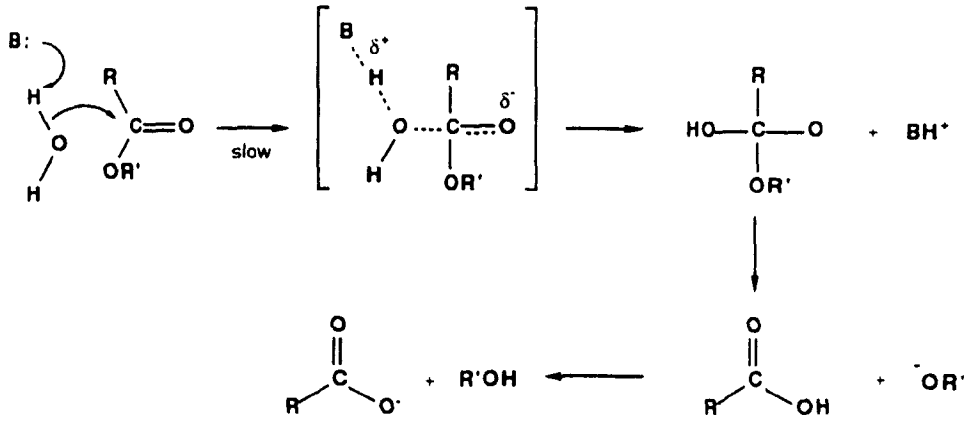

Figure 4.7 General base catalyzed hydrolysis of esters (ref 85)

Nucleophilic catalysis occurs if the attacking nucleophile is more basic than the alkoxy leaving group. For example, esters of relatively acidic alcohols (in particular, phenols) are hydrolyzed by the nucleophilic catalysis mechanism in the presence of imidazole[85] A more detailed analysis of this mechanism will be presented in the discussion concerning nucleophilic catalysis of esters (section 6.1.1).

[85] J F Kirsch and W P Jencks, *J Am Chem Soc*, **1964**, 86, 837

4.3 MECHANISM OF AMIDE HYDROLYSIS

The mechanisms for amide hydrolysis are more complex compared with the mechanism for ester hydrolysis. The hydrolysis of amides to carboxylic acids and amines requires considerably more vigorous conditions than those for ester hydrolysis. Recently, Kahne and Still[86] have developed a sensitive radioassay capable of measuring peptide bond hydrolysis at neutral pH and room temperature. The pseudo-first-order rate constant of hydrolysis of a tripeptide was reported to be 3×10^{-9} s^{-1} which corresponds to a half-life of approximately seven years. In general, amides are thousands of times less reactive than esters (table 4.1). Because of the inherent stability of amide bonds, most studies involving amide hydrolysis deal with activated amides.

Table 4.1 Second-order rate constants for hydroxide ion catalyzed hydrolysis of esters and amides at 25 °C

Substrate	k ($M^{-1}s^{-1}$)	Rel. rate	ref.
CH_3COOCH_3	1.5×10^{-1}	2027	107
CH_3CONH_2	7.4×10^{5}	1	a
$HCON(CH_3)_2$	1.8×10^{4}	2.43	b

a T. Yamana, Y. Mizukami, A. Tsuji, Y. Yasuda, and K. Masuda, *Chem. Pharm. Bull.* **1972**, 20, 881.
b J. P. Guthrie, *J. Am. Chem. Soc.*, **1974**, 96, 3608.

In some amide hydrolyses, the breakdown of the tetrahedral intermediate may proceed through the formation of a dianion. For example, the mechanism of hydrolysis of p-nitroacetanilide[87] (fig. 4.8) involves nucleophilic attack of hydroxide ion to form a tetrahedral intermediate, followed by ionization to a dianion, and rate determining unimolecular breakdown to acetate ion and anilide ion. At pH>13, the addition of hydroxide to form the tetrahedral intermediate becomes the rate-determining step.

[86]D. Kahne and W. C. Still, *J. Am. Chem. Soc.*, **1988**, 110, 7529.
[87]R. M. Pollack and M. L. Bender, *J. Am. Chem. Soc.*, **1970**, 92, 7190.

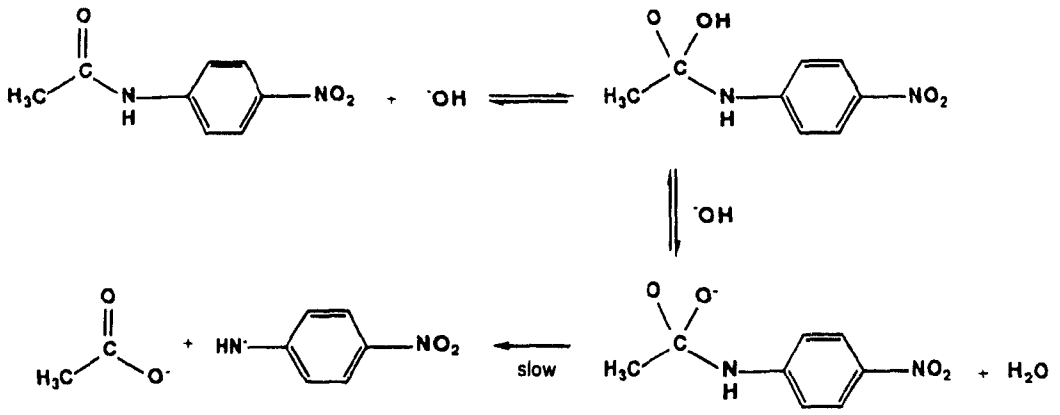

Figure 4.8 Hydroxide ion catalyzed hydrolysis of p-nitroacetanilide (ref 87)

For acyl-activated amides, simple proton transfer to the leaving group in the tetrahedral intermediate is rate determining for poor leaving groups ($pK_b<9$) with the subsequent C-N bond cleavage being rapid, while good leaving groups ($pK_b>9$) follow rate-determining fission of the C-N bond proceeded by fast proton transfer (fig. 4.9)[88]

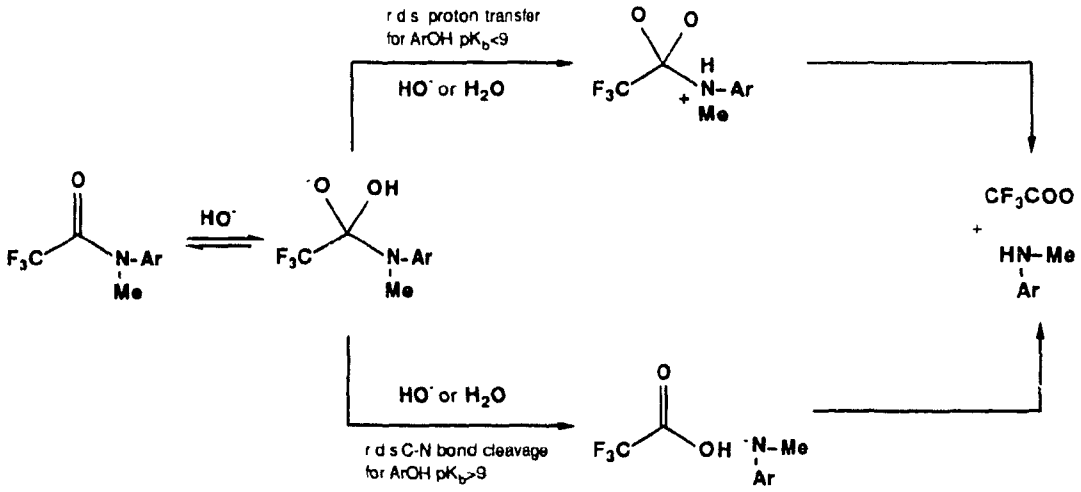

Figure 4.9 Hydrolysis of acyl-activated amides (ref 88)

[88a] L. D. Kershner and R. L. Schowen, *J Am Chem. Soc* , **1971**, 93, 2014

The principal difference between ester and amide hydrolysis (i.e. for unactivated esters and unactivated amides) lies in the poorer ability of amide ions (formally RNH^-) to act as leaving groups compared to alkoxides. As a result, protonation at nitrogen is required prior to or in concert with the breakdown of the tetrahedral intermediate. For amides without any special structural features (i.e. unactivated amides), hydrolysis at neutral pH proceeds according to a rate-limiting tetrahedral intermediate breakdown mechanism (fig. 4.10). The mechanism involves addition of the hydroxide to the amide, forming the tetrahedral intermediate **T1** followed by proton transfer **T2** and the rate-determining expulsion of the amine leaving group.[89]

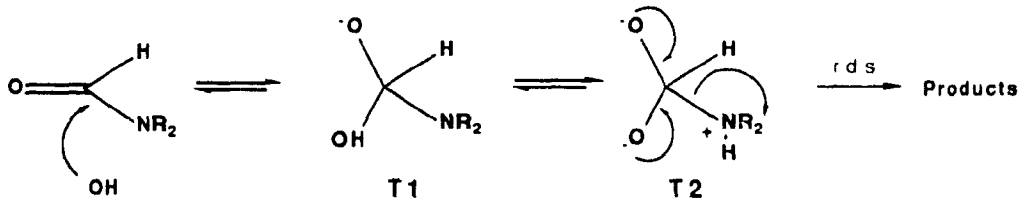

Figure 4.10 Hydrolysis of unactivated amides

General acid/base catalysis can also greatly facilitate amide hydrolysis.[89] It is not unusual to observe bifunctional buffer catalysis where the actual structure of the buffer is important towards catalysis. For example, Cunningham and Schmir[89d] observed that imidazole buffers were ineffective at catalyzing the breakdown of the tetrahedral intermediate in the hydrolysis of 4-hydroxybutyranilide. Catalysis was observed only for those buffers which carried both a proton and a basic centre such as phosphate or bicarbonate ions (fig. 4.11). For 4-hydroxybutyranilide hydrolysis, the breakdown of the tetrahedral intermediate is rate determining at low phosphate concentrations and is accelerated at increasing phosphate concentrations until it is as fast as the formation of the intermediate. At higher concentrations of phosphate, the first step, formation of the tetrahedral intermediate, becomes rate determining and the rate becomes independent of buffer concentration.

---

[89]a) D. Drake, R. L. Schowen, and H. Jayaraman, *J. Am. Chem. Soc.*, **1973**, 95, 454. b) I. Meresaar and L. Bratt, *Acta Chem. Scand.*, **1974**, A 28, 2. c) S. O. Eriksson and C. Holst, *Acta Chem. Scand.*, **1966**, 20, 1892. d) A. J. Kirby and A. Fersht, *Prog. Bioorg. Chem.*, **1971**, 1, 1. e) R. W. Hay, A. K. Basak, M. P. Pujari, and A. Perotti, *J. Chem. Soc. Dalton Trans.*, **1989**, 197.

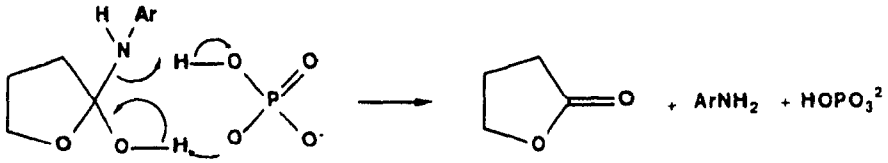

Figure 4.11 Phosphate buffer catalyzed hydrolysis of 4-hydroxybutyroanilide (ref 89d)

4.4 METAL ION PROMOTED HYDROLYSIS OF ESTERS AND AMIDES

In 1951, Kroll[28] discovered that Cu^{2+} catalyzed the hydrolysis of amino acid esters (fig. 1 15). For phenylalanine ethyl ester, the rate enhancement due to Cu^{2+} was 10^6 at pH 7 3. Since that time there have been numerous studies on metal ion promoted hydrolyses of α-amino acid esters and amides. Most studies involved substitutionally inert Co(III) complexes so that reaction intermediates could be identified and mechanisms could be differentiated.[90]

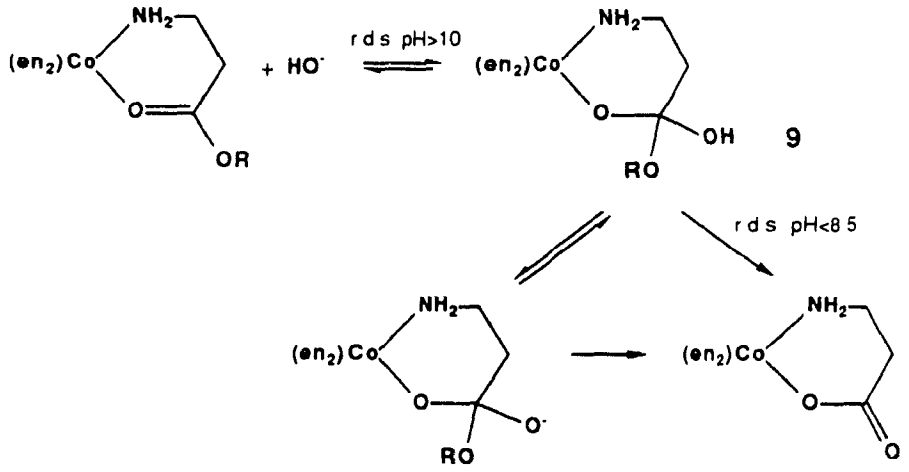

Figure 4.12 Co(III)-promoted hydrolysis of β-alanine ester (ref 90)

Cobalt(III) complex promoted hydrolysis of amino acid esters can occur by two mechanisms· 1) by coordination of the metal ion to the acyl oxygen followed by intermolecular hydroxide attack, 2) by intramolecular nucleophilic attack of a cobalt bound hydroxide ion. ^{18}O-tracer studies with the glycine and β-alanine chelates showed that the

[90]For a review see P A Sutton and D A Buckingham, *Acc Chem Research*, **1987**, 20, 357.

chelate ring remains intact during hydrolysis and that acyl-oxygen cleavage occurs for esters of primary and secondary alcohols. The directly activated esters are accelerated 10^6 fold by the metal. However, for t-butyl esters, alkyl-oxygen bond fission occurs and only a 30 fold rate enhancement is detected. For the chelated β-alanine ester, elimination of ^-OR is rate determining below pH 8.5 but above this pH, deprotonation of **9** (fig. 4.12) becomes significant so that by pH 10, rapid loss of ^-OR from its conjugate base is the preferred route and addition of hydroxide ion becomes rate determining.

Hydrolysis of amino acid esters by coordinated hydroxide ion was first demonstrated by Buckingham et al.[91] in 1969 (fig. 4.13). Metal-hydroxide attack was found to be the rate-determining step. For the β-alanine ester system, hydrolysis by this mechanism is 3×10^5 times slower compared with the Lewis acid mechanism. However, since the intramolecular metal-hydroxide mechanism is dependent on chelate ring size, such differences cancel in forming five-membered ring systems.

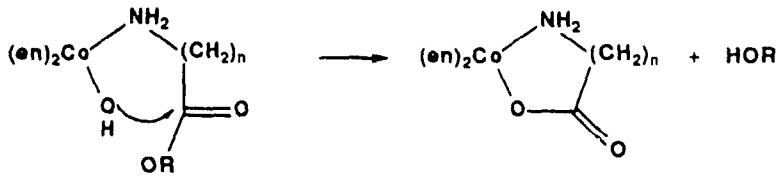

Figure 4.13 Metal-hydroxide mechanism for Co(III)-promoted hydrolysis of amino acid esters (ref. 90).

Amides of amino acids are also susceptible to hydrolysis by Co(III) complexes[91], however, the rate enhancements brought about are very much lower than those observed for the corresponding esters. This is due to the greater basicity or the poor leaving group nature of the amino function. Amide hydrolysis promoted by Co(III) complexes was shown to occur by both Lewis acid and metal-hydroxide mechanisms. At pH 7, the intramolecular metal-hydroxide mechanism is 100 times faster than the Lewis acid mechanism.

The effectiveness of metal-hydroxides in hydrolyzing esters in bimolecular reactions have also been investigated.[92] The results of these studies show that metal-bound hydroxide ions can be effective catalysts in hydrolyses reactions where good leaving groups are involved, such as 4-nitrophenyl acetate, 2,4-dinitrophenyl acetate, and

---

[91] D. A. Buckingham, D. M. Foster, A. M. Sargeson, *J. Am. Chem. Soc.*, **1969**, 91, 4102.

[92] D. A. Buckingham, *Biological Aspects of Inorganic Chemistry*, A. W. Addison, W. R. Cullen, D. Dolphin, B. R. James, Eds., Wiley, New York, 1976, Ch. 5.

propionic anhydride The catalysis involves the direct attack by metal-hydroxide on the carbonyl centre The catalytic ability of M-OH was found to depend solely on the pKa of the metal-bound water, however, this dependence was found to be small For example, for the hydrolysis of propionic anhydride, the metal-hydroxide catalyzed rate increases by less than a factor of 100 when the pKa of the metal-bound water is increased by six.

Metal ion promoted hydrolysis of unactivated esters and amides have been shown to occur only in the presence of some concentrating factor which forces the reactants into juxtaposition Duerr and Czarnik[93] reported Cu^{2+} catalyzed hydrolysis of an unactivated ester covalently linked to a chelating ethylenediamine unit. The system involved the well known reversible conjugate addition of amines to enones (fig 4.14) It was observed that Cu(II) catalyzed the hydrolysis of the methylacrylate adduct by a factor of 16000 over the uncatalyzed rate.

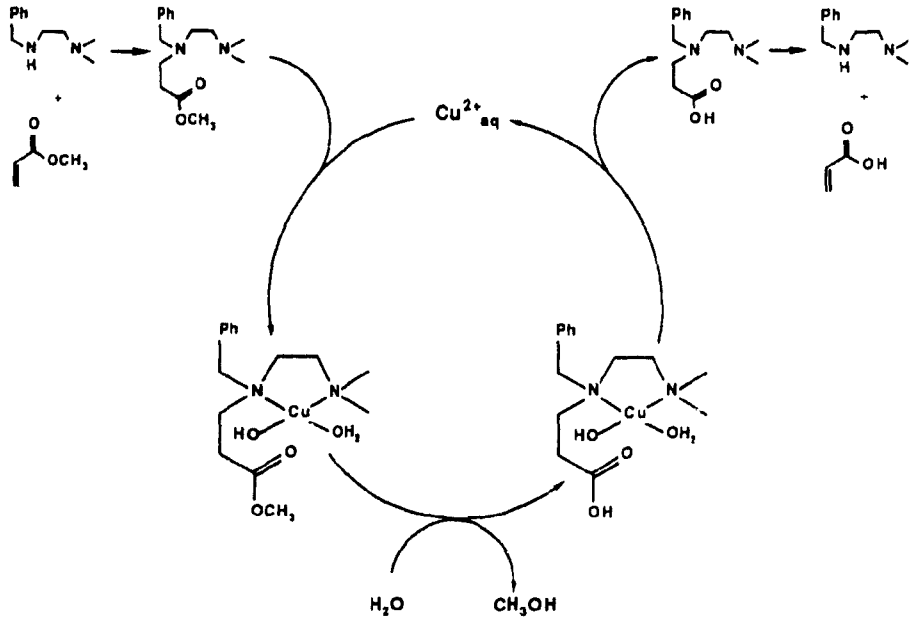

(ref. 93)

Figure 4.14 Cu(II) hydrolysis of an unactivated ester based on reversible conjugate addition

Groves and Dias[29] reported Cu(II) promoted hydrolysis of a metal coordinating lactam (fig. 1.16). At pH 7.6, the copper-hydroxide mechanism displayed a rate enhancement of approximately 1 x 10^6 times greater than that calculated for the base

[93]B F Duerr and A W Czarnik, *Tetrahedron Lett*, **1989**, 30, 6951

catalyzed hydrolysis of the amide at the same pH. The authors reasoned that such a large rate enhancement was observed because of two factors: 1) Ideal proximity and orientation of the metal-hydroxide with respect to the amide carbonyl. This arrangement should highly favour a nucleophilic M-OH attack leading to the tetrahedral intermediate. 2) Rate-determining breakdown of the tetrahedral intermediate is greatly facilitated due to conformational restrictions imposed on this intermediate. Deslongchamp's investigations of stereoelectronic control during hydrolyses reactions indicate that cleavage of a C-O or C-N bond is facilitated only when two heteroatoms of the tetrahedral intermediate each have a lone pair oriented antiperiplanar to the departing O-alkyl or N-alkyl group. Such a situation exists in the Cu(II) promoted hydrolysis reaction, thus, in the metal-bound intermediate, anchimeric assistance from antiperiplanar lone pairs facilitates breakdown of the tetrahedral intermediate (fig. 4.15). In the absence of a metal ion, the tetrahedral intermediate involved is much more flexible with free rotation about C-O bonds.

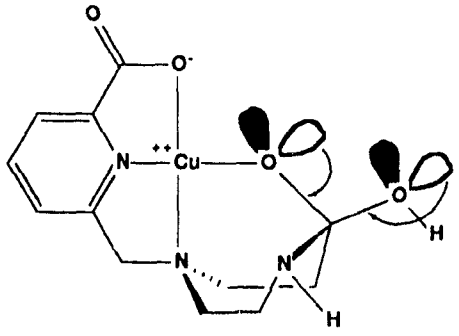

Figure 4.15 Anchimeric assistance from antiperiplanar lone pairs facilitates breakdown of the tetrahedral intermediate (ref 29)

Other examples of metal ion promoted hydrolysis of amides will be discussed in section 6.6.2.

4.5 PLAN OF STUDY

There is a great deal of interest in developing catalysts that efficiently hydrolyze carboxylic esters and amides. Numerous reports exist for metal ion promoted or catalyzed hydrolysis of esters and amides. However, these systems either possess both the ester (or amide) and the metal-binding ligand covalently linked together, or the substrates being hydrolyzed are highly activated esters and amides.

The plan is to study the mechanism of hydrolysis of various esters (pNPA, MTA, MeOAc) and amides (DMF) catalyzed by simple Cu(II) complexes. The efficiencies of different Cu(II) complexes are to be compared in order to determine the structural requirements of a metal catalyst for hydrolyzing carboxylic esters and amides. A detailed kinetic analysis shall provide a mechanistic rationale for the observed reactivities. It will also give an insight towards the mechanism of metal containing peptidases such as carboxypeptidase A.

5.0 RESULTS

5.1 Cu(II) COMPLEX CATALYZED HYDROLYSIS OF ESTERS

The rate constants for hydrolysis of pNPA, MTA, and MeOAc by various catalysts are listed in table 5.1. Catalyzed hydrolysis of MTA and MeOAc were measured by the pH stat method, following the production of acetic acid. The rate of hydrolysis of pNPA was measured spectrophotometrically by following the production of p-nitrophenolate ion at 400 nm.

Table 5.1 Rate constants (s^{-1}) for hydrolysis of pNPA and MeOAc at 25 °C and MTA at 5 °C with and without catalysts (1mM) at pH 8.0

Catalyst	pNPA	MTA	MeOAc
none	9.56×10^{-6}	1.2×10^{-2}	1.5×10^{-7} (a)
imidazole	5.8×10^{-4}	1.2×10^{-2}	(b)
[Cu(terpy)(OH_2)]	2.3×10^{-4}	3.0×10^{-2}	2.0×10^{-7} (c)
[Cu(dpa)(OH_2)$_2$]	2.1×10^{-4}	1.6×10^{-2}	9.8×10^{-7}

(a) extrapolated from the hydroxide rate
(b) too slow to be detected
(c) at 10 mM copper complex concentration

Imidazole is an efficient catalyst for hydrolyzing pNPA but not for hydrolyzing MTA and MeOAc. In contrast, the Cu(terpy)-complex is efficient at catalyzing the hydrolysis of pNPA and MTA but not MeOAc. The Cu(dpa)-complex efficiently hydrolyzes all three esters.

The pH-rate profiles for Cu(dpa)-complex catalyzed hydrolysis of MeOAc and for Cu(terpy)-complex catalyzed hydrolysis of MTA are shown in figures 5.1 and 5.2 respectively. Data points are averages from at least three consecutive runs. The rate of acetic acid production is given by $k_{obs}[Cu_T][ester]$ where $[Cu_T]$ is the total Cu(II) catalyst concentration and k_{obs} is given by equation 5.1.

$$k_{obs} = C\left[\frac{Ka}{Ka + [H]}\right] \qquad (5\ 1)$$

where Ka is the acid dissociation constant for the coordinated water molecule. The data were fit according to equation 5.1 using an iterative non-linear least squares curve fitting program.† For Cu(dpa)-complex catalyzed hydrolysis of MeOAc, $C = k_2K_1$ where K_1 is the equilibrium constant for complexation of the ester substrate to the copper complex and k_2 is the rate constant for metal-hydroxide attack on coordinated ester. The constants, C and Ka, obtained from the calculated curve are listed underneath the appropriate pH-rate plots.

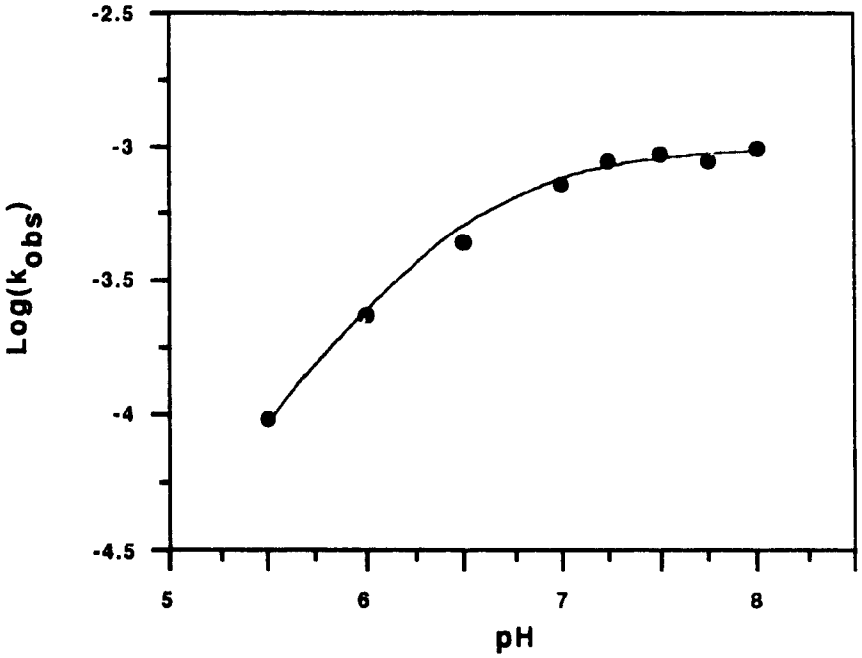

Figure 5.1 pH-rate profile for Cu(dpa) (1mM) catalyzed hydrolysis of methyl acetate (1 M) at 25 °C. Ka = 2.8 x 10^{-7}, K_1k_2 = 1 x 10^{-3} $M^{-1}s^{-1}$

The data for the pH-rate plots are listed in tables 5.2 and 5.3. For the Cu(terpy) catalyzed hydrolysis of MTA, the background rate of hydrolysis was subtracted from the observed rate of hydrolysis. At pH>8.5, the background rate of hydrolysis (i.e. the hydroxide rate) becomes faster than the copper complex catalyzed rate.

† *Kaleidograph*, version 2.0.2, developed by Abelbeck software.

Table 5.2 Second-order rate constants, k_{obs}, for the hydrolysis of MeOAc (1 M) catalyzed by $[Cu(dpa)(OH_2)_2]^{2+}$ (1mM) at 25 °C at different pH values.

pH	$k_{obs} \times 10^4$ ($M^{-1}s^{-1}$)	log (k_{obs})
5.5	0.96	-4 02
6.0	2.33	-3 63
6.5	4 33	-3.36
7.0	7.17	-3.14
7.25	8.83	-3.05
7 5	9.33	-3.03
7 75	8 83	-3.05
8.0	9 83	-3.00

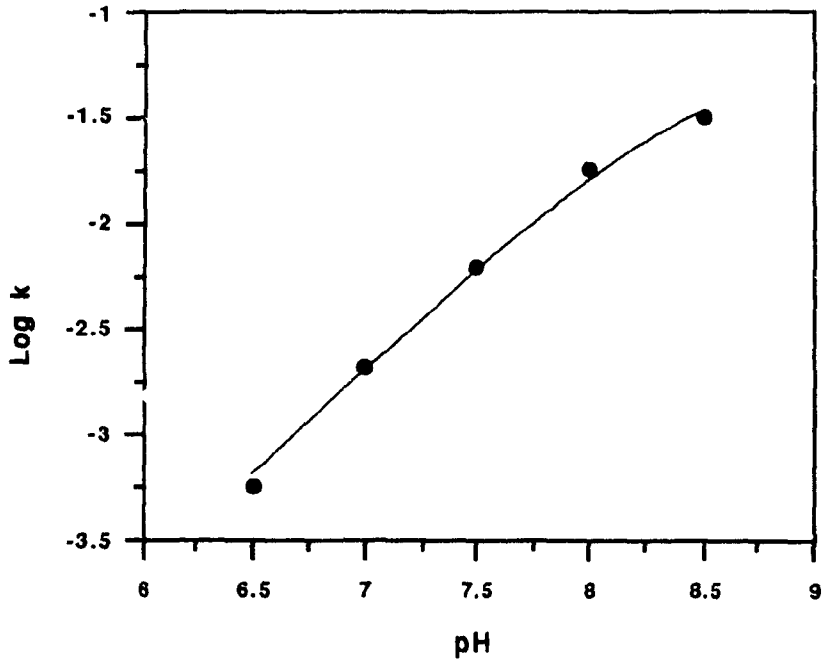

Figure 5.2 pH-rate profile for Cu(terpy) (1mM) catalyzed hydrolysis of MTA (2 mM) at 25 °C. Ka = 2.8×10^{-9}, C = 7.1×10^{-2} s^{-1}.

Table 5.3 Rate constants (s^{-1}) for hydrolysis of MTA (2mM) catalyzed by $[Cu(terpy)(OH_2)]^{2+}$ (1mM) at different pH values

pH	k_{obs} [a]	k_{uncat} [b]	k [c]	log k
6.5	6.5×10^{-3}	6.0×10^{-3}	5.6×10^{4}	-3.2
7.0	9.0×10^{-3}	6.9×10^{-3}	2.1×10^{-3}	-2.7
7.5	1.6×10^{-2}	9.7×10^{-3}	6.2×10^{-3}	-2.2
8.0	3.0×10^{-2}	1.2×10^{-2}	1.8×10^{-2}	-1.7
8.5	5.8×10^{-2}	2.6×10^{-2}	3.2×10^{-2}	-1.5

a) k_{obs} = observed rate of hydrolysis uncorrected for the spontaneous (control) hydrolysis
b) k_{uncat} = spontaneous rate of hydrolysis in the absence of metal complex
c) $k = k_{obs} - k_{uncat}$

Production of methanol due to Cu(dpa)-complex catalyzed hydrolysis of MeOAc was confirmed by ^1H NMR. Figure 5.3 shows the disappearance of the MeOAc signals (δ 2.05 and δ 3.65) and the appearance of the methanol signal (δ 3.3). The acetate signal is quenched owing to interaction of acetate with the paramagnetic copper complex. The non-coordinating buffer, 2,6-lutidine, was used to maintain a constant pH of 7 throughout the course of the reaction. The ^1H NMR signal arising from the methyl groups of lutidine (δ 2.4) were omitted for clarity. No observable production of methanol was detected using Cu(terpy) as the catalyst.

The rate constants for the base catalyzed and $[Cu(dpa)(OH_2)_2]^{2+}$ catalyzed hydrolysis of methyl acetate and acetylcholine are compared in table 5.4. The Cu(II)-complex hydrolyzes the less reactive ester, MeOAc, more efficiently. No catalysis is observed from the one to one aqueous addition of $CuCl_2$ and bis-[2-(5-carboxypyridyl)]methylamine (1mM each) at neutral or alkaline pH. For this ligand, metal complexation does not occur, thus at pH>7, precipitation of $Cu(OH)_2$ is observed.

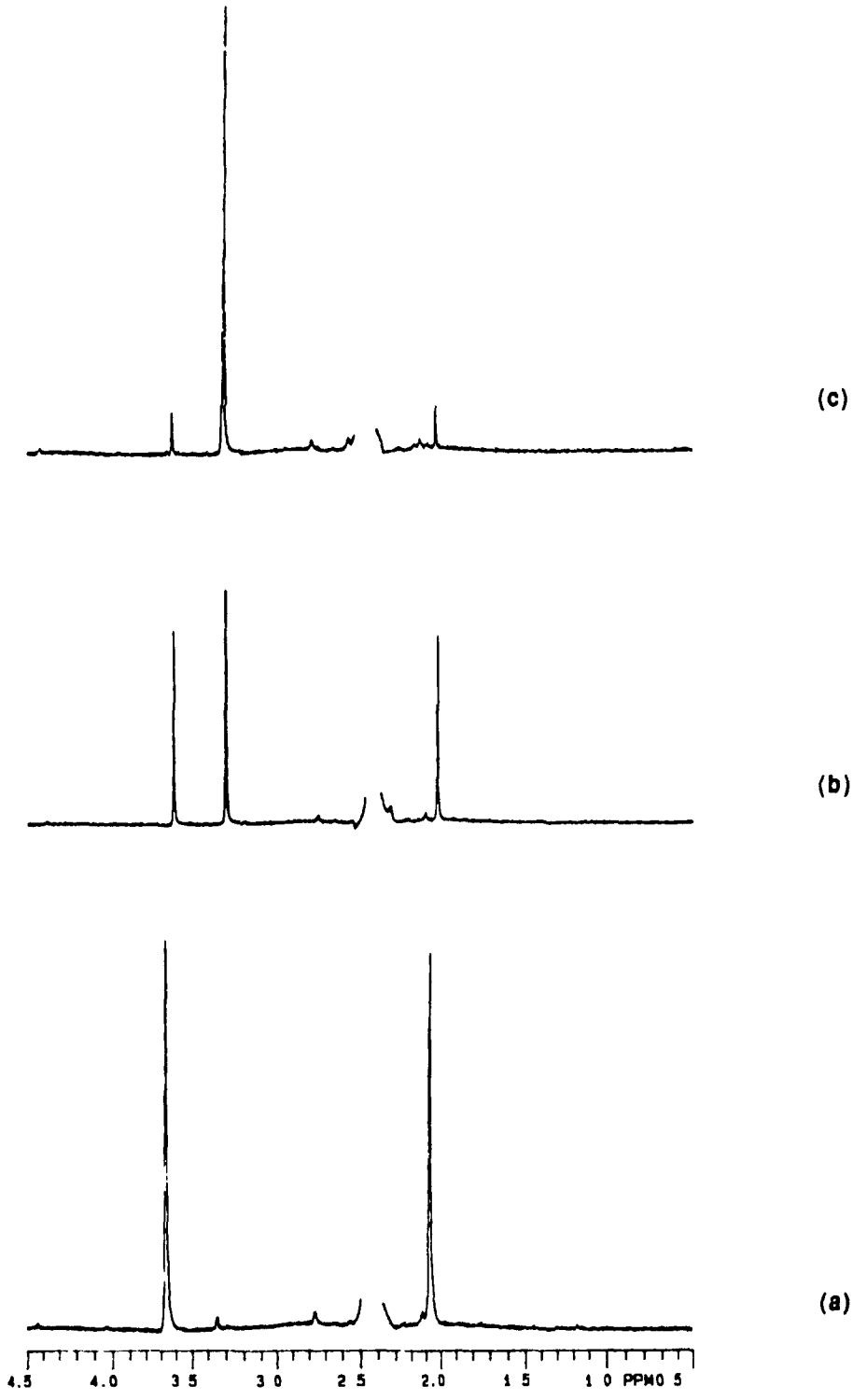

Figure 5.3 ^1H NMR spectra of methyl acetate (20 mM) in D_2O after adding $[Cu(dpa)(OH_2)_2]^{2+}$ (10 mM) in 2,6-lutidine buffer (100 mM) at pD 7, 25 °C Elapsed time: **(a)** 0 min, **(b)** 2 days, **(c)** 7 days.

Table 5.4 Rate constants (s^{-1}) for hydrolysis of methyl acetate and acetylcholine (1 M) with and without $[Cu(dpa)(OH_2)_2]^{2+}$ (1 mM) at pH 7 0, 25 °C

Ester	k_{OH}	$[Cu(dpa)(OH_2)_2]^{2+}$
AcCh	$2\,0 \times 10^{-7}$ [a]	$4\,5 \times 10^{7}$
MeOAc	$0\,15 \times 10^{-7}$ [b]	$7\,2 \times 10^{-7}$

a M Nakagaki and S Yokoyama, *Bull Chem Soc Jpn*, **1986**, 59, 1925
b from ref 107

5.2 Cu(II) COMPLEX CATALYZED TRANSESTERIFICATION AND SYNTHESIS OF MeOAc

Figure 5.4 shows the ^1H NMR spectral changes due to Cu(NMedpa)-complex catalyzed transesterification of ethyl acetate to methyl acetate and ethanol in CD_3OD Toluene was added to the system as a reference (δ 2.3) The disappearance of the ethyl acetate signal (δ 4 1, quartet) is accompanied by the appearance of the ethanol signal (δ 3 6, quartet). The Cu(dpa) complex could not be used because of its insolubility in methanol, however, the transesterification reaction may be observed using the Cu(dpa) complex in CD_3OD in the presence of 15% DMSO. Production of MeOAc from acetic acid in CD_3OD can also be detected by ^1H NMR. Figure 5.5 shows the appearance of the MeOAc signal (δ 2.05) at different time intervals. Toluene (δ 2.3) was added to this system as a reference marker. In all cases, acetate signals are quenched owing to the interaction of acetate with the paramagnetic copper complexes. Tridentate Cu(II) complexes which possess only one free coordination site, such as Cu(terpy) and Cu(dien), do not catalyze these reactions.

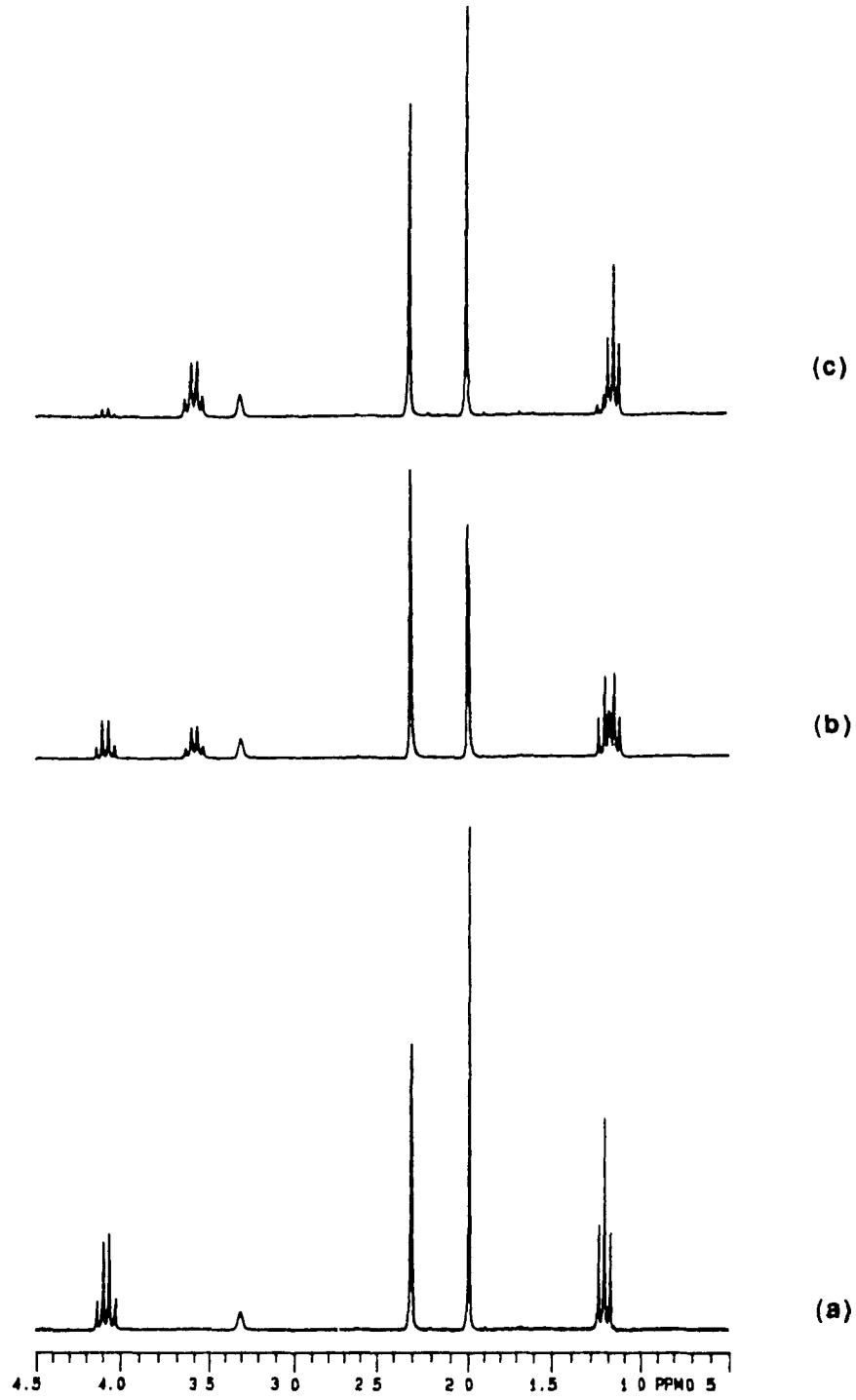

Figure 5.4 ^1H NMR of ethyl acetate (80 mM) in CD_3OD after adding $[Cu(NMedpa)(CH_3OH]^{2+}$ (20 mM) at pD 8, 50 ^0C. Toluene (80 mM) is added as reference, δ 2.3 Elapsed time **(a)** 0 min, **(b)** 21 hrs, **(c)** 74 hrs.

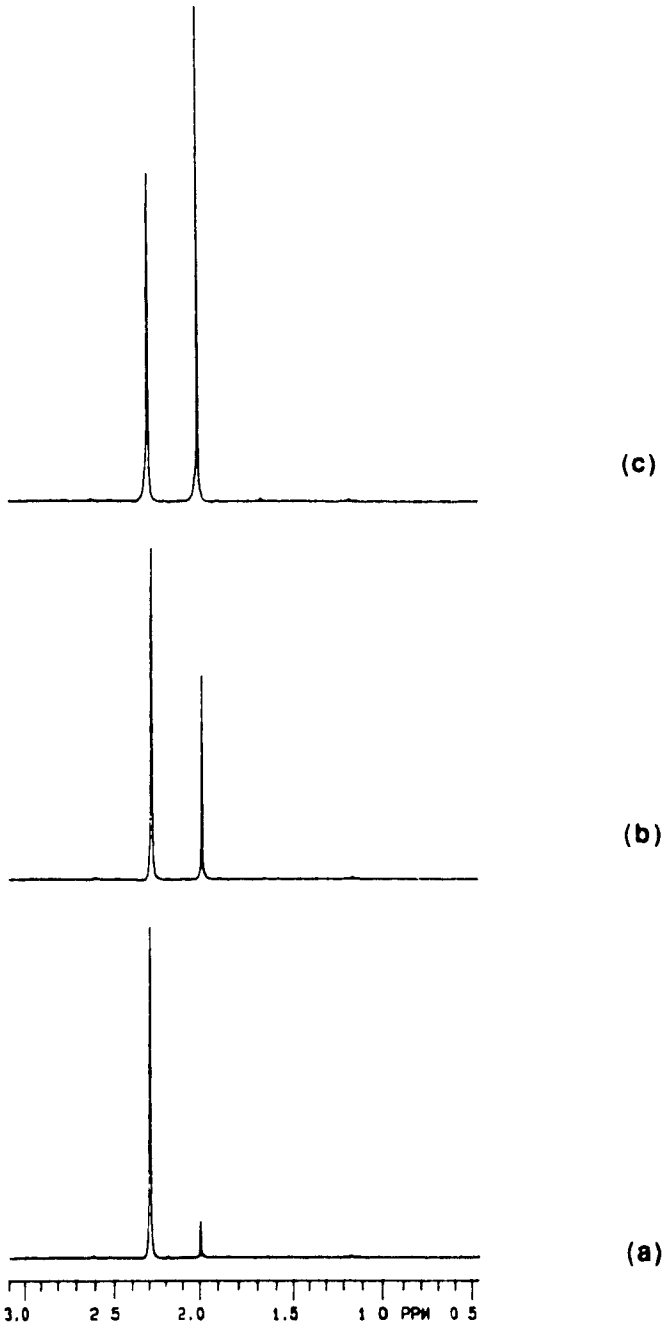

Figure 5.5 ^1H NMR of acetic acid (80 mM) in CD_3OD after adding $[Cu(NMedpa)(MeOH)_2]^{2+}$ (20 mM) at pD 8, 50 °C Toluene (80 mM) is added as a reference marker, δ 2 3 Elapsed time: **(a)** 1 day, **(b)** 6 days, **(c)** 16 days

5.3 ACETATE BINDING TO $[Cu(dpa)(OH_2)_2]^{2+}$

It has been shown by X-ray crystallography that acetate binds to the Cu(dpa) complex as a bidentate ligand forming a four-membered ring.[60] The equilibrium constant, K_d, for the dissociation of acetate from $[Cu(dpa)(OH_2)_2]^{2+}$ was obtained by potentiometric titration. The pH corresponding to the midpoint of the buffer region of the titration curve for $[Cu(dpa)(OH_2)_2]^{2+}$ increases when increased amounts of acetate are added. This relationship is due to binding of acetate to the copper complex. Representative titration curves for $[Cu(dpa)(OH_2)_2]^{2+}$ in the presence of varying concentrations of acetate are shown in figure 5.6.

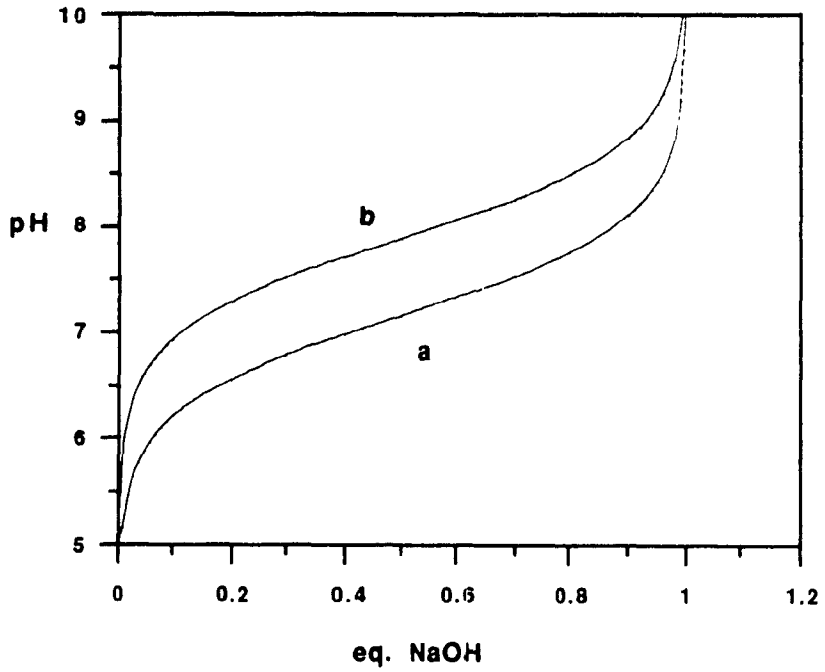

Figure 5.6 Titration curves for the $[Cu(dpa)(OH_2)_2]^{2+}$ system **a)** 1mM $[Cu(dpa)(OH_2)_2]^{2+}$ + 1mM AcOH **b)** 1mM $[Cu(dpa)(OH_2)_2]^{2+}$ + 20 mM AcOH. The buffer region for AcOH is omitted for clarity. 1 eq. NaOH represents 1 mM NaOH added.

The following equilibria are considered to take place during titration

$$[(L)Cu] + OAc \rightleftharpoons [(L)Cu'OAc]$$

$$[(L)Cu(OAc)] \rightleftharpoons [(L)Cu] + OAc$$

$$K_d = \frac{[(L)Cu]\,[OAc]}{[(L)Cu(OAc)]} \qquad (5\,2)$$

$$[(L)Cu] \rightleftharpoons [(L)Cu(OH)] + H^+$$

$$Ka = \frac{[(L)Cu(OH)]\,[H^+]}{[(L)Cu]} \qquad (5\,3)$$

$$C_T = [(L)Cu] + [(L)Cu(OH)] + [(L)Cu(OAc)] \qquad (5\,4)$$

where K_d is the equilibrium constant for dissociation of acetate anion (OAc) from $[Cu(dpa)(OH_2)_2]^{2+}$ (represented as [(L)Cu]). Ka represents the acid dissociation constant of the coordinated water molecule, and C_T represents the total concentration of Cu(II)-complex present in solution. Water molecules coordinated to the copper complex are omitted for clarity

By substituting equations 5 2 and 5.3 into equation 5 4, one obtains the total copper complex concentration as a function of the concentration of the hydroxy-aqua species present in solution (eqn. 5.5).

$$C_T = [(L)Cu(OH)]\left[\frac{[H]}{Ka} + 1 + \frac{[H]\,[OAc]}{Ka\,K_d}\right] \qquad (5\,5)$$

At the midpoint of the titration curve, the concentration of the hydroxy-aqua species should be one half the total metal complex concentration (i.e $[(L)Cu(OH)] = C_T/2$), therefore

$$C_T = \frac{C_T}{2}\left[\frac{[H]_{mid}}{Ka} + 1 + \frac{[H]_{mid}\,[OAc]}{Ka\,K_d}\right] \qquad (5\,6)$$

Rearranging equation 5 6 produces,

$$\frac{1}{[H]_{mid}} = \frac{[OAc]}{Ka\,K_d} + \frac{1}{Ka} \qquad (5\,7)$$

where $[H]_{mid}$ is the H^+ concentration at the midpoint of the titration curve at a given acetate concentration. A plot of $1/H_{mid}$ versus acetate concentration gives a straight line with a slope of $1/KaK_d$ and intercept of 1/Ka. (see figure 5.7). The calculated values for these constants are listed in the caption of fig 5 7

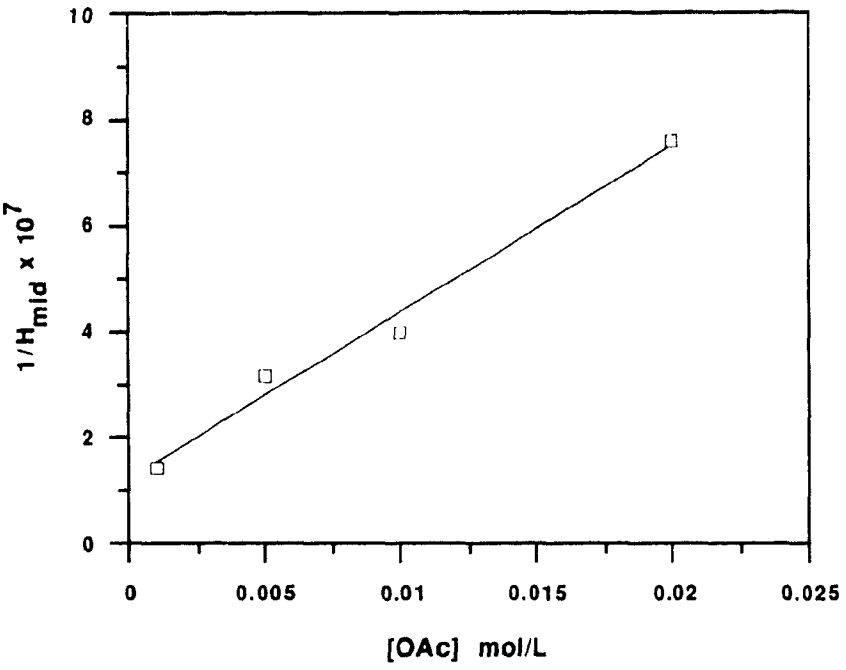

Figure 5.7 Dependence of $1/H_{mid}$ on acetate ion concentration Slope = $1/KaK_d$ = 3 14 x 10^9, y-intercept = 1/Ka = 1 2 x 10^7, thus, Ka = 8 3 x 10^{-8}, K_d = 3 8 x 10^{-3} M

5.4 TURNOVER FOR $[Cu(dpa)(OH_2)_2]^{2+}$ CATALYZED HYDROLYSIS OF MeOAc

The turnover time for $[Cu(dpa)(OH_2)_2]^{2+}$ catalyzed hydrolysis of MeOAC is 23 min at pH 7.0, 25 °C. At 1mM catalyst concentration, the aforementioned turnover time translates to a reaction rate of 7.2 x 10^{-7} M^{-1} acetic acid produced per second. [10^{-3}/23 x

60]. Figure 5.8 shows the turnover versus time plot for $[Cu(dpa)(OH_2)_2]^{2+}$ catalyzed hydrolysis of MeOAc. Up to three turnovers are observed without a significant decrease in rate.

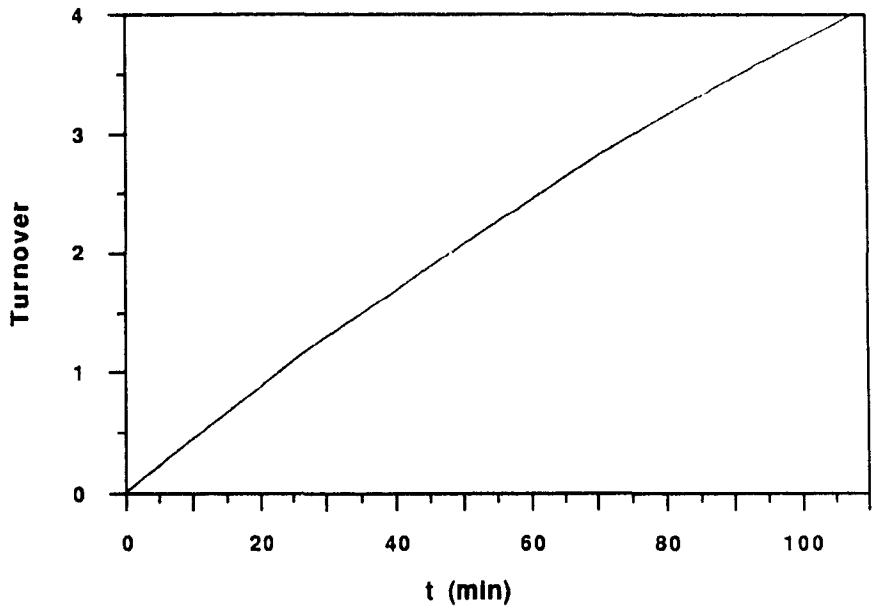

Figure 5.8 Catalyzed hydrolysis of MeOAc (1M) using $[Cu(dpa)(OH_2)_2]^{2+}$ (1mM) at pH 7.0, 25 °C

5.5 Cu(II) COMPLEX CATALYZED HYDROLYSIS OF AMIDES.

The rate constants for $[Cu(dpa)(OH_2)_2]^{2+}$ and hydroxide ion catalyzed hydrolysis of DMF are compared in table 5.5. $[Cu(dpa)(OH_2)_2]^{2+}$ mediated hydrolysis is observed at pD 8 and 100 °C.

Table 5.5 Rate constants (s^{-1}) for $[Cu(dpa)(OH_2)_2]^{2+}$ (10mM) and hydroxide ion catalyzed hydrolysis of DMF (10 mM), 100 °C, pH 8

Catalyst	k (s^{-1})	rel. rate
$[Cu(dpa)(OH_2)_2]^{2+}$	1.3×10^{-6}	44
^{-}OH	2.97×10^{8} (a)	1

(a) extropolated from data ranging from 70 to 90 °C
S. Langlois and A. Broche, *Bull. Soc. Chem. Fr.*, **1964**, 812

Under similar conditions, other cis-diaqua Cu(II) complexes, such as $[Cu(phen)(OH_2)_2]^{2+}$ and $[Cu(en)(OH_2)_2]^{2+}$ are inactive at hydrolyzing the amide, whereas $[Cu(neo)(OH_2)_2]^{2+}$ and $[Cu(tmen)(OH_2)_2]^{2+}$ decompose at 100 °C. Mono-aqua Cu(II) complexes are also not active at catalyzing the hydrolysis of DMF. Catalyzed hydrolysis of DMF by $[Cu(terpy)(OH_2)_2]^{2+}$ could not be observed, however, $[Cu(dpa)(OH_2)_2]^{2+}$ is two orders of magnitude less reactive than $[Cu(dpa)(OH_2)_2]^{2+}$ at hydrolyzing formamide.[94]

The catalyzed hydrolysis of DMF by $[Cu(dpa)(OH_2)_2]^{2+}$ was monitored by ^1H NMR spectroscopy (fig. 5.9). With the progress of the hydrolysis reaction, the decrease in the ^1H NMR signals of DMF (δ 7.92, δ 3.00 and δ 2.85) is accompanied by an increase in the dimethylamine peak (δ 2.71). The formate signal is quenched by the interaction of formate with the paramagnetic copper complex.

To 10 mM $[Cu(dpa)(OH_2)_2]^{2+}$, buffer catalysis was not observed with the addition of such buffers as acetate (20 mM), 2,6-lutidine (100mM); DMAP (10 mM); and N,N,N',N'-tetramethyldiaminomethane (100 mM). Addition of phosphate buffer (10 mM) inhibits the copper catalyzed hydrolysis reaction. With the addition of hydrazine (10 mM) and upon heating the reaction to 100 °C, decomposition of the Cu(dpa) complex was observed.

---

[94] J. Chin, V. Jubian, and K. Mrejen, *J. Chem. Soc , Chem. Commun* , **1990**, 1326.

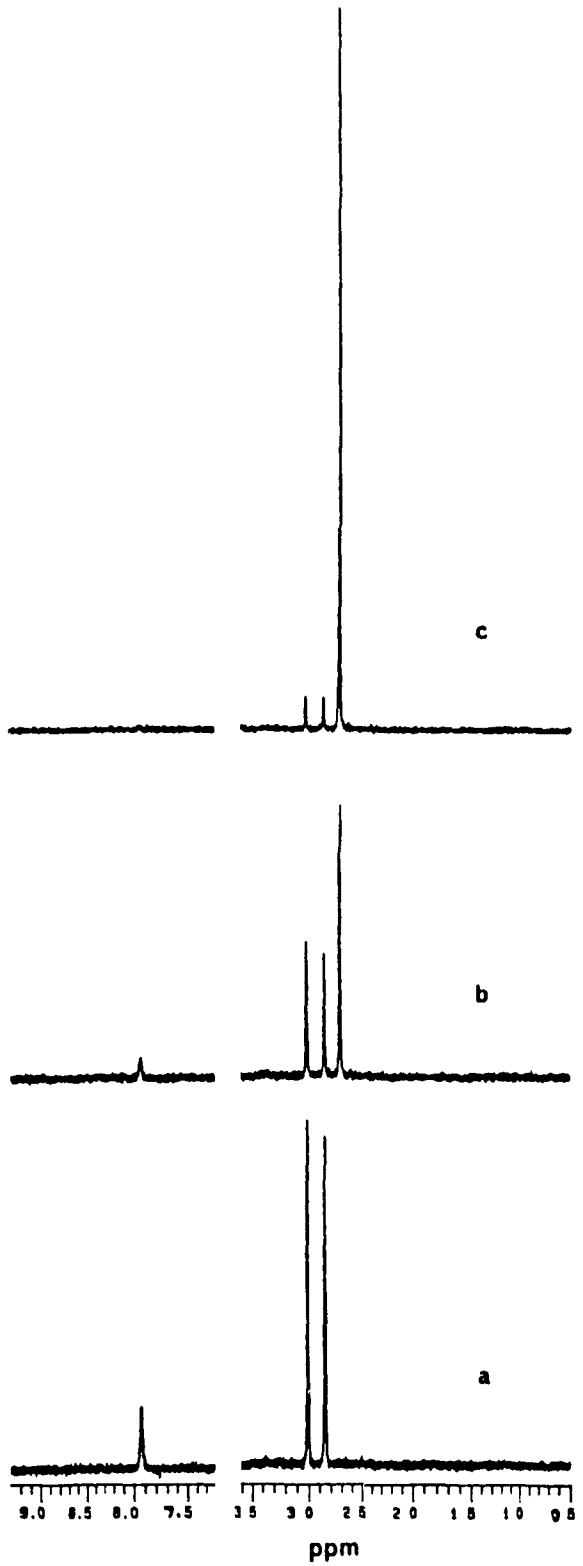

Figure 5.9 ^{1}H NMR of N,N-dimethyl formamide (10 mM) after adding $[Cu(dpa)(OH_2)_2]^{2+}$ (10mM) at pD 8, 100 ^{0}C. Elapsed time (**a**) 0 hr, (**b**) 150 hrs, (**c**) 600 hrs

6. DISCUSSION

6.1 Cu(II) COMPLEX CATALYZED HYDROLYSIS OF ESTERS WITH GOOD LEAVING GROUPS

6.1.1 The p-Nitrophenyl Ester Syndrome

Catalysts which are efficient at hydrolyzing esters with good leaving groups will not necessarily be successful at hydrolyzing esters with poor leaving groups. Recently, Menger and Ladika[95] coined the phrase *p-nitrophenyl ester syndrome* to caution researchers of the common misconception that catalysts which are reactive towards activated substrates should also be reactive towards unactivated substrates. A remarkable 3.3 x 10^5 acceleration in hydrolysis rate was observed by Breslow et al.[96] when p-nitrophenyl 3-ferrocenylacrylate was fully bound to β-cyclodextrin (fig. 6.1). This corresponds to a half-life of 7.4 seconds. However, Menger and Ladika observed that the analogous ethyl ester, which is only 56 times less reactive than the p-nitrophenyl ester towards basic hydrolysis, did not react with a half-life of a few minutes, (i.e. 56 x 7.4 s) as one may anticipate, but reacted with a half-life of at least two years. Insufficient binding or a different mode of complexation of the substrate to the cyclodextrin host was not a factor. In other words, large rate enhancements occurred for esters with good leaving groups but not for esters possessing poor leaving groups.

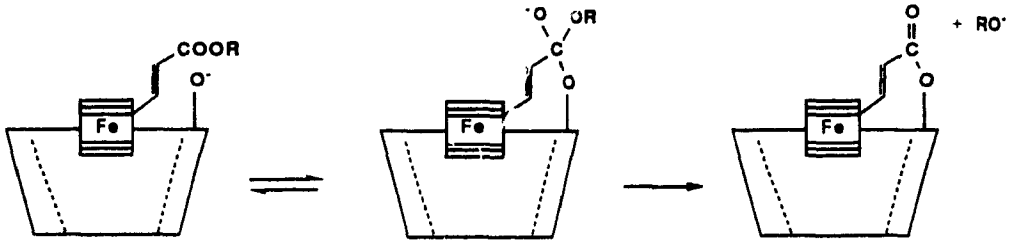

Figure 6.1 Cyclodextrin catalyzed hydrolysis of esters of 3-ferrocenylacrylate. (ref. 95, 96)

---

[95] F. M. Menger and M. Ladika, *J. Am. Chem. Soc.*, **1987**, 109, 3145.

[96] a) R. Breslow, G. Trainor, and A. Ueno, *J. Am. Chem. Soc.*, **1983**, 105, 2739. b) R. Breslow, M. F. Czarnieki, and J. Emert, H. Hamaguchi, *J. Am. Chem. Soc.*, **1980**, 102, 762.

Another example of this dilemma is the well known imidazole-catalyzed hydrolysis of esters.[85] Imidazole is an efficient nucleophilic catalyst for hydrolyzing esters with good leaving groups (e.g. p-nitrophenyl acetate) and is comparable with hydroxide ion but for hydrolyzing esters with poor leaving groups (e.g. methyl acetate), imidazole is millions of times less reactive than hydroxide ion.

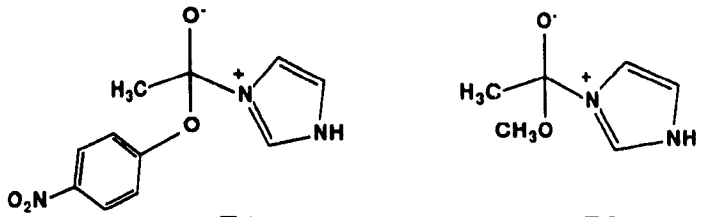

T1 T2

Figure 6.2 Tetrahedral intermediates for imidazole catalyzed hydrolysis of esters

These observations can be rationalized in terms of partitioning the tetrahedral intermediates **T1** and **T2** for the imidazole catalyzed hydrolysis of p-nitrophenyl acetate and methyl acetate respectively (fig 6.2). The **T1** intermediate should easily break down to either acetyl imidazole or p-nitrophenyl acetate since the basicities of the two leaving groups are comparable. For esters of poorer leaving groups (eg methyl acetate), the tetrahedral intermediate **T2** reverts back to the starting materials since imidazole is a much better leaving group than methoxide. In fact, a nucleophilic mechanism is no longer observed and imidazole now acts as a general base to catalyze the hydrolysis of methyl acetate.

The same analysis can be applied to metal-monoaqua complexes. The mechanism of hydrolysis of p-nitrophenyl acetate (pNPA) by metal-monoaqua complexes, such as Cu(terpy), involves a metal-hydroxide nucleophilic attack on the ester substrate.[92] The resulting tetrahedral intermediate (**T3** in fig. 6.3) should break down to products since the basicity of the metal-hydroxide is greater than p-nitrophenolate. However, Cu(terpy) does not catalyze the hydrolysis of methyl acetate since methoxide is much more basic (i e a poorer leaving group) than the M-OH, thus, the tetrahedral intermediate reverts back to the starting materials.

6.2 Cu(II) COMPLEX CATALYZED HYDROLYSIS OF ESTERS WITH POOR LEAVING GROUPS

6.2.1 Hydrolysis of Methyl Trifluoroacetate (MTA)

The $[Cu(terpy)(OH_2)]^{2+}$ complex is an efficient catalyst for hydrolyzing pNPA and MTA but not for hydrolyzing MeOAC. Figure 5.2 shows the pH-rate profile for $[Cu(terpy)(OH_2)]^{2+}$ catalyzed hydrolysis of MTA. The efficiency of the catalyst increases with increase in the solution alkalinity and then begins to level off near the pH corresponding to the pKa of the copper bound water molecule (pKa=8.0). There is only one free coordination site available in the Cu(terpy) complex; thus, there are two classical mechanisms that can account for the observed pH-rate profile. One is the metal-hydroxide mechanism involving direct nucleophilic attack of the copper-hydroxide on the ester and the other is the Lewis acid mechanism involving free hydroxide attack on the metal-coordinated ester. These two mechanisms are kinetically indistinguishable. However, based on the reactivity-selectivity principle, the Lewis acid mechanism can be ruled out. According to the reactivity-selectivity principle, selectivity decreases with increase in reactivity. Since metal coordinated esters are more reactive towards nucleophilic attack than the corresponding free esters, hydroxide should be less selective towards the metal coordinated esters than to the free esters. It follows that less reactive the ester, the greater the expected rate acceleration upon coordination of the ester to the metal. Experimentally, a greater rate acceleration is observed for MTA hydrolysis than for MeOAc hydrolysis which is inconsistent with the Lewis acid mechanism. At pH 8 and 1mM Cu(terpy), a rate acceleration of 2 5 over the uncatalyzed rate is observed for MTA hydrolysis whereas catalyzed hydrolysis of MeOAc is undetected under similar conditions (table 5.1). In contrast, the metal-hydroxide mechanism is consistent with the experimental results. Metal-hydroxides are less nucleophilic than free hydroxides and hence are more selective towards esters than are free hydroxides. Therefore, metal hydroxides are expected to give a greater rate acceleration for MTA hydrolysis than for MeOAc hydrolysis.

In the previous section (6.1.1), one may conclude that metal catalysts which act on their ester substrates solely by a metal-hydroxide mechanism will not be efficient at hydrolyzing esters with poor leaving groups. If the results for Cu(terpy) catalyzed hydrolysis of MTA are rationalized in terms of partitioning the tetrahedral intermediate **T3** (fig. 6.3) then the tetrahedral intermediate should break down to the starting materials more rapidly than to the products since the metal-hydroxide is a much better leaving group than methoxide. If this is the case then it is easy to understand why Cu(terpy) does not catalyze

the hydrolysis of MeOAc but why does Cu(terpy) efficiently catalyze the hydrolysis of MTA?

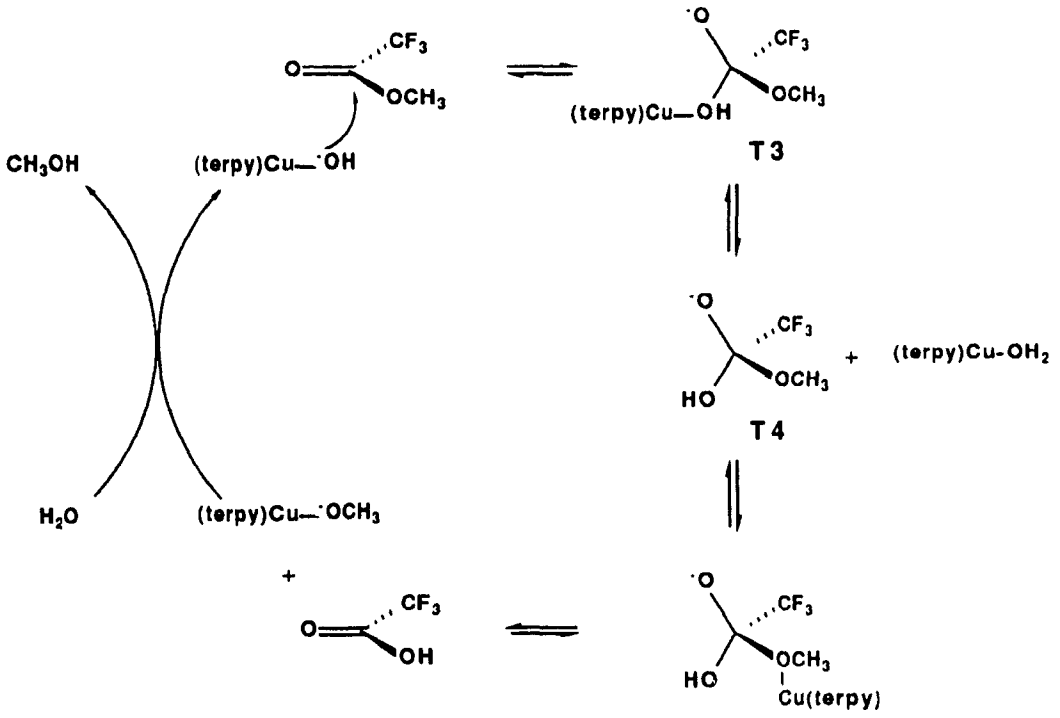

Figure 6.3 Proposed mechanism for $[Cu(terpy)(OH_2)]^{2+}$ catalyzed hydrolysis of MTA

The metal-hydroxide mechanism for Cu(terpy) catalyzed hydrolysis of MTA is shown in figure 6.3. In hydrolyzing esters with poor leaving groups, there is a relationship between effective nucleophilic catalysis and the lifetime of the tetrahedral intermediate.[97] The lifetime of the tetrahedral intermediate **T4** (fig. 6.3) for MTA hydrolysis is much longer than that for MeOAc hydrolysis. Reversion of **T3** to the starting materials can be significantly reduced if the metal-oxygen bond is cleaved more rapidly than the carbon-oxygen (metal hydrate) bond. The stability of **T4** enables "metal transfer" to take place. Coordination of the metal complex to the methoxide moiety makes it a better leaving group so that breakdown to products is now feasible. For metal-complex catalyzed hydrolysis of MTA there is enough time for **T4** to encounter the metal complex and break

[97]J. Chin and X. Zou, *J Am Chem Soc*, **1984**, 106, 3687

down to the products or to the starting materials. If the breakdown of **T4** is catalytic its formation must also be catalytic according to the principle of microscopic reversibility.

For MeOAc, metal catalysis cannot occur by this mechanism because, compared to the lifetime of **T4**, the lifetime of the corresponding tetrahedral intermediate for methyl acetate hydrolysis is too short to encounter the metal catalyst. Therefore, metal complexes possessing only one free coordination site (i.e. monoaqua complexes) can only hydrolyze activated esters (pNPA, MTA) via a metal-hydroxide mechanism but do not hydrolyze, to any significant extent, unactivated esters such as methyl acetate.

6.2.2 Hydrolysis of Methyl Acetate (MeOAc): Structural Requirements for a Metal Catalyst

In order for a metal catalyst to efficiently hydrolyze MeOAc, the lifetime of the tetrahedral intermediate corresponding to **T4** should be increased and the metal migration should be made to be more efficient. Both of these goals may be realized with a cis-diaqua metal complex such as $[Cu(dpa)(OH_2)_2]^{2+}$. It was anticipated that the Cu(dpa) complex may form the tetrahedral intermediate **T5.** The only difference between **T5** and **T4** is that the anionic oxygen of the tetrahedral intermediate is coordinated to the metal in **T5.** This should stabilize the intermediate and at the same time provide an intramolecular mechanism for the metal to coordinate to the methoxide leaving group. It is not possible for monoaqua complexes, such as Cu(terpy), to form this type of intermediate in the hydrolysis of MeOAc. Furthermore, even if Cu(terpy) were to form the tetrahedral intermediate corresponding to **T5** this interaction would be non-productive. Although Cu(terpy) will stabilize the tetrahedral intermediate to the same extent as the Cu(dpa) complex, Cu(terpy) has no additional coordination site available to facilitate an intramolecular metal migration; thus, Cu(terpy) is inactive at catalyzing the hydrolysis of MeOAc.

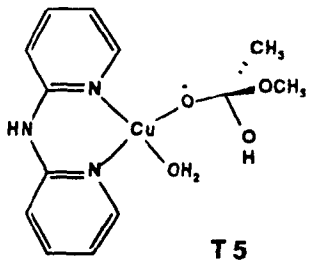

T5

6.3 $[Cu(dpa)(OH_2)_2]^{2+}$ CATALYZED HYDROLYSIS OF MeOAc

6.3.1 Mechanism

The hydrolysis of all three esters (pNPA, MTA, and MeOAc) are efficiently catalyzed by $[Cu(dpa)(OH_2)_2]^{2+}$. Based on the pKa of the copper coordinated water molecule and the pH-rate profile (fig. 5.1), the proposed mechanism for $[Cu(dpa)(OH_2)_2]^{2+}$ catalyzed hydrolysis of MeOAc involves coordination of the ester to the metal followed by intramolecular metal hydroxide attack on the coordinated ester as shown in figure 6.4. The proposed mechanism is similar to the one proposed for $[Cu(dpa)(OH_2)_2]^{2+}$ promoted hydrolysis of phosphate esters and requires the formation of a four-membered ring. Since Cu(II) is substitutionally labile, K_1 should not be the rate-determining step; thus, either formation or breakdown of the tetrahedral intermediate is the rate-limiting step.

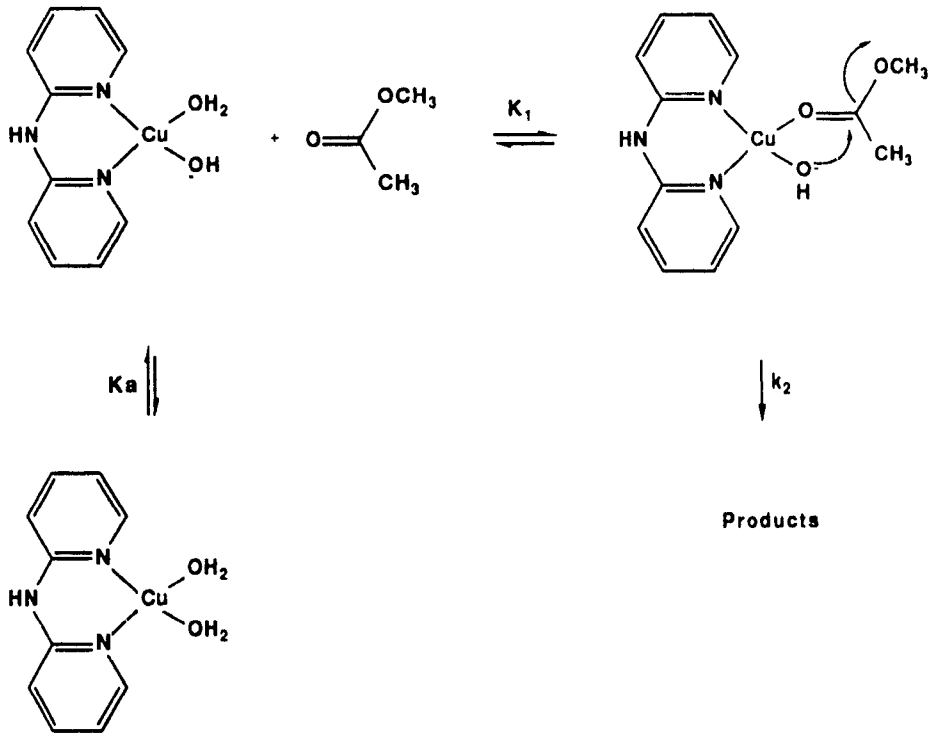

Figure 6.4 Proposed mechanism for $[Cu)dpa)(OH_2)_2]^{2+}$ catalyzed hydrolysis of MeOAc

The k_2 step in figure 6.4 may be broken down into several steps. Two paths may exist for the breakdown of the tetrahedral intermediate **T6** (fig. 6.5). In path A, hydrogen-oxygen bond cleavage occurs followed by product formation. This mechanism is not unreasonable if we consider the breakdown of the tetrahedral intermediate as a nucleophilic displacement (of methoxide) at carbon by the lone pairs on the two oxygens. In path B, **T6** undergoes metal-oxygen bond cleavage followed by ligand exchange to yield products.

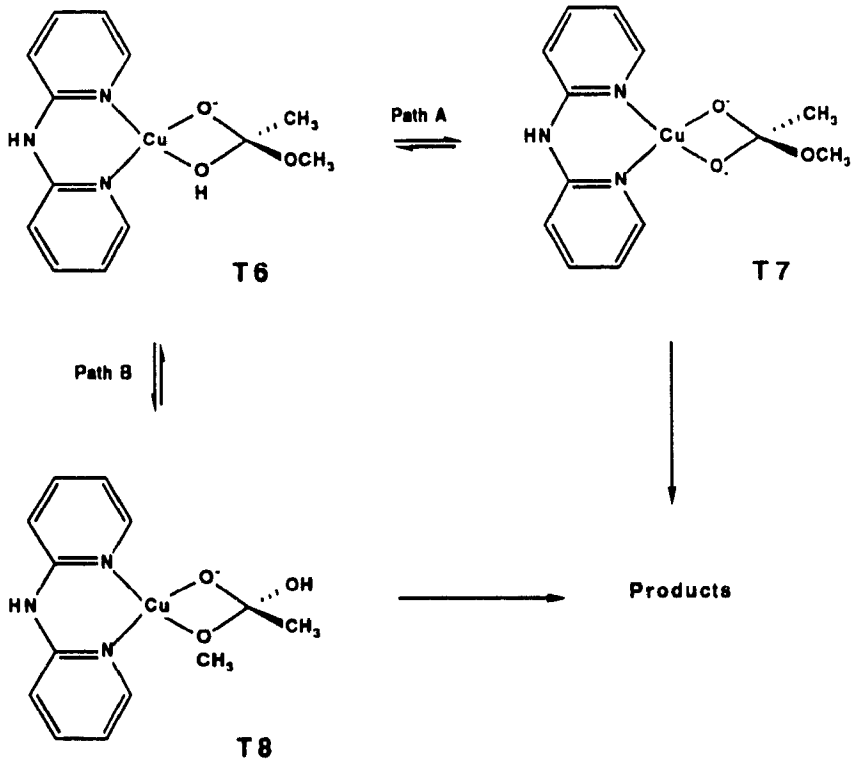

Figure 6.5 Possible pathways for the breakdown of the tetrahedral intermediate for the $[Cu(dpa)(OH_2)_2]^{2+}$ catalyzed hydrolysis of MeOAc.

The mechanism for path B is similar to the one proposed for Cu(terpy) catalyzed hydrolysis of MTA in figure 6.3. The only difference between the mechanisms shown in fig. 6.3 and 6.5 is that, in fig. 6.5, the anionic oxygen of **T8** is coordinated to the metal. This satisfies the requirements for catalyzed hydrolysis of unactivated esters as discussed in the previous sections (6.2.1. and 6.2.2).

For both pathways the possibility of buffer catalysis exists. In path A, the situation is ideal for a proton switch mechanism similar to the one depicted in figure 4.11 However, buffers which possess this capability, such as phosphate, coordinate strongly to the metal complex and inhibit the hydrolysis reaction Buffer catalysis was not observed when the non-coordinating buffer, 2,6-lutidine, was used.

For path B, the role of a buffer would be to deprotonate the alcohol moiety of **T8** in order to accelerate its breakdown to products. Buckingham et al [91] observed mild catalysis with non-nucleophilic buffers, such as α-picoline and 2,6-lutidine, in the Co(III)-promoted hydrolysis of β-alanine ester (fig. 4 12). However, no increase in rate was observed in the present system using lutidine as buffer. In the Co(III) case, (fig. 4.12) the leaving group is not coordinated to the metal, thus, deprotonation is required to aid in the expulsion of alkoxide. In contrast, the leaving group is coordinated in **T8**, therefore, deprotonation is not necessary to accelerate the breakdown of this intermediate.

Path A can be ruled out; this mechanism is not in accord with the pH-rate profile If path A is operative, then an additional inflection point near the pKa of the coordinated alcohol moiety of **T6** should be observed. No such increase in rate, attributable to the formation of **T7** is observed.

If the mechanism of hydrolysis follows path B, then the metal complex should be an efficient catalyst for transesterification processes. Experimentally this is the case; ethyl acetate is smoothly converted to methyl acetate in methanol at neutral pH when the Cu(NMedpa) complex is added. Figure 5.4 shows the ^{1}H NMR spectral changes due to the metal complex catalyzed transesterification of ethyl acetate to methyl acetate in CD_3OD The proposed mechanism is analogous to path B and is shown in figure 6 6

If $[Cu(dpa)(OH_2)_2]^{2+}$ is a true catalyst, then catalytic turnover should be observed (see section 6.3.2) and it should also catalyze the reverse of the hydrolysis reaction. Indeed, methyl acetate is formed when a catalytic amount of the complex is added to a solution of acetic acid in methanol (fig 5.4) In accordance with the principle of microscopic reversibility, the mechanism for synthesis of methyl acetate should be the reverse of the hydrolytic mechanism shown in fig 6 7

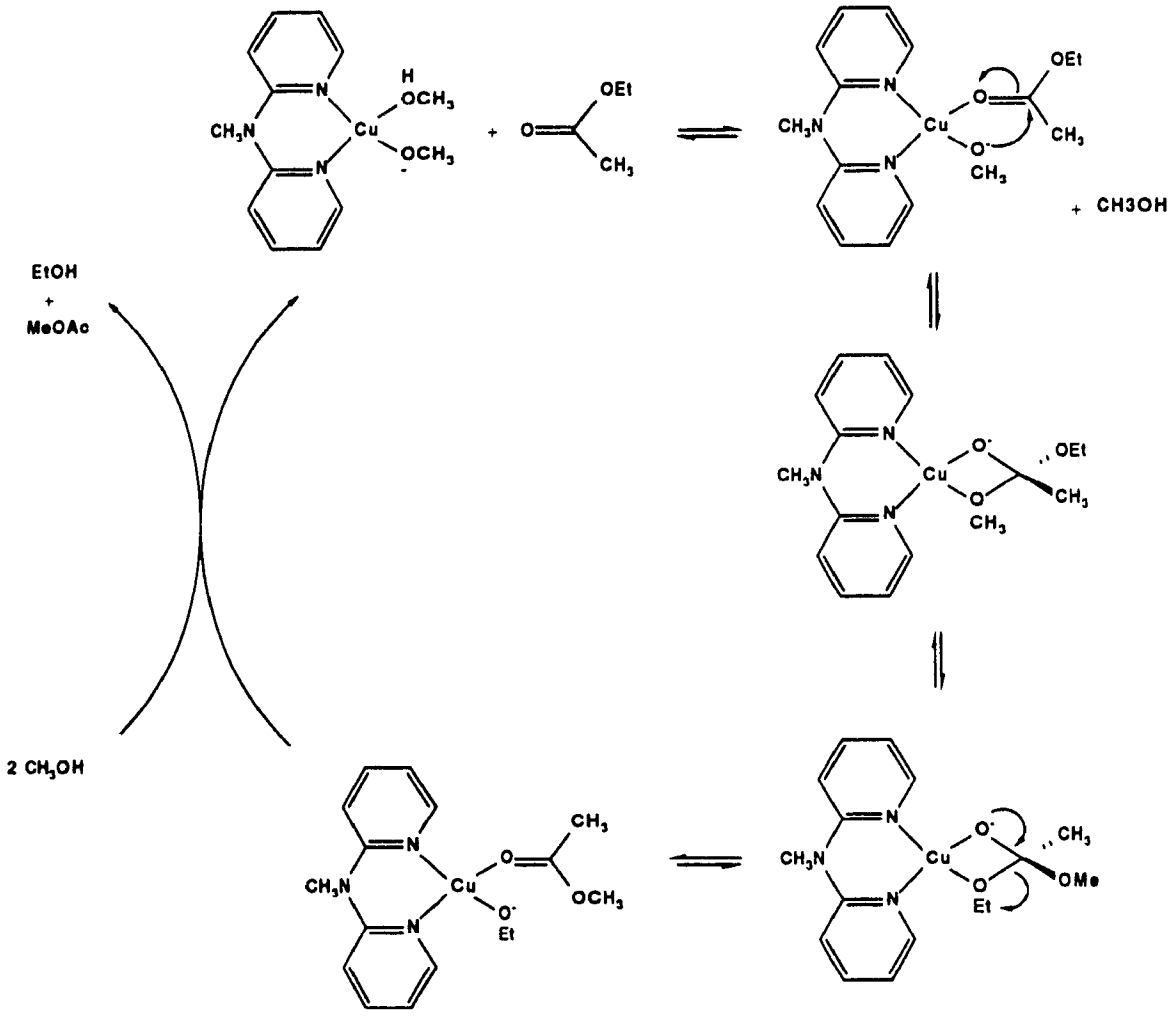

Figure 6.6 Copper complex catalyzed transesterification of EtOAC to MeOAc

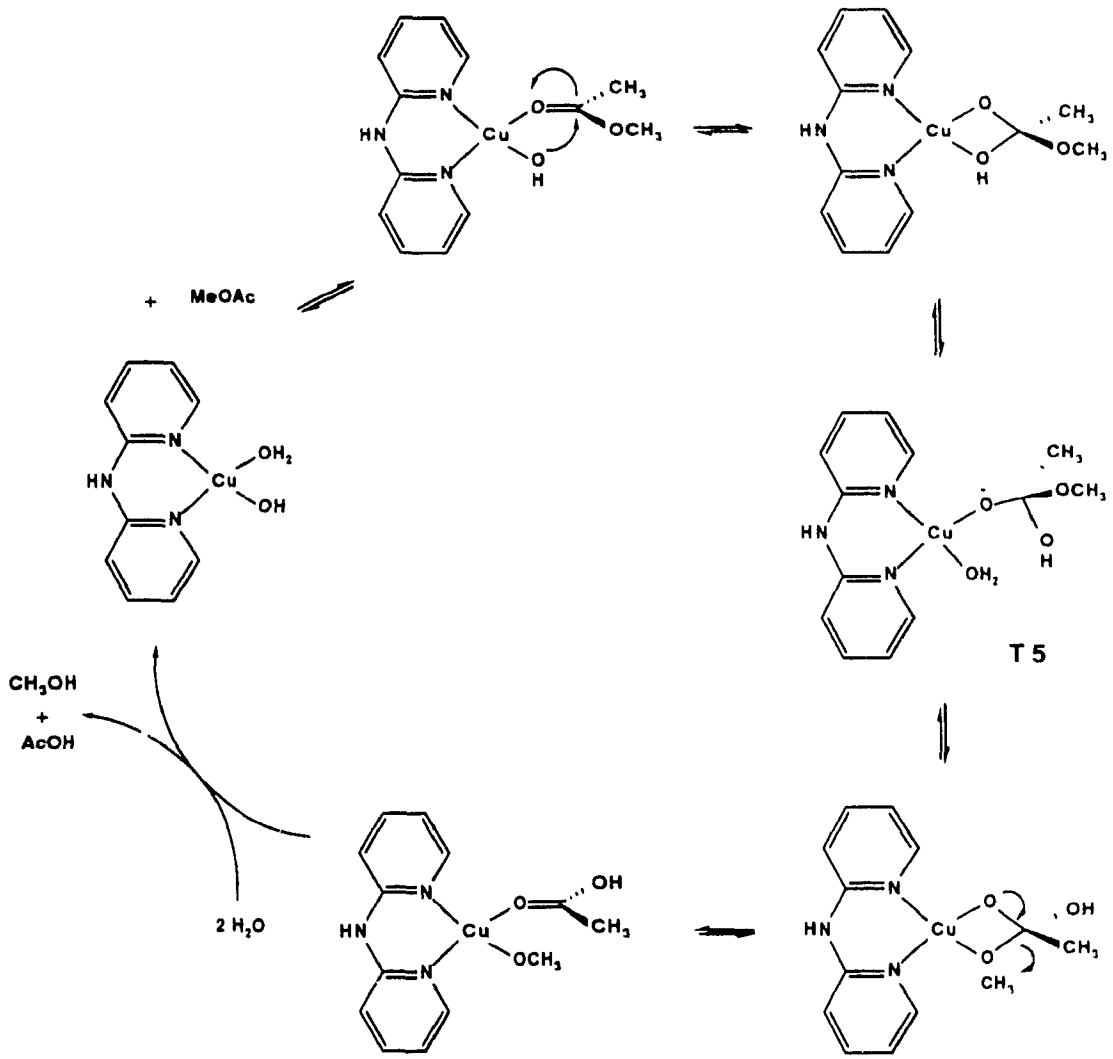

Figure 6.7 Proposed mechanism for $[Cu(dpa)(OH_2)_2]^{2+}$ catalyzed hydrolysis of MeOAc

6.3.2 Binding of Acetate to $[Cu(dpa)(OH_2)_2]^{2+}$ and Turnover

The mechanism for $[Cu(dpa)(OH_2)_2]^{2+}$ catalyzed hydrolysis of MeOAc involves the formation of a four-membered ring. Although generally four-membered rings are unstable, it has been shown by X-ray crystallography that the product of MeOAc hydrolysis, acetate, is able to bind to $[Cu(dpa)(OH_2)_2]^{2+}$ as a bidentate ligand to form a four-membered ring.[60] The dissociation constant, K_d, for acetate dissociating from

$[Cu(dpa)(OH_2)_2]^{2+}$ was determined to be 3.8 x 10^{-3} M (log K_d = -2.4). This value is similar to the corresponding K_d value for aqueous Cu(II) (log K_d = -2.2).[98] The difference in log K_d values between $[Cu(dpa)(OH_2)_2]^{2+}$ and aqueous Cu(II) is similar to the difference between $[Cu(bpy)(OH_2)_2]^{2+}$ and aqueous Cu(II).[99] Our results are somewhat surprising, from the K_d values, there is no observable increase in stability from which a chelate formation could be deduced, yet it is known from X-ray crystallographic studies that chelation of acetate to $[Cu(dpa)(OH_2)_2]^{2+}$ is possible.

The $[Cu(dpa)(OH_2)_2]^{2+}$ complex catalyzes the hydrolysis of MeOAc at pH 7 and 25 °C with a turnover time of 23 minutes (fig. 5.8). In this system, product inhibition should be negligible when the product concentration is less than the dissociation constant. Indeed, up to three turnovers can be observed without significant decrease in the hydrolysis rate.

6.3.3 Rate Comparison to Real Enzymes

In order to compare the efficiency of the copper complex with real enzymes the constants K_1 and k_2 (fig. 6.4) must be determined. The equilibrium constant, K_1, for complexation of methyl acetate to the copper complex cannot be measured directly. However, K_1 can be approximated as follows. There is a linear free energy relationship between the basicity of the ligands, L, and the equilibrium constant for complexation of L to aqueous Cu(II) (equation 6.1)[100],

$$\log K = 0.45 (pKa - 7) + 3.26 \qquad (6.1)$$

where $K=[Cu(H_2O)_5(L)]^{2+}/\{[Cu(H_2O)_6]^{2+} + [L]\}$ and pKa is the acid dissociation constant for the conjugate acid of L. The pKa of protonated methyl acetate is approximately -6.0.[101] Therefore, using equation 6.1, the equilibrium constant for binding methyl acetate to aqueous Cu(II) should be about 2.6 x 10^{-3} M^{-1}. This is an extended extrapolation considering that equation 6.1 is based on a series of 3-, 4-, and 5-substituted pyridines. However, log K for $L=H_2O$ calculated from equation 6.1 {log K =

---

[98] *Stability Constants of Metal-Ion Complexes*, Compiled by L. G. Sillen and A. E. Martell, Special publication No. 17, The chemical Society, Burlington House, W. 1, London, 1964.

[99] R. Griesser, B. Prijs, and H. Sigel, *Inorg. Nucl. Chem. Letters*, **1969**, 5, 951.

[100] a) M. S. Sun and D. G. Brewer, *Can. J. Chem.*, **1967**, 45, 2729. b) J. Hine, *Structural Effects On Equilibria in Organic Chemistry*, Wiley, New York, 1975, p. 214.

[101] R. A. Cox and K. Yates, *J. Am. Chem. Soc.*, **1978**, 100, 3861.

0.45(-1.72 - 7) + 3.26 = -0.66} is in good agreement with what it should be {log K = log(6/55) = -0.96}.

Kinetic analysis of the pH-rate profile (fig. 5.1) gives K_1k_2=1 x 10^{-3} $M^{-1}s^{-1}$ Assuming that the affinity of methyl acetate for aqueous copper and for $[Cu(dpa)(OH_2)_2]^{2+}$ are comparable, then k_2 = 3.8 x 10^{-1} s^{-1} (half-life = 2 s) This is a 10^9 fold rate enhancement over the water rate (3 x 10^{-10} s^{-1})[102] for free methyl acetate hydrolysis This is truly a spectacular rate acceleration for such a simple catalyst The k_2 value is comparable to the k_{cat} values for chymotrypsin catalyzed hydrolyses of esters (5 x 10^{-1} s^{-1}).[103] However, nature's most efficient esterase, which hydrolyzes the neurotransmitter, acetylcholine, is in a league by itself (acetylcholinesterase: k_{cat} = 2.5 x 10^{4} s^{-1}) [104]

The rate of $[Cu(dpa)(OH_2)_2]^{2+}$ catalyzed hydrolysis of acetylcholine is actually slower than that observed for MeOAc even though the uncatalyzed rate of hydrolysis of acetylcholine is faster than MeOAc (table 5.4). This is probably due to a smaller binding constant of acetylcholine to the metal arising from unfavourable electrostatic interactions between the two positively charged molecules It was anticipated that binding of acetylcholine to the metal complex would be increased by placing carboxylate groups in the 5 positions of the dipyridylamine ligand as shown below.

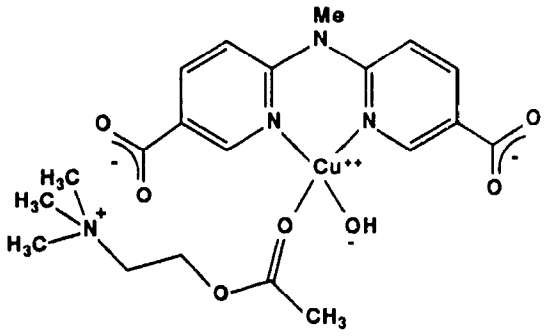

Unfortunately, this system was inactive at catalyzing the hydrolysis of esters. Placing negatively charged groups at the aforementioned positions makes the ligand inaccessible for N,N-coordination to Cu(II), as a result, precipitation of the metal occurs in neutral to alkaline pH.

---

[102]J. P Guthrie, *J Am Chem Soc* , **1973**, 95, 6999

[103]C. Walsh, *Enzymatic Reaction Mechanisms*, Freeman, San Francisco, 1979, p 79

[104]L. Stryer, *Biochemistry*, Freeman, New York, 1981, 2nd Edition p 890

6.4 REQUIREMENTS FOR METAL COMPLEX CATALYZED HYDROLYSIS OF AMIDES vs ESTERS

There is a great deal of interest in developing catalysts that hydrolyze amides. Researchers who are designing, synthesizing and examining organic systems that in some way mimic or model enzyme activity very often use p-nitrophenyl esters as substrates.[95] It is convenient for the scientist to use p-nitrophenyl esters since their hydrolyses can be followed easily by spectrophotometry. In contrast, amides are much less reactive than esters and the hydrolyses reactions are much more difficult to monitor. There is a real need to test the activity of artificial enzymes directly on amides since the structural requirements of a catalyst for hydrolyzing a p-nitrophenyl ester (or an unactivated ester such as MeOAc) are not the same as those for hydrolyzing an amide.

There have been only a few examples of significant catalysis of amide bond hydrolysis. A prime reason for this lack of reactivity is that many divalent metal complexes deprotonate in weakly basic solution to give complexes of the type **10**[105] (fig. 6.8) when coordinated to primary and secondary amides. When deprotonated, these complexes are not susceptible to nucleophilic attack by hydroxide ion.[106] Amide hydrolysis at neutral pH proceeds according to a rate-limiting tetrahedral intermediate breakdown mechanism, because, contrary to ester hydrolysis, which involves the relatively facile expulsion of an alkoxide leaving group, amide hydrolysis involves a poor leaving group (RNH^-) which must be protonated either prior to, or in concert with C-N cleavage. Therefore, in order for a metal catalyst to display significant rate accelerations for hydrolyzing amides, it is necessary for the catalyst to facilitate the rate-limiting tetrahedral intermediate breakdown step.

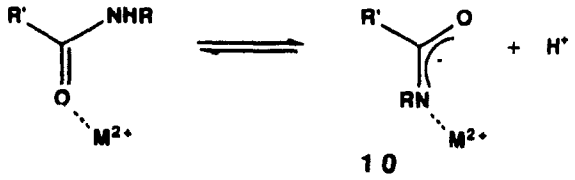

Figure 6.8 Metal ion deprotonation of primary or secondary amides.

There are two major requirements for a metal catalyst to efficiently hydrolyze amides. One criterion stems from stereoelectronic considerations: the large rate

---

[105]For a review see H. Sigel and R. B. Martin, *Chem Rev* , **1982**, 82, 385.

[106]R. W. Hay, A. K. Basak, M. P Pujari, and A. Perotti, *J. Chem Soc Dalton Trans.*, **1989**, 197 and references therein.

enhancements for amide bond hydrolysis displayed by Groves' model (fig. 4.15) was partly attributed to favourable lone pair orientations which facilitated the C-N bond cleavage step. Therefore, any geometrical restrictions imposed on the amide by the metal complex should not preclude such stereoelectronic requirements. The other requirement is that the metal should not interact with the leaving nitrogen at the tetrahedral intermediate stage where the nitrogen has developed full basic character, since, this would inhibit the required protonation at nitrogen. A metal coordinated to the leaving nitrogen (RNH_2-M) cannot be nearly as good a leaving group as a proton (RNH_3^+).[107] A different situation exists for ester hydrolysis, where, in contrast to C-N cleavage with amides, C-O cleavage occurs without prior protonation. Thus, coordination of the metal to the leaving alkoxide oxygen (as shown in fig. 6.7) improves leaving group ability in this case. Therefore, $[Cu(dpa)(OH_2)_2]^{2+}$ mediated hydrolysis of amides and esters should not occur by the same mechanism.

6.5 Cu(II) COMPLEX CATALYZED HYDROLYSIS OF AMIDES

The $[Cu(dpa)(OH_2)_2]^{2+}$ complex catalyzes the hydrolysis of DMF at a rate of 1.3 x 10^{-4} $M^{-1}s^{-1}$ at pD 8.0, 100 °C, whereas $[Cu(terpy)(OH_2)]^{2+}$ does not catalyze the hydrolysis of DMF to any significant extent. It is estimated that the diaqua complex is at least two orders of magnitude more reactive than the monoaqua complex in hydrolyzing the amide.[94]

For monoaqua complexes such as $[Cu(terpy)(OH_2)]^{2+}$, two kinetically indistinguishable mechanisms are possible: the Lewis acid mechanism (mechanism **a**), and the metal-hydroxide mechanism (mechanism **b**). For diaqua complexes an additional mechanism is possible (mechanism **c**) in which the Lewis acid mechanism and the metal-hydroxide mechanism are combined (fig. 6.9). If either mechanism **a** or mechanism **b** is more efficient than mechanism **c** then the reactivity of monoaqua metal complexes should be comparable to that of diaqua metal complexes. If mechanism **c** is most efficient then diaqua metal complexes should be more reactive than monoaqua complexes. It is unlikely that the difference in reactivity between the two complexes is due to any steric effect since $[Cu(terpy(OH_2)]^{2+}$ is slightly more reactive than $[Cu(dpa)(OH_2)_2]^{2+}$ in hydrolyzing pNPA (table 5.1). Also, it is unlikely that the difference in reactivity is due to any electronic effect since the difference in the acidity of the water molecules coordinated to the metal ion in

[107]L. M. Sayre, *J Am. Chem Soc* , **1986**, 108, 1632

$[Cu(dpa)(OH_2)_2]^{2+}$ (pKa = 7.2) and $[Cu(terpy)(OH_2)]^{2+}$ (pKa = 8.0) is less than an order of magnitude.

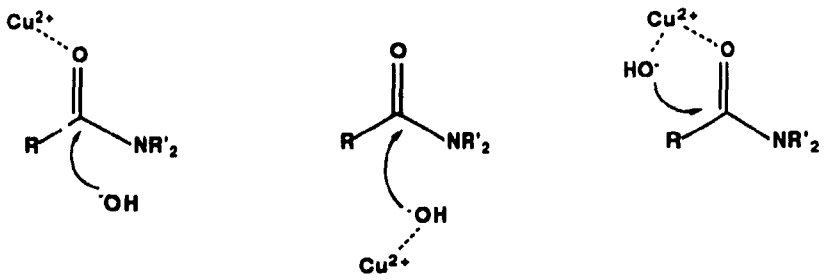

Figure 6.9 Possible mechanisms for Cu(II)-complex catalyzed hydrolysis of amides.

The simplest mechanism that can account for the difference in the reactivity between $[Cu(terpy)(OH_2)]^{2+}$ and $[Cu(dpa)(OH_2)_2]^{2+}$ is shown in figure 6.10.

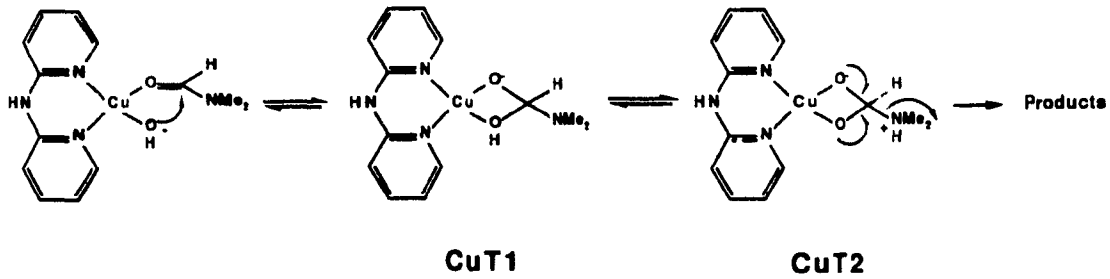

Figure 6.10 Proposed mechanism for $[Cu(dpa)(OH_2)_2]^{2+}$ catalyzed hydrolysis of amides.

Except for the involvement of the metal complex, the mechanism shown in fig. 6.10 is essentially the same as that for the uncatalyzed mechanism for amide hydrolysis (fig. 4.10). The proposed mechanism shows an acceleration for the formation of the tetrahedral intermediate **CuT1.** Although the rate-determining step is most likely loss of amine from the tetrahedral intermediate, it would be wrong to suggest that the catalytic acceleration of the attack of water will result in no observable catalysis of the overall hydrolysis. The effect of the metal is to increase the concentration of a normally insignificant, but highly reactive, intermediate species. Therefore, one way to accelerate the rate of amide

hydrolysis would be to stabilize the tetrahedral intermediate **T2** (fig. 4.10) thereby increasing its steady-state concentration. $[Cu(dpa)(OH_2)_2]^{2+}$ stabilizes **T2** by chelation (**CuT2**). This four-membered ring intermediate is similar to the one proposed for $[Cu(dpa)(OH_2)_2]^{2+}$ catalyzed hydrolysis of MeOAc.

The cleavage of the C-N bond is rate determining but this does not make the distinction between mechanisms **a**, **b**, or **c** moot. Mechanism **c** can be much more efficient than mechanism **a** or **b** if the equilibrium concentration of the doubly coordinated tetrahedral intermediate is greater than the equilibrium concentration of the singly coordinated tetrahedral intermediate (arising from mechanism **a** or **b**). Furthermore, it is not the acceleration of the tetrahedral intermediate formation step that makes mechanism **c** more efficient than the other two mechanisms but it is the consequences of such a mechanism on the C-N bond cleavage step. The tetrahedral intermediates arising from mechanism **a**, **b**, and **c** are depicted in figure 6.11. The reactive intermediates are **CuT2** and **CuT4.** It is more likely that **CuT4** will arise from **CuT3** (mechanism **b**) than from **CuT5** (mechanism **a**) since metal bound alcohols are more acidic than free alcohols. Breakdown of the tetrahedral intermediates to products can be thought of as a nucleophilic displacement (of nitrogen) at carbon by the lone pairs on the two oxygens, and the rate of this process should be directly related to the nucleophilicity of the electrons on the oxygens in the tetrahedral intermediate. If this is the case, then **CuT4** (mechanism **b**) should be more reactive than **CuT2** (mechanism **c**). However, mechanism **c** provides stabilization of the tetrahedral intermediate through metal chelation, thus, the lower reactivity of **CuT2** compared with **CuT4** is more than compensated for by its greater concentration. What makes mechanism **c** most efficient is stabilization of the tetrahedral intermediate through chelation, and the pKa lowering effect of the metal to enhance the nucleophilicity of the second oxygen in the tetrahedral intermediate.

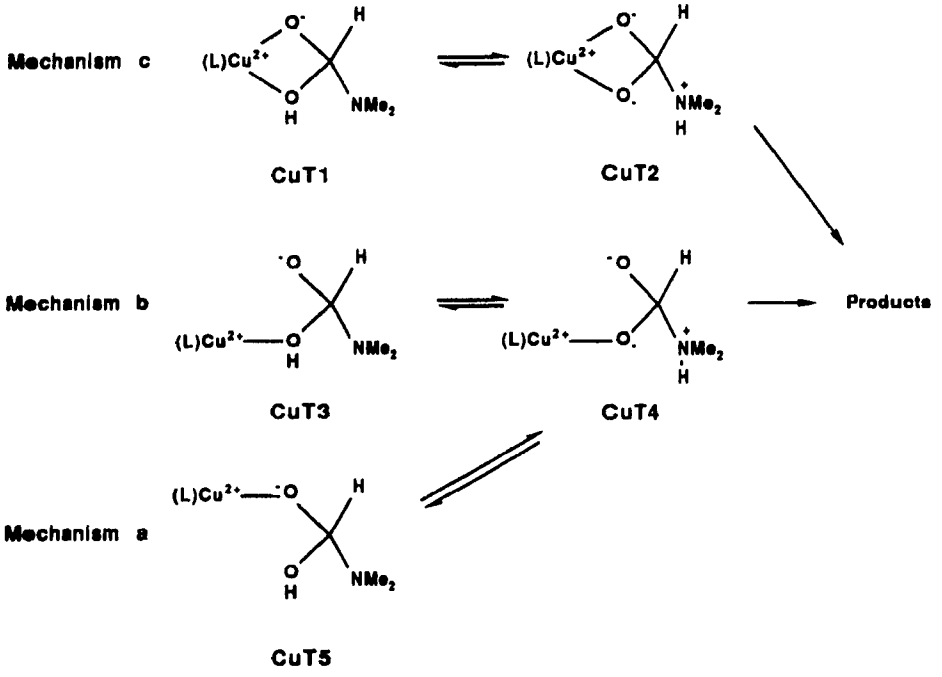

Figure 6.11 Proposed tetrahedral intermediates arising from mechanisms **a** , **b**, and **c** for Cu(II)-complex catalyzed hydrolysis of amides

There are other possible mechanisms which are available for diaqua metal complexes but not for monoaqua metal complexes. Figure 6.12 depicts one other possibility.

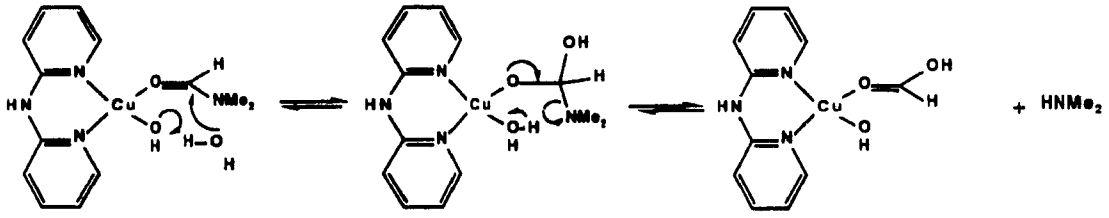

Figure 6.12 $[Cu(dpa)(OH_2)_2]^{2+}$ general base/acid catalyzed hydrolysis of amides.

In this mechanism, the intermediate **CuT6** may arise from the metal-hydroxide mechanism, Lewis acid mechanism, or as shown in the figure, it may arise from a general base

mechanism. The rate-limiting C-N cleavage step may be accelerated by the coordinated water molecule acting as a general acid catalyst. Based on the success for $[Cu(dpa)(OH_2)_2]^{2+}$ mediated hydrolysis of phosphate esters and carboxylic esters, and the ease with which this complex may form four-membered rings, the mechanism shown in fig. 6.10 is preferred over the one shown in fig. 6.12. The mechanism in fig. 6.10, which employs simultaneous carbonyl activation and intramolecular metal-hydroxide participation, parallels the mechanisms proposed for Cu(II)-complex mediated hydrolysis of phosphate diesters and MeOAc, while at the same time it satisfies the requirements necessary for metal-complex catalyzed hydrolysis of amides discussed in the previous section.

Although the reaction is carried out near neutral pH, high temperatures (100 °C) are required to observe amide hydrolysis. The rate enhancement for $[Cu(dpa)(OH_2)_2]^{2+}$ catalyzed hydrolysis of DMF is not spectacular. The Cu(II)-complex catalyzes the hydrolysis of DMF only 40 times faster than the free hydroxide rate under the same conditions (table 5.5). However, $[Cu(dpa)(OH_2)_2]^{2+}$ is two orders of magnitude more reactive at hydrolyzing unactivated amides than $[Cu(terpy)(OH_2)]^{2+}$. The former complex is unique in that it is able to stabilize four-membered chelates and it does not decompose at high temperatures. Other Cu(II)-diaqua-complexes are not stable at high temperatures.

6.6 CARBOXYPEPTIDASE A: AMIDE HYDROLYSIS MECHANISM

6.6.1 CPA Active Site

Bovine carboxypeptidase A is a hydrolytic metalloenzyme of molecular weight 34,472 containing one zinc ion bound to a simple polypeptide chain of 307 amino acids [108]. Its biological function is the hydrolysis of C-terminal amino acids from polypeptide substrates, and it displays a preference toward those substrates possessing large, hydrophobic C-terminal side chains such as phenylalanine.

The enzyme is active in the pH range 6.9 to 9.0 with the maximum activity occuring around neutrality. The zinc ion is essential for maintaining the enzyme's activity. The apoenzyme produced by removal of the metal ion by competitive complexation with chelating agents such as 1,10-phenanthroline is completely inactive, but the enzyme's reactivity is restored on adding the required amount of metal ion. Aside from peptidase

---

[108] D. W. Christianson and W. N. Lipscomb, *Acc. Chem. Res.*, **1989**, 22, 62.

activity, CPA has also been shown to possess esterase activity. Other transition metal ions like Co^{2+}, Ni^{2+}, Mn^{2+}, and Fe^{2+} are known to be good substitutes for Zn^{2+} but with varying degrees of enzyme activity.[109]

The first high resolution X-ray structure of carboxypeptidase A included the slow reacting substrate glycyltyrosine in the enzyme's active site.[110] The X-ray structure revealed that the zinc ion was coordinated to the enzyme through two histidines (His-69, His-196) and glutamic acid (Glu-72). The carbonyl oxygen of the amide substrate coordinated to the metal by displacing the metal bound water molecule. The only parts of CPA which are near enough to the peptide bond to be directly involved in the catalysis are Glu-270, Tyr-248, Arg-127, and Zn^{2+}. The only other group of the protein within 3Å of the substrate's amide bond is Arg-145 is considered to aid in substrate binding.[110] A generalized picture of this complex is shown in figure 6.13.

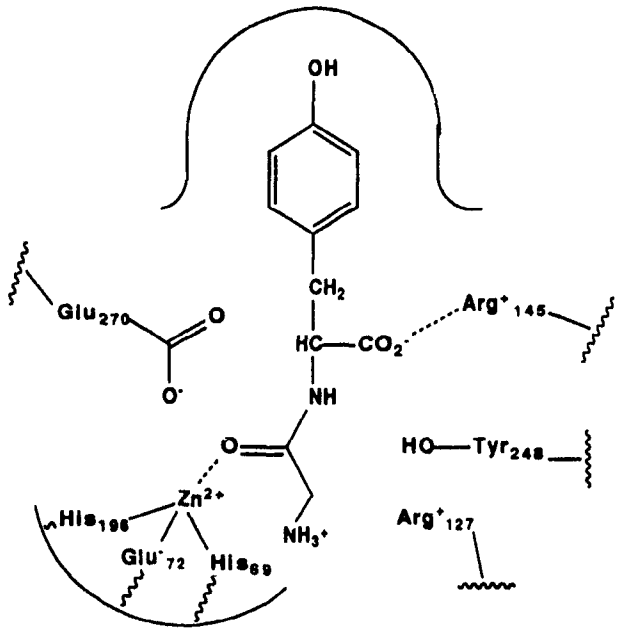

Figure 6.13 Glycyltyrosine in active site of Carboxypeptidase A. (ref. 110)

[109]J. T. Groves and R. M. Dias in *The Coordination Chemistry of Metalloenzymes*, I. Bertini, R. S. Drago, C. Luchinat, Eds., D. Reidel Publishing. Dordrecht, 1983, pp 79-92.
[110]W. N. Lipscomb, *Acc Chem Res*, **1970**, 3, 81.

6.6.2 Possible Mechanisms Proposed From Previous Model and Enzyme Studies

The hydrolytic mechanism of CPA has been the topic of much debate. Based on the arrangement of functional groups in the enzyme's active site, there have been several different mechanisms proposed for the action of carboxypeptidase A. It is now generally accepted that Tyr-248 is not involved in catalysis. Using site directed mutagenesis, Tyr-248 was replaced by phenylalanine. This Phe-248 mutant of CPA retained its catalytic ability to hydrolyze peptides or relate esters at near normal activity [111]

Investigations on the hydrolysis catalyzed by CPA on its natural and artificial substrates have resulted in some conflicting opinions regarding the mechanism of the hydrolytic reactions. There are currently three basic hydrolytic pathways under consideration. The first X-ray structure of CPA complexed with the pseudo-substrate glycyltyrosine revealed that the substrate was bound to the enzyme with its carbonyl oxygen coordinated to the zinc ion of the enzyme. Naturally, researchers thought that the metal must act as a Lewis acid, thus, the first two mechanisms that will be discussed will involve the metal acting in this manner. In the first mechanism, the Glu-270 carboxylate serves as a nucleophile to afford an acyl enzyme intermediate which is subsequently labile to hydrolysis (fig. 6.14(a)). Evidence for this mechanism includes the apparent spectroscopic detection of an accumulating intermediate, presumably the acyl enzyme, of certain ester substrates at subzero temperature.[112] However, Breslow and Wernick[113] demonstrated in a landmark ^{18}O isotope labelling experiment that an acyl enzyme intermediate is not involved in the synthesis or hydrolysis of typical peptide substrates. It was demonstrated that CPA catalyzes the ^{18}O exchange in benzoylglycine only in the presence of an added amino acid like phenylalanine. As the principle of microscopic reversibility would dictate, a hydrolytic enzyme should also catalyze the synthesis of peptides. Thus, the observed ^{18}O exchange of benzoylglycine in the presence of an added amino acid can be explained as that taking place during the hydrolysis of the dipeptide synthesized by CPA. By the same principle, the existence of an acyl-enzyme intermediate in the hydrolytic step would also require ^{18}O exchange to take place without the added amino acid, which is not observed. However, these researchers did not rule out an acyl-enzyme intermediate in esterolysis.

---

[111]a) S. J. Gardell, C S Craik, D. Hilvet, M. S. Urdea, and W J Rutter, *Nature (London)*, **1985**, 317, 551. b) D Hilvert, SD. J Gardell, W. J Rutter, and E T Kaiser, *J Am Chem Soc*, **1986**, 108, 5298

[112]a) M. W. Makinen, L. C Kuo, and J J Dymowski, *J Biol Chem*, **1976**, 254, 356 b) M W.Makinen, K. Yamamura, and E T. Kaiser, *Proc Natl Acad. Sci U SA* **1976**, 73, 3882

[113]R Breslow and D. L. Wernick, *J Am Chem Soc*, **1976**, 98, 259 b) R. Breslow and D L Wernick, *Proc. Natl Acad Sci U S A*, **1977**, 74, 1303

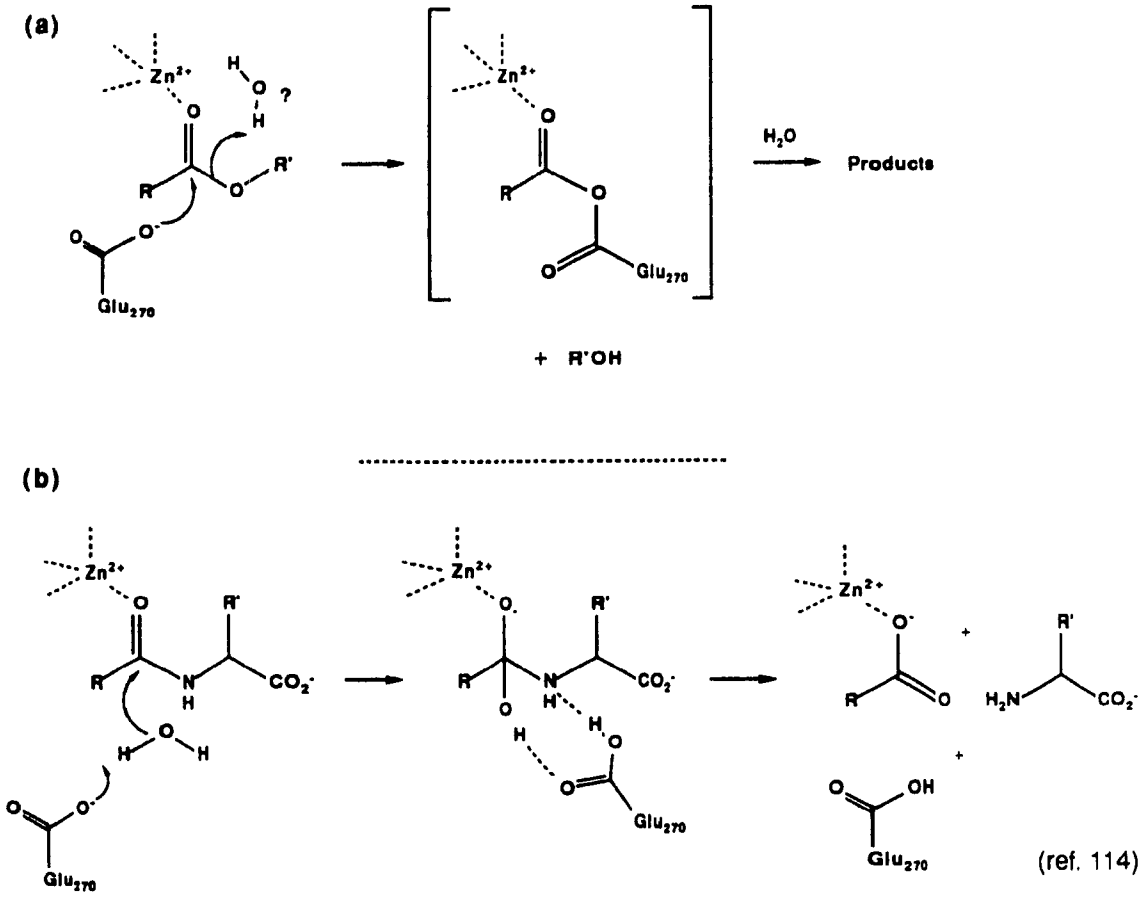

Figure 6.14 Proposed Lewis acid mechanisms for CPA catalyzed reactions:
(a) Nucleophilic mechanism for Glu-270.
(b) General base mechanism for Glu-270.

In the second mechanism, the zinc ion acts as a Lewis acid and the Glu-270 behaves as a general base delivering a hydroxide ion to the carbonyl group to form the tetrahedral intermediate. In the second step, Glu-270 acts as a proton switch by transferring a proton from the oxygen of the tetrahedral intermediate to the leaving nitrogen thus permitting a catalyzed decomposition of the tetrahedral intermediate in the forward direction.[114] The mechanism is shown in figure 6.14(b). Evidence for such a mechanism is given in Schepartz and Breslow's enzyme model for carboxypeptidase A.[114] In this model,

[114]A. Schepartz and R. Breslow, *J Am. Chem Soc* , **1987**, 109, 1814.

Co(III)-chelated amides undergo hydrolysis with bifunctional buffer catalysis. The Co(III) centre behaves as a Lewis acid and acetate buffer (or phosphate buffer) mimics the role of Glu-270 (fig. 6.15).

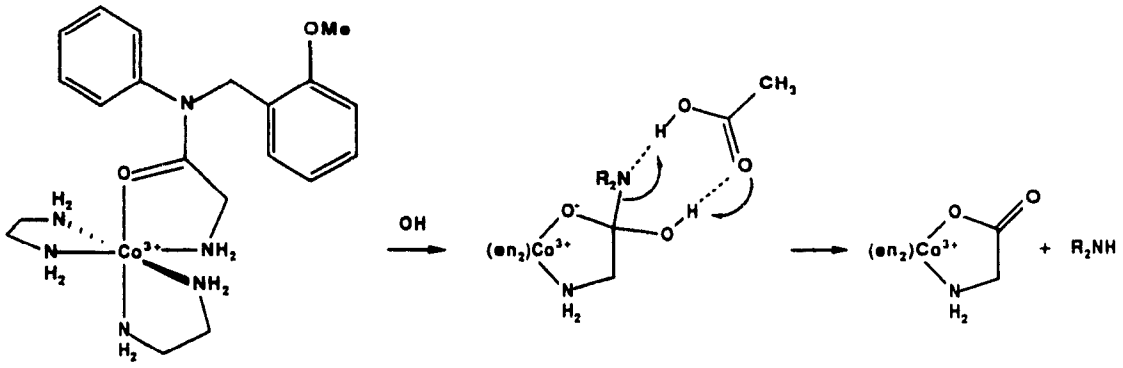

Figure 6.15 Hydrolysis of an amide in a carboxypeptidase model using Co(III) and bifunctional catalysis. (ref. 114)

Some researchers believe that glycyltyrosine may be bound with CPA in a nonproductive manner. The structural information on enzyme-pseudo substrate complex, though extremely useful, may not totally represent the binding of the enzyme and the typical reactive substrates. More recently, the X-ray structure of CPA-glycyltyrosine complex has been determined with higher resolution (1.6 Å resolution) [115] It was determined that both the peptide carbonyl oxygen and the amino terminus (as the free base) coordinate to the zinc ion in a chelate interaction. The zinc-carbonyl coordination may be simply a consequence of the chelate effect. The N-unprotected dipeptide, glycyltyrosine, is hydrolyzed nearly 5000 times more slowly than N-protected peptides; therefore, the zinc-carbonyl interaction cannot model a productive interaction in the mechanism of peptide hydrolysis. It is likely that all dipeptide substrates of CPA that carry an unprotected amino terminus are poor substrates because of such favourable bidentate coordination to the metal ion of the enzyme.

Lipscomb, as well as other researchers, believe that a more productive representation of enzyme-substrate interaction may be found in the complex of CPA with the substrate analog, 2-benzyl-3-(p-methoxybenzoyl)propanoic acid, in which the intact

---

[115]D. W. Christianson and W N. Lipscomb, *Proc Natl Acad Sci U S A*, **1986**, 83, 7568

carbonyl of this ketone is not coordinated to the metal but is H-bonded to the guanidinium moiety of Arg-127. The mechanistic role of the metal may be to promote a water molecule, with the assistance of Glu-270, to attack a peptide bond polarized by Arg-127.

Evidence for a metal-hydroxide mechanism was provided in Groves and Baron's enzyme model.[116] In this model, due to geometric restrictions, coordination of the amide carbonyl oxygen to the metal is prevented. Rate enhancements of 1.7×10^7 and 5.3×10^8 over the free hydroxide rate are observed for the Co(III) mediated amide hydrolysis of **11** and **12** respectively (fig 6.16). The mechanism involves a metal-hydroxide attack on the amide acyl carbon. Compared with **11**, the presence of a pendant carboxylate ion as in **12** increases the observed rate of hydrolysis by two fold. The carboxylate mimics the role of Glu-270 by removing the proton from the initially formed tetrahedral intermediate and transfering it to the leaving nitrogen in order to facilitate decomposition of the tetrahedral intermediate.

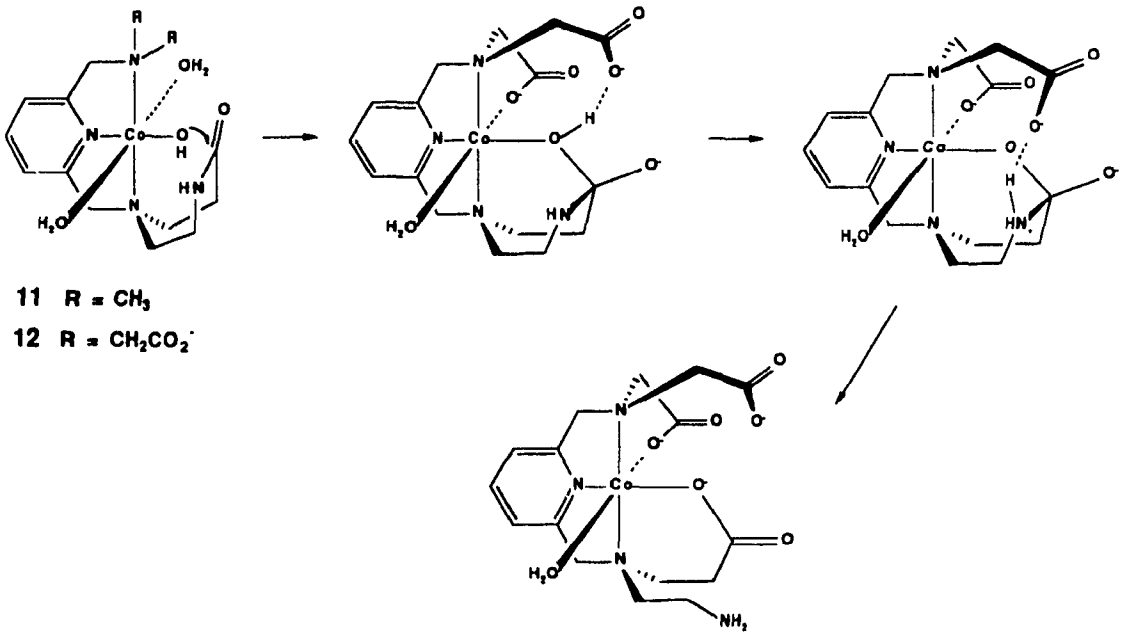

11 R = CH_3

12 R = $CH_2CO_2^-$

Figure 6.16 CPA model for the metal hydroxide mechanism. (ref 116)

Recently, X-ray structures of nonactivated ketones such as 5-benzamido-2-benzyl-4-pentanoic acid and N-(tert-butoxycarbonyl)-5-amino-2-benzyl-4-oxo-6-phenylhexanoic

[116]J. T. Groves and L. A. Baron, *J Am Chem. Soc* , **1989**, 111, 5442.

acid complexed to the enzyme were determined.[108] The structures show that these ketones bind to the enzyme as tetrahedral hydrates, more importantly, the hydrated ketones coordinate in a bidentate fashion to the active site zinc ion of carboxypeptidase A (fig 6.17(a)). The result is surprising considering that these ketones are estimated to exist less than 0.2% in the hydrated form in solution. The enzyme has performed a hydration reaction on the intact carbonyls of the ketones to result in the gem-diolate analogue of the proteolytic tetrahedral intermediate.

Christianson and Lipscomb have classified these ketones as *reaction coordinate analogues*. This term describes reversibly reactive substrate analogues that bind to enzyme active sites as analogues of catalytic intermediates. A reaction coordinate analogue can undergo a reversible chemical reaction identical with the first elementary step(s) of catalysis, yet it cannot complete the chemistry of the entire catalytic cycle due to a subsequently insurmountable barrier (e.g. in this case, the expulsion of an unfavourable carbanion).[108]

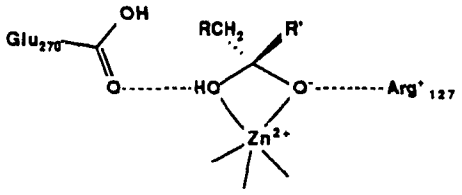

(a) Carbonyl-containing reaction-coordinate analogues bind to the Zn^{2+} of CPA as hydrate adducts in a bidentate fashion (ref 108)

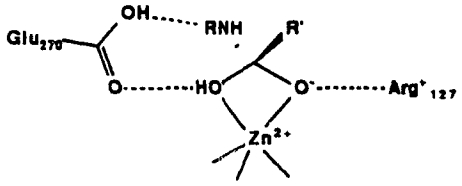

(b) Proposed tetrahedral intermediate for CPA catalyzed hydrolysis of peptides (ref 108)

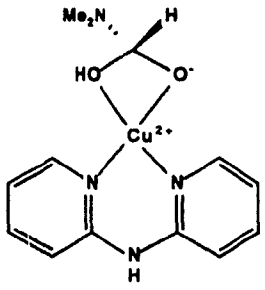

(c) Proposed tetrahedral intermediate for $[Cu(dpa)(OH_2)_2]^{2+}$ catalyzed hydrolysis of DMF

Figure 6.17

6.6.3 Proposed Alternative Mechanism

It is impossible to prove enzyme mechanisms based on simple model studies or structures of enzyme-pseudosubstrate complexes. Nevertheless detailed mechanistic studies on simple enzyme models can provide valuable insight into how enzymes work. Interestingly, the mechanism for $[Cu(dpa)(OH_2)_2]^{2+}$ catalyzed hydrolysis of dimethylformamide appears to parallel the mechanism for carboxypeptidase A catalyzed hydrolysis of peptides Both reactions involve the formation of a four-membered ring bidentate complex (fig 6 17). Christianson and Lipscomb used the X-ray structure of the CPA-hydrated-ketone complex to support a metal-hydroxide mechanism, (mechanism **b** of fig. 6.9) but considering the present results on Cu(II)-complex catalyzed hydrolysis of amides, the aforementioned X-ray structure supports a double activation mechanism (mechanism **c**) even better. The role of Glu-270 would be to act as a proton switch to transfer a proton from the oxygen of the tetrahedral intermediate to the leaving nitrogen. Unfortunately, in the Cu(II)-complex model, buffer catalysis is not observed. Addition of phosphate to mimic the role of Glu-270 inhibits the Cu(II) catalyzed reaction due to complexation of the phosphate to the metal ion. Similarly, buffer catalysis is not observed with the addition of acetate buffer.

There has been much controversy as to whether the metal ion catalyzed hydrolysis of amides by CPA would occur by a Lewis acid (mechanism **a**) or by a metal-hydroxide mechanism (mechanism **b**). Enzyme models exist to support either mechanism, however, this distinction may not be critical since mechanism **c** was observed to be more efficient than either mechanism **a** or **b** for Cu(II)-complex catalyzed hydrolysis of formamides. Furthermore, the mechanism seems to parallel the mechanism for CPA catalyzed hydrolysis of peptides. In future enzyme model studies, a bifunctional mechanism (mechanism **c**) for the role of the metal ion of CPA should be taken into consideration.

EXPERIMENTAL (PART I and PART II)

7.1 GENERAL

^1H NMR and ^{13}C NMR were taken on Varian XL-200 and XL-300 spectrometers respectively. Data is reported in parts per million (ppm) downfield from the following references: tetramethylsilane ($CDCl_3$) and 3-(trimethylsilyl)-1-propane-sulfonic acid (D_2O) for ^1H NMR; $^{13}CDCl_3$ (δ 77.0), $^{13}CD_3S(O)CD_3$ (δ 39.5), or 1,4-dioxane (δ 66.5 used for D_2O solutions) for ^{13}C NMR. The residual proton signals of DMSO and methanol (assigned values of δ 2.49 and δ 3.3 for ^1H NMR) were used as reference in these solvents.

Kinetic studies were carried out by a UV-vis method using a Hewlett-Packard 8451 diode array spectrophotometer equipped with a Lauda RM6 thermostat or a PYE UNICAM PU88 UV/VIS spectrophotometer equipped with an Accuron SPX 876 Series 2 Temperature Programme Controller.

Titrations of metal complexes were carried out with a Radiometer PHM63 pH meter equipped with a Radiometer RTS822 automatic titrator and a water bath thermostat.

Elemental analysis were performed by Guelph Chemical Laboratories Ltd.

Tetrahydrofuran was distilled from sodium benzophenone ketyl. Toluene was dried over sodium wire. N,N-Dimethylformamide was dried by shaking with KOH followed by distillation, at reduced pressure, from BaO.

Thin-layer chromatography (t.l.c.) was performed using Kieselgel 60 F_{254} aluminum-backed plates (0.2 mm thickness) and visualized by UV (λ 254 nm) using a Ultraviolet Products Inc. Model UVG-54 Mineralight Lamp. Kieselgel 60 (Merck 230-400 mesh) silica gel was employed for column chromatography.

7.2 MATERIALS

The following chemicals were purchased from Aldrich Chemical Company and used without further purification: 1,10-phenanthroline, neocuproine, 2,2'-dipyridylamine, 2,2'-dipyridylketone, 2,2':6',2"-terpyridine, 4-nitrophenyl acetate, methyl trifluoroacetate, methyl acetate, and 4-ethylmorpholine. Bis(p-nitrophenyl)phosphate and the biological buffers, MES and CHES were purchased from Sigma Chemical Company

The following compounds were synthesized according to the literature procedures: Bis(2,4-dinitrophenyl)phosphate[21c], 2,4-dinitrophenyl phosphate[117], 2,2-dipyridylmethane[118], 2,2'-dipyridylsulfide[119], and 5-nitroneocuproine[120], and trpn.[14]

7.3 SYNTHESIS OF LIGANDS

2,9-diethyl-1,10-phenanthroline

This compound has previously been synthesized in 45% yield by nucleophilic alkylation of 1,10-phenanthroline using 2 equivalents of ethyllithium[121]. The following procedure avoids the difficult preparation of an ethyllithium solution: To a stirred solution of phenyllithium (4.32 mmol) in cyclohexane/ether (2.26 mL, 70:30 v/v), neocuproine (0.3 g, 1.44 mmol) dissolved in 10 mL anhydrous tetrahydrofuran was added dropwise under a flow of nitrogen. The stirring was continued for 1 h at room temperature during which time a dark red solution resulted. The reaction mixture was placed in an ice bath and chilled to 0-5 °C. Iodomethane (0.27 mL, 4.32 mmol) was then added, the temperature was slowly raised to room temperature, and the reaction was allowed to stir overnight. During this time, the red colour disappeared. Water (10 mL) was slowly added followed by concentrated HCl (~2 mL). The aqueous layer was removed and neutralized with sodium carbonate. The crude reaction product separated as an oil and was extracted with methylene chloride (4 x 15 mL). The extracts were combined, dried (Na_2SO_4), and rotory-evaporated yielding a yellow oil. The product was purified by flash column chromatography over silica gel (ethyl ether, R_f 0.54). Recrystallization from ether/water afforded the desired product as a colorless solid (0.15 g, 40% yield): m.p. (monohydrate) 40-43 °C (lit.[121] 43-44 °C). ^{1}H NMR ($CDCl_3$, 200 MHz) δ 1.40 (t, 6H, CH_3), 3.26 (q, 4H, CH_2), 7.52 (d, 2H, ArH3, ArH8), 7.66 (s, 2H, ArH5, ArH6), 8.12 (d, 2H, ArH4, ArH7). Coupling constants (Hertz): $J_{CH_2,CH_3} = 7.6$, $J_{ArH3,ArH4} = 8.3$.

---

[117] G Rawji and R. M. Milburn, *J Org Chem*, **1981**, 46, 1205

[118] A. J. Canty and N. J. Minchin, *Aus J Chem*, **1986**, 39, 1063.

[119] C Chachaty, G.C. Pappalardo, G Scarlata, *J Chem Soc, Perkin II*, **1976**, 1234.

[120] L. P Hammett, G H. Walden, Jr, and S. M. Edmonds, *J Am Chem. Soc*, **1934**, 56, 1092.

[121] P. J Pijper, H. Van der Goot, H Timmerman, and W. Th. Nauta, *Eur J Med Chem -Chim Ther.*, **1984**, 19, 399.

Bis-(2-pyridyl)methylamine

Under a flow of nitrogen, 2-(methylamino)pyridine (3 g, 28 mmol) was added slowly to a stirred suspension of sodium hydride (60% oil disp., 1 g, 30 mmol) in dry toluene (50 mL). The mixture was gently refluxed for 3 h. 2-Bromopyridine (4.42 g, 28 mmol) in dry toluene (10 mL) was added dropwise to the above mixture over a period of 1 h and then refluxed for 24 h. The reaction was monitored by t.l.c. (EtOAc, R_f 0.94 for 2-bromopyridine, R_f 0.38 for 2-(methylamino)pyridine, and R_f 0.55 for the desired product). After cooling, water was slowly added (1-2 mL), the mixture was filtered, and the solids washed with methylene chloride. The filtrates were combined and evaporated *in vacuo* to give a yellow liquid. Vacuum distillation (90 °C, 0.01 mm) afforded the desired product (4.4 g, 85% yield) as a colourless liquid. ^{1}H NMR ($CDCl_3$, 200 MHz) δ 3.63 (s, 3H, CH_3), 6.83-6.89 (ddd, 2H, pyH5), 7.15-7.20 (ddd, 2H, pyH3), 7.49-7.58 (ddd, 2H, pyH4), 8.33-8.37 (ddd, 2H, pyH6). Coupling constants (Hertz). $J_{pyH3\text{-}pyH4}$ = 8.42, $J_{pyH3\text{-}pyH5}$ = 0.96, $J_{pyH3\text{-}pyH6}$ = 0.84, $J_{pyH4\text{-}pyH5}$ = 7.18, $J_{pyH4\text{-}pyH6}$ = 2.00, $J_{pyH5\text{-}pyH6}$ = 4.96; ^{13}C NMR ($CDCl_3$, 75.4 MHz) 35.79 ppm (CH_3), 114.04 (C3), 116.66 (C5), 136.90 (C4), 147.88 (C6), 157.49 (C2). Anal. Calcd for $C_{11}H_{11}N_3$: C, 71.33; H, 5.99; N, 22.69. Found: C, 70.91; H, 6.10; N, 22.82.

Bis-[2-(5-bromopyridyl)]methylamine

Bis-(2-pyridyl)methylamine (3 g, 1.62 x 10^{-2} mol) dissolved in dioxane (30 mL) was gradually added to a stirring solution of bromine (5.82 g, 3.65 x 10^{-3} mol) in dioxane (60 mL) at 0-5 °C. After the addition, the reaction was allowed to stir overnight at room temperature. Aqueous sodium hydroxide (5% w/v) was added to the reaction mixture until it was alkaline to litmus (~90 mL). The mixture was then allowed to stir for a few minutes. The resulting precipitate was collected and crystallized in methanol. Recrystallization afforded the product as a white fluffy solid (4.72 g, 85% yield). m.p. 103 °C, ^{1}H NMR ($CDCl_3$, 200 MHz) δ 3.57 (s, 3H, CH_3), 7.11 (d, 2H, pyH3), 7.64 (dd, 2H, pyH4), 8.36 (d, 2H, pyH6). Coupling constants (Hertz): $J_{pyH3\text{-}pyH4}$ = 8.29, $J_{pyH4\text{-}pyH6}$ = 2.23, ^{13}C NMR ($CDCl_3$, 75.4 MHz) 36.16 ppm (CH_3), 112.21 (C5), 115.50 (C3), 139.67 (C4), 148.73 (C6), 155.77 (C2). Anal. Calcd for $C_{11}H_9Br_2N_3$: C, 38.52; H, 2.64, Br, 46.59, N, 12.25. Found: C, 38.42; H, 2.49; Br, 47.00; N, 12.15.

Bis-[2-(5-cyanopyridyl)]methylamine

Under a flow of nitrogen, bis-[2-(5-bromopyridyl)]methylamine (3 g, 8.75 mmol) was added to dry N,N-dimethylformamide (30 mL) containing copper(I) cyanide (3.13 g, 350 mmol). The mixture was refluxed overnight. While still hot, the dark brown mixture was poured into a flask containing concentrated ammonium hydroxide (150 mL) and water (150 mL). The mixture was stirred while allowed to cool to room temperature. Methylene chloride (250 mL) was added, the flask was stoppered and then shaken until a fine suspension resulted. The reaction mixture was filtered, the organic layer of the filtrate was separated and washed with a dilute ammonia solution (2 x 100 mL) followed by water (1x 100 mL). The organic extract was dried (Na_2SO_4), filtered, and rotary evaporated to a solid. This crude yellowish solid was recrystallized in methanol to afford a colourless solid (1.49 g, 77% yield): m.p. 200-205 °C; ^1H NMR ($CDCl_3$, 200 MHz) δ 3.71 (s, 3H, CH_3), 7.41 (d, 2H, pyH3), 7.85 (dd, 2H, pyH4), 8.63 (d, 2H, pyH6). Coupling constants (Hertz): $J_{pyH3\text{-}pyH4}$ = 8.83, $J_{pyH4\text{-}pyH6}$ = 2.33; ^{13}C NMR ($CDCl_3$, 75.4 MHz) 35.13 ppm (CH_3), 102.99 (C5), 114.25 (C3), 117.10 (CN), 140.12 (C4), 151.82 (C6), 158.11 (C2). Anal. Calcd for $C_{13}H_9N_5$: C, 66.37; H, 3.86; N, 29.77. Found: C, 66.58; H, 4.07; N, 29.62.

Bis-[2-(5-carboxypyridyl)]methylamine

Bis-[2-(5-cyanopyridyl)]methylamine (1.22 g, 5.46 mmol) was dissolved in concentrated HCl (40 mL) and refluxed overnight. The solution was allowed to cool and the precipitate was collected. The product was recrystallized from water/DMSO to afford a yellowish solid (1.2 g, 80 % yield). ^1H NMR (D_2O and KOH, pD>9, 200 MHz) δ 3.34 (s, 3H, CH_3), 7.03 (d, 2H, pyH3), 7.94 (dd, 2H, pyH4), 8.49 (d, 2H, pyH6). Coupling constants (Hertz): $J_{pyH3\text{-}pyH4}$ = 8.86, $J_{pyH4\text{-}pyH6}$ = 2.25; ^{13}C NMR (D_2O and KOH, pD>9, 75.4 MHz) 36.78 ppm (CH_3), 114.46 (C3), 126.06 (C5), 139.39 (C4), 148.80 (C6), 158.51 (C2), 173.07 (COO^-). Anal. Calcd for $C_{13}H_{11}N_3O_4 \cdot H_2O$: C, 53.61; H, 4.5; N, 14.43. Found: C, 53.57; H, 4.19; N, 14.45.

2-Bromo-6-methylpyridine

Bromine (7.5 mL, 0.15 mol) was added dropwise to a stirred solution containing 2-amino-6-picoline (5.4 g, 0.05 mol) in HBr (48% w/v, 19 mL, 0.11 mol) at 0-5 °C. A solution of sodium nitrite (8.71 g, 0.15 mol) in water (12.6 mL) was added dropwise over a period of 0.5 h while keeping the temperature at 0-5 °C. The stirring was continued for an additional 20 minutes. A solution of sodium hydroxide (13.2 g, 0.33 mol) in water (15 mL) was added at such a rate so that the temperature did not rise above 20-25 °C. The reaction solution was extracted with methylene chloride (3 x 20 mL), the organic extracts were combined, dried (Na_2SO_4), and concentrated *in vacuo* to give an oil which was vacuum distilled (b.p. 76-79 °C, 12 mm) [lit.[122] b.p. 65 °C (4 mm)]. ^{1}H NMR ($CDCl_3$, 200 MHz) δ 2.55 (s, 3H, CH_3), 7.12 (d, 1H, pyH5), 7.31 (d, 1H, pyH3), 7.45 (t, 1H, pyH4). Coupling constants (Hertz): $J_{pyH3\text{-}pyH4}$ = 7.5, $J_{pyH4\text{-}pyH5}$ = 7.5. ^{13}C NMR ($CDCl_3$, 75.4 MHz) 14.83 ppm (CH_3), 120.45 (C5), 127.72 (C3), 141.38 (C4), 147.41 (C2), 159.69 (C6).

2-Bromo-5-methylpyridine

This compound was prepared in 90% yield in a manner identical to that described for the preparation of 2-bromo-6-methylpyridine from 2-amino-5-methylpyridine. Vacuum distillation gave a colourless liquid: b.p. 80 °C (80 mm), which solidified at room temperature, m.p. 41-44 °C, lit.[123] (45 °C). ^{1}H NMR ($CDCl_3$, 200 MHz) δ 2.30 (s, 3H, CH_3), 7.35, 7.38 (s, 1 each, pyH3 and pyH4), 8.20 (s, 1H, pyH6). ^{13}C NMR ($CDCl_3$, 75.4 MHz) 17.66 ppm (CH_3), 127.41 (C3), 132.40 (C5), 138.85, 139.23 (C2 and C4), 150.31 (C6).

Bis-[2-(6-methylpyridyl)]amine·HBr

2-amino-6-picoline (0.31 g, 2.9 mmol) was placed in a flask containing 2-bromo-6-picoline (0.5 g, 2.9 mmol) and was fused at 180 °C for 2 days. The progress of the reaction was monitored by t.l.c. (EtOAc : R_f 0.82 for 2-bromo-6-picoline, R_f 0.36 for 2-

---

[122]G. R. Newkome, D. C Pantaleo, W. E Puckett, P L Ziefle, and W A Deutsch, *J Inorg Nucl Chem*, **1982**, 43, 1529.
[123]G. Thyagarajan and E. L May, *J Het Chem*, **1971**, 8, 465

amino-6-picoline, and R_f 0.62 for product). The black solid obtained after cooling was dissolved in methanol, decolorizing charcoal was added and the mixture was boiled with stirring for 5-10 min. While still hot, the mixture was filtered, the filtrate was rotary evaporated to a solid, and the crude product was recrystallized from H_2O as the hydrobromide salt (0.48 g, 60% yield). ^1H NMR (DMSO-d_6, 200 MHz) δ 2.62 (s, 6H, CH_3), 3.38 (broad s, 1H, NH), 7.17 (apparent t, 4H, pyH3 and pyH5), 8.0 (apparent t, 2H, pyH4). ^{13}C NMR (DMSO-d_6, 75.4 MHz) 20.94 ppm (CH_3), 110.17 (C3), 116.35 (C5), 141.27 (C4), 151.18 (C6), 159.26 (C2). Anal. Calcd for $C_{12}H_{14}BrN_3 \cdot 2H_2O$: C, 45.58; H, 5.74; Br, 25.27; N, 13.29. Found: C, 45.67; H, 5.38; Br, 25.5; N, 12.96.

Bis-[2-(5-methylpyridyl)]amine

Under a flow of nitrogen, 2-amino-5-methyl pyridine (0.63 g, 5.82 mmol) in dry toluene (~20 mL) was added dropwise to a stirred solution containing sodium hydride (60% oil disp., 0.233 g) in dry toluene (20 mL). The mixture was allowed to stir at room temperature for 2 h during which time the colour of the reaction mixture became dark brown. 2-Bromo-5-methylpyridine dissolved in dry toluene (20 mL) was then added dropwise over a period of 1 h. The reaction mixture was refluxed overnight. After cooling, any unreacted sodium hydride was destroyed by the slow addition of water. The reaction solution was washed with water (2 x 30 mL). The toluene layer was isolated, decolorizing charcoal was added, and the mixture was heated to a gentle boil for 10-15 min and then filtered. The pale-yellow filtrate was dried (Na_2SO_4), filtered, and rotory evaporated to dryness leaving a yellow oil. The product was purified by flash column chromatography over silica gel (1:1, hexanes:EtOAc, v/v, R_f 0.34) yielding a yellowish solid (0.68 g, 60% yield): m.p. 93-94 °C. ^1H NMR ($CDCl_3$, 200 MHz) δ 2.25 (s, 6H, CH_3), 7.4 (two closely spaced s, 4H, pyH3 and pyH4), 7.75 (broad s, 1H, NH), 8.0 (broad s, 2H, pyH6). ^{13}C NMR ($CDCl_3$, 75.4 MHz) 17.57 ppm (CH_3), 110.99 (C3), 124.88 (C5), 138.44 (C4), 147.28 (C6), 152.24 (C2). Anal. Calcd for $C_{12}H_{13}N$: C, 72.34; H, 6.58; N, 21.09. Found: C, 72.16; H, 6.75; N, 21.43.

7.4 PREPARATION OF METAL COMPLEXES

7.4.1 Preparation Of 1:1 Complexes Of $CuCl_2$ With Diamine Ligands

All Cu(II) complexes were prepared by the 1:1 addition of an ethanolic solution of ligand to an ethanolic solution of copper(II) chloride The following is a general procedure for the preparation of Cu(II) complexes of the type, $[(L)Cu(Cl)_2]$, where L represents a diamine bidentate ligand:

A solution of diamine (3 mmol) in absolute ethanol (10 mL) was added slowly, with magnetic stirring, to a solution of anhydrous copper(II) chloride (0.4 g, 3 mmol) in absolute ethanol (15 mL). The resulting precipitate was collected by vacuum filtration and was washed with cold ethanol (4 x 20 mL).

$[Co(neo)(Cl)_2]$ and $[Ni(neo)(Cl)_2]$ was prepared as described above by substituting copper(II) chloride by cobalt(II) chloride and nickel(II) chloride respectively.

7.4.2 Preparation Of Co(III) Complexes

$[(trpn)Co(OH_2)_2]^{3+}$ was prepared by acid hydrolysis of the corresponding carbonato complex.

$[(trpn)Co(CO_3)]ClO_4 \cdot 2H_2O$ This complex was prepared by the method of Dasgupta and Harris[124], with some minor modifications. To a stirred suspension of lead dioxide (12 g, 50 mmol), trpn (4.71 g, 25 mmol), and sodium hydrogen carbonate (0.42 g, 50 mmol) in ice-cold water (150 mL), was slowly added $Co(ClO_4)_2\,6H_2O$ (9 15 g, 25 mmol) in water (100 mL). The mixture was allowed to stir vigorously for two days at room temperature. Aqueous perchloric acid (70% v/v, 6.5 mL, 50 mmol) was then added slowly. The mixture was filtered and the volume of the solution was reduced to half by evaporation *in vacuo*. The crude product slowly precipitated out of solution which was then recrystallized from water (7.88 g, 70 % yield). UV-vis: λ_{max} 536 nm (ε 120), 368 nm (ε 148), Lit.[125] λ_{max} 532 nm (ε 125), 363 nm (ε 153).

---

[124]T. P. Dasgupta and G. M. Harris, *J Am Chem Soc*, **1975**, 97, 1733.
[125]S. S. Massoud, and R M. Milburn, *Inorg Chim Acta* **1988**, 154, 115

$[(trpn)Co(H_2O)_2](ClO_4)_3 \cdot 2H_2O$ The carbonato complex was converted to the corresponding diaqua species by adding aqueous perchloric acid (5 M, 0.5 mL) to the finely divided carbonato complex (1 mmol). The resulting effervescent solution was stirred *in vacuo* (water aspirator) for two hours. The solid diaqua complex is isolated by removing the water by freeze drying.[126]

7.5 TITRATIONS

Titrations to determine the pKa of the water bound to metal complexes were performed on solutions of metal-ligand complex (5 mL, 1mM) and titrated from pH 3 to 10 using sodium hydroxide (0.01 M). The determination of the pKa of the copper coordinated water molecule for complexes of the type, $[(L)Cu(OH_2)_2]^{2+}$, is compounded by dimerization of the copper complex. The acidity of the water molecule and the equilibrium constant for dimerization of these complexes were obtained by carrying out titrations at various concentrations of copper complex (0.25 mM to 10 mM). Sodium hydroxide (0.01 M) titrant was used to titrate Cu(II) complexes (5 mL) of 0.25 mM, 0.5 mM, 1 mM, and 2 mM. NaOH (0.1M) titrant was used to titrate Cu(II) complexes (5 mL) of 5 mM and 10 mM concentrations.

The equilibrium constant for binding of acetate to $[Cu(dpa)(OH_2)_2]^{2+}$ was determined by titrating the copper complex (5mL, 1 mM), from pH 5 to 10 using sodium hydroxide (0.01 M) as titrant, in the presence of varying amounts of acetate (1 to 20 mM).

---

[126]M. Banaszczyk, Ph.D. thesis, McGill University, 1989.

7.6 KINETICS

7.6.1 Hydrolysis of Phosphate Esters and pNPA.

The hydrolysis of BNPP, BDNPP, DNPP, and pNPA were monitored spectrophotometrically by following the production of p-nitrophenolate or 2,4-nitrophenolate at 400 nm. The reactions were carried out under pseudo-first-order reaction conditions with a large excess of the copper complex over the ester. Buffers were used to maintain a constant pH during the course of the hydrolysis reaction. For pH 5.5 to 6.5, MES buffer was utilized; pH 7 to 8, N-ethylmorpholine buffer; and for pH 8.5 to 10, CHES buffer was used. The utilization of these buffers did not increase nor inhibit the copper complex promoted hydrolysis reaction.

First order rate constants were calculated from the initial slopes of the linear plots of optical density against time by converting to concentration units (ε_{400} = 18000 for p-nitrophenolate, ε_{400} = 12500 for 2,4-dinitrophenolate) and dividing by the initial phosphate ester concentration . Reactions performed at pH<9 for BNPP and NPA hydrolysis were corrected for the degree of ionization of p-nitrophenol (Ka = 7.08 x 10^{-8}).

In a typical kinetics experiment, a 1-cm cuvette was filled with a freshly prepared aqueous solution (2 mL) containing the Cu(II) complex (1 mM) and buffer (0.01 M) that had been preadjusted to the desired pH. The hydrolysis reaction was initiated by injecting a stock solution of ester (5 μL, 0.01 M) to the above solution. For BNPP an aqueous stock solution was prepared whereas a stock solution in acetonitrile was prepared for BDNPP, DNPP, and pNPA. The pH of the reaction did not change during the course of the reaction.

7.6.2 Hydrolysis of MTA and MeOAc

Hydrolysis of MeOAc and MTA were monitored by the pH-stat method.

MTA hydrolysis: A MTA stock solution (20 μL, 0.5 M in dioxane) was added to the metal complex (5 mL, 1 mM) at 5 °C. The production of trifluoroacetic acid was followed by pH-stat, the pH being maintained with sodium hydroxide (0.01 M) titrant The hydrolysis reaction was monitored to completion and the rate constant was obtained by fitting the first three half-lives of the reaction according to a first order kinetics equation

MeOAc Hydrolysis: To an aqueous solution of Cu(II) complex (5 mL, 1mM) at 25 °C, MeOAc was added (0.4 mL, final conc. 1M). The production of acetic acid was followed by the identical manner for MTA hydrolysis. The reaction can be followed up to 4 turnovers.

Production of methanol from $[Cu(dpa)(OH_2)_2]^{2+}$ promoted hydrolysis of MeOAc can be detected by ^1H NMR. MeOAc (20 mmol) was mixed with $[Cu(dpa)(Cl)_2]$ (10 mM) in a D_2O solution buffered with lutidine (0.01 M) at pD 7 or pD 8, 25 °C. ^1H NMR spectra were recorded at different time intervals.

7.6.3 Transesterification

Production of ethanol from the transesterification of ethyl acetate to methyl acetate in methanol was detected by ^1H NMR. Due to the low solubility of $[Cu(dpa)(Cl)_2]$ and [Cu(terpy)(Cl)]Cl in methanol, $[Cu(NMedpa)(Cl)_2]$ and [Cu(dien)(Cl)]Cl were used as potential catalysts. In a typical experiment, ethyl acetate (80 mM) was mixed with $[Cu(NMedpa)(Cl)_2]$ (20 mM) in CD_3OD (pD 8) at 50 °C for 3 days during which time the reaction proceeded to 95% completion.

The transesterification reaction can be carried out with [Cu(terpy)(Cl)]Cl or $[Cu(dpa)(Cl)_2]$ as the potential catalyst by the addition of 15% DMSO-d_6. This allows the complex to dissolve in the methanolic solution.

7.6.4 MeOAc Synthesis

Production of methyl acetate from acetic acid and methanol was detected by ^1H NMR by following the increase in the ^1H NMR signal due to methyl acetate (δ 2.05). Acetic acid/sodium acetate (3:1, 80mM total) was mixed with $[Cu(NMedpa)(Cl)_2]$ (20 mM) and toluene (80 mM) in CD_3OD. The toluene was used as an internal marker. The progress of the reaction can be quantified by comparing the integration area underneath the toluene and MeOAc signals. The integration area of toluene's methyl peak represents 100% completion of the reaction. The solution was placed in an NMR tube, sealed, and heated to 50 °C for 2 weeks during which time the reaction proceeded to 95% completion.

7.6.5 Hydrolysis Of Methyl Phosphate

The hydrolysis of methyl phosphate was monitored by ^1H NMR by following the increase in the ^1H NMR signal due to methanol. In a typical experiment, 1 eq. of methyl phosphate (disodium salt, 4 x 10^{-5} mol) was added to a D_2O solution containing $[Co(trpn)(OH_2)_2]^{3+}$ (4 mL, 10 mM). The solution was stirred for a few minutes at room temperature. The reaction is initiated by the addition an aliquot (1 mL) of the above solution to a D_2O solution containing $[Cu(dpa)(OH_2)_2]^{2+}$ (1 mL, 10 mM) at pD 7. The reaction is placed in a NMR tube, sealed, and heated to 40 °C. NMR spectra were recorded at different time intervals.

7.6.6 Hydrolysis of DMF

The hydrolysis of DMF in the presence of Cu(II) complexes was monitored by ^1H NMR by following the decrease in the ^1H NMR signal due to DMF (δ 7.92, δ 3.0, and δ 2.85) and following the increase in the dimethylamine peak (δ 2.71). In a typical kinetic experiment, DMF (10-30 mM) was added to a D_2O solution containing $[Cu(dpa)(OH_2)_2]^{2+}$ (5-10 mM) at pD 8. The solution was placed in a NMR tube, sealed, and heated to 100 °C. NMR spectra were recorded at different time intervals.

CONTRIBUTIONS TO KNOWLEDGE

Considerable progress has been made in understanding the mechanism of hydrolysis of phosphate diesters promoted by simple transition metal complexes.

1) The efficiencies of a series of structurally related Cu(II) complexes of the type $[(L)Cu(OH_2)_2]^{2+}$, where L represents a bidentate diamine ligand, have been determined to differ significantly depending on the ligand structure. The mechanism involves an intramolecular metal-hydroxide attack on the coordinated phosphate ester producing a four-membered ring intermediate. A structure-reactivity relationship has been elucidated based on the mechanism of the hydrolysis reaction.

2) The complex $[Cu(dpa)(OH_2)_2]^{2+}$ has been shown to be the most efficient in promoting the hydrolysis of BDNPP; the rate of hydrolysis (1 mM $Cu(dpa)(OH_2)_2]^{2+}$) at pH 8, 25 °C, is 1.5×10^6 times faster than the hydroxide rate under the same conditions.

3) The mechanism of hydrolysis of phosphate diesters promoted by $[(L)Cu(OH_2)_2]^{2+}$ has been determined to be the same as that promoted by $[(N_4)Co(OH_2)_2]^{2+}$, and in both cases, slight modifications to the ligand structure greatly influenced the reactivity of the complex. The understanding of this ligand effect may lead to the rational design of better catalytic systems which will be of considerable value in developing artificial restriction enzymes.

The hydrolysis of carboxylic esters and amides catalyzed by simple Cu(II) complexes has also been investigated.

4) The minimum structural requirements of a metal catalyst necessary for hydrolyzing esters and amides have been explained in terms of a detailed mechanistic analysis.

5) Successful catalyzed hydrolysis of unactivated esters has been achieved. The complex $[(dpa)Cu(OH_2)_2]^{2+}$ efficiently catalyzes the hydrolysis of methyl acetate under ambient conditions. A 10^9 fold rate enhancement over the water rate for free methyl acetate hydrolysis was displayed. This spectacular rate enhancement is comparable to that achieved by enzymes.

6) The efficiencies of two Cu(II) complexes for catalyzing the hydrolysis of amides in neutral water have been investigated. Diaqua copper complexes (e.g. $[Cu(dpa)(OH_2)_2]^{2+}$) catalyze the hydrolysis of simple amides whereas monoaqua copper complexes (e.g. $[Cu(terpy)(OH_2)]^{2+}$) do not. The Cu(II)-dpa complex has been proposed as an enzyme model for Carboxypeptidase A, where the hydrolysis proceeds by a bifunctional mechanism.

The following papers have been published as a result of my Ph.D. study:

1. Jik Chin, Vrej Jubian, and Karen Mrejen.
"Catalytic Hydrolysis of Amides at Neutral pH."
Journal of the Chemical Society: Chemical Communications, **1990**, 1326-1328.

2. Jik Chin and Vrej Jubian.
"A Highly Efficient Copper(II) Complex Catalyzed Hydrolysis of Methyl Acetate at pH 7.0 and 25 °C."
Journal of the Chemical Society· Chemical Communications, **1989**, 839-841.

3. Jik Chin, Mariusz Banaszczyk, Vrej Jubian, and Xiang Zou.
"Co(III) Complex Promoted Hydrolysis of Phosphate Diesters: Comparison in Reactivity of Rigid cis-Diaquotetraazacobalt(III) Complexes."
Journal of the American Chemical Society, **1989**, 111, 186-190.

4. Jik Chin, Mariusz Banaszczyk, and Vrej Jubian.
"Novel Ligand Effect on Cobalt(III) Complex Promoted Hydrolysis of a Phosphate Diester."
Journal of the Chemical Society· Chemical Communications, **1988**, 735-736.

8 APPENDIX

Derivation of equation 2.1

Cu(II) complexes of the type $[(L)Cu(OH_2)_2]^{2+}$, dimerize to give a dihydroxy bridged dimer, $[(L)Cu]_2$, that is unreactive in promoting the hydrolysis of esters. The concentration of the active monomeric species, [(L)Cu], present in solution may be determined from the following relationships:

$$2\,[(L)Cu] \underset{}{\overset{K_{dim}}{\rightleftharpoons}} [(L)Cu]_2$$

$$K_{dim} = \frac{[(L)Cu]_2}{[(L)Cu]^2} \qquad (1)$$

$$C_T = [(L)Cu] + 2[(L)Cu]_2 \qquad (2)$$

where C_T represents the total concentration of Cu(II) complex present in solution. By substituting equation 1 into equation 2 one obtains the total concentration of copper complex as a function of the concentration of the monomeric Cu(II) species present in solution (eq. 3).

$$C_T = 2K_{dim}[(L)Cu]^2 + [(L)Cu] \qquad (3)$$

Equation 3 rearranges to the quadratic equation 4,

$$0 = 2K_{dim}[(L)Cu]^2 + [(L)Cu] - C_T \qquad (4)$$

and solving the quadratic equation gives the concentration of the monomeric copper complexes present in solution (eq. 5)

$$[(L)Cu] = \frac{-1 + \sqrt{1 + 8K_{dim}C_T}}{4K_{dim}} \qquad (5)$$

The rate of BDNPP hydrolysis promoted by [(L)Cu] is given by k*[(L)Cu]*[ester], where k is the second-order rate constant for [(L)Cu] mediated hydrolysis of BDNPP. Therefore,

$$k_{obs} = k \left[\frac{-1 + \sqrt{1 + 8K_{dim}C_T}}{4K_{dim}} \right] \qquad (2\ 1)$$

where k_{obs} is the pseudo-first-order rate constant for [(L)Cu] promoted hydrolysis of BDNPP.